

Electronic Thesis and Dissertation Repository

---

6-1-2018 1:30 PM

# 1-Dimensional Hydraulic and Sediment Transport Modelling of an Emergency Spillway

Ryan Weise, *The University of Western Ontario*

Supervisor: Simonovic, Slobodan P., *The University of Western Ontario*

A thesis submitted in partial fulfillment of the requirements for the Master of Engineering Science degree in Civil and Environmental Engineering

© Ryan Weise 2018

Follow this and additional works at: <https://ir.lib.uwo.ca/etd>



Part of the [Hydraulic Engineering Commons](#)

---

## Recommended Citation

Weise, Ryan, "1-Dimensional Hydraulic and Sediment Transport Modelling of an Emergency Spillway" (2018). *Electronic Thesis and Dissertation Repository*. 5551.  
<https://ir.lib.uwo.ca/etd/5551>

This Dissertation/Thesis is brought to you for free and open access by Scholarship@Western. It has been accepted for inclusion in Electronic Thesis and Dissertation Repository by an authorized administrator of Scholarship@Western. For more information, please contact [wlsadmin@uwo.ca](mailto:wlsadmin@uwo.ca).

## Abstract

Hydropower dams are complex structures that require a high level of safety. Systems approach and system simulation have provided new insights into evaluating dam safety. System simulation of hydropower dams requires that the physical state of the critical infrastructure be represented. A 1-dimensional hydraulic and sediment transport model was developed within HEC-RAS to address erosion in an emergency spillway for an existing system simulation model. Various inflow events were simulated, and the ensuing erosion was evaluated. A range of Manning's roughness coefficients were tested and the sensitivity was minimal. Erosion and deposition values were not accurate but offer an understanding of the patterns and relationships with various overflow events. The model will allow for a representation of the physical state of the emergency spillway within the system simulation model for the Cheakamus Dam in British Columbia.

## Keywords

1-dimensional hydraulic model, sediment transport model, emergency spillway, HEC-RAS, systems engineering, GIS, erosion.

## Acknowledgments

Dr. Simonovic, thank you so much for the opportunity to complete this research under your supervision. I have learned so much from you and will be forever grateful for this experience. Thank you for your patience and guidance through the last two years. It has been a pleasure working with you.

Thank you, Leanna, for your help through the project. It was a lot of fun and I look forward to seeing your final work.

Thank you, Dr. Hartford and Derek, for your advice and feedback through the project. It was always a pleasure discussing the project with you both.

To the members of FIDS, I thank you for your help and guidance along the way. Thank you all for your support.

To my friends and family who helped me along the way, I thank you. I appreciate the support and willingness to listen when things were difficult.

Mom and Dad – thank you so much for your support along the way. I wouldn't have made it without you.

# Table of Contents

Abstract.....	i
Acknowledgments.....	ii
Table of Contents .....	iii
List of Tables .....	vi
List of Figures.....	vii
List of Appendices .....	xi
Chapter 1 .....	1
1 Introduction.....	1
1.1 Systems Approach to Dam Safety .....	1
1.1.1 System Simulation Model of a Hydropower Dam.....	1
1.1.2 Systems Approach to Dam Safety .....	3
1.1.3 Oroville Dam Safety Incident .....	5
1.2 Problem Definition.....	6
1.3 Research Objective .....	8
1.4 Literature Review.....	8
1.4.1 Hydraulic Modelling of Open Channel Flow .....	8
1.4.2 Sediment Transport.....	12
1.5 Oroville Dam Incident of 2017.....	16
1.6 Cheakamus Dam Case Study .....	18
1.7 Thesis Organization .....	19
Chapter 2.....	20
2 Methodology for 1-Dimensional Modelling of an Emergency Spillway.....	20
2.1 Introduction.....	20
2.1.1 Research Objective .....	20

2.1.2	Software Utilized .....	21
2.1.3	Research Process.....	22
2.2	Data Acquisition .....	24
2.2.1	Required Data for Hydraulic and Sediment Modelling .....	24
2.3	Data Preprocessing.....	25
2.3.1	Geospatial Elevation Data Interpolation.....	25
2.3.2	Preparing the Geospatial Data with HEC-GeoRAS.....	26
2.3.3	Reservoir Routing with Vensim.....	26
2.3.4	Sediment Data and Manning’s Values.....	29
2.4	Hydraulic Modelling of Open Channel Flow .....	30
2.4.1	Introduction.....	30
2.4.2	Overview of Computational Process of Hydraulic Model.....	30
2.4.3	Hydraulic Accuracy Issues .....	33
2.5	Sediment Transport Modelling .....	34
2.5.1	Introduction.....	34
2.5.2	Computational Process of Sediment Transport Model .....	35
2.6	Processing Hydraulic and Sediment Transport Results .....	43
2.6.1	Stability.....	43
2.6.2	Hydraulic Open Channel Flow Results.....	43
2.6.3	Sediment Transport Results .....	44
2.7	Conclusion .....	44
Chapter 3	.....	45
3	Case Study: Cheakamus Dam .....	45
3.1	Introduction.....	45
3.1.1	Site Specifics of Cheakamus Dam .....	45
3.1.2	Overview of the Case Study .....	48

3.2	Analyses for the Cheakamus Dam .....	49
3.2.1	Geometry Data .....	49
3.2.2	Processing of Hydraulic Data and Reservoir Routing .....	50
3.2.3	Processing of Sediment Data for the Cheakamus Dam .....	57
3.2.4	HEC-GeoRAS Preprocessing of the Cheakamus Dam Data .....	61
3.2.5	HEC-RAS Model Preparation for the Cheakamus Dam.....	66
3.3	Results for the Cheakamus Dam 1-Dimensional Model.....	71
3.3.1	Hydraulic Results.....	71
3.3.2	Sediment Transport Results .....	77
3.3.3	Manning’s Sensitivity .....	80
3.4	Discussion .....	96
Chapter 4	.....	99
4	Conclusion .....	99
4.1	Overview.....	99
4.2	Future Work .....	99
Chapter 5	.....	101
5	Bibliography.....	101
Appendices	.....	106

## List of Tables

Table 1: Cheakamus Dam Emergency Spillway - Manning's Coefficients for Various Areas .....	59
Table 2: Manning's Scenarios for the Cheakamus Dam Emergency Spillway .....	80

## List of Figures

Figure 1: Hydropower System Control Loop (King et al, 2017) .....	2
Figure 2: Diagram of an Emergency Spillway (Groenier, 2012).....	7
Figure 3: Research Process Flow Chart .....	23
Figure 4: Reservoir Routing Model .....	28
Figure 5: Comparison of Unsteady and Quasi-Unsteady Hydrographs.....	29
Figure 6: Flow Chart of HEC-RAS Quasi-Unsteady Flow Calculation .....	31
Figure 7: Flow Chart of HEC-RAS Sediment Transport Calculation .....	36
Figure 8: Equilibrium Depth Scenarios (Brunner, 2016).....	41
Figure 9: Distribution of Eroded or Deposited Material (Brunner, 2016).....	42
Figure 10: Cheakamus Dam (photo taken by Ryan Weise on August 11, 2015).....	46
Figure 11: Map of the Cheakamus Dam System (BC Hydro, 2005).....	47
Figure 12: Aerial Photograph of Concrete Spillway and Emergency Spillway (BC Hydro, 2005) .....	48
Figure 13: Map of the Cheakamus Dam Elevation Point Data.....	50
Figure 14: Probable Maximum Flood for the Cheakamus Dam Reservoir (BC Hydro, 2013) .....	51
Figure 15: Scaled Down Probable Maximum Flood for the Cheakamus Dam .....	52
Figure 16: Reservoir Elevation-Storage Relationship for the Cheakamus Dam (BC Hydro, 2013) .....	53
Figure 17: Reservoir Elevation-Discharge Relationships for Various Outflow Structures of the Cheakamus Dam (BC Hydro, 2013).....	54



Figure 18: Cheakamus Dam Concrete Spillway Elevation-Discharge Relationship (BC Hydro, 2013) ..... 55

Figure 19: Cheakamus Dam Emergency Spillway Overflow Hydrographs for Probable Maximum Flood Scenarios ..... 56

Figure 20: Cheakamus Dam Emergency Spillway Overflow Quasi-Unsteady Hydrograph.. 57

Figure 21: Aerial Photograph of the Cheakamus Dam Emergency Spillway Vegetation (after Google Maps January 2018) ..... 58

Figure 22: Cheakamus Dam Emergency Spillway Map of Different Manning’s Areas ..... 60

Figure 23: Cheakamus Dam Sample of Soil Gradations (BC Hydro, 2008) ..... 61

Figure 24: Cheakamus Dam Triangular Irregular Network Including Outline of Main Concrete Dam and Spillway, Highway, and Saddle Dams..... 63

Figure 25: Cheakamus Dam Emergency Spillway with HEC-GeoRAS Layers ..... 65

Figure 26: Cheakamus Dam Emergency Spillway Aerial View of HEC-RAS Model Cross Sections with the Concrete Spillway as a Blocked Obstruction ..... 67

Figure 27: Cheakamus Dam Emergency Spillway Cross Section at Station 250..... 68

Figure 28: Cheakamus Dam Emergency Spillway HEC-RAS Soil Gradation Editor..... 69

Figure 29: Cheakamus Dam Emergency Spillway Cross Section at Station 250 Showing Maximum Erodible Depth ..... 70

Figure 30: Cheakamus Dam Emergency Spillway Side Profile Plot Showing Maximum Erodible Depth ..... 71

Figure 31: Cheakamus Dam Emergency Spillway Side Profile Water Surface Elevation at Peak Outflow ..... 72

Figure 32: Cheakamus Dam Emergency Spillway 3-Dimensional Water Surface Elevation at Peak Outflow ..... 73

Figure 33: Cheakamus Dam Emergency Spillway Cross Section at Station 236 Showing Water Surface Elevation .....	74
Figure 34: Cheakamus Dam Emergency Spillway Shear Stress Map for 100% PMF and Normal Manning's Conditions .....	75
Figure 35: Cheakamus Dam Emergency Spillway Velocity Map for 100% PMF and Normal Manning's Conditions.....	76
Figure 36: Cheakamus Dam Emergency Spillway Cross Section at Station 236 Showing Erosion for 100% PMF and Normal Manning's Conditions .....	78
Figure 37: Cheakamus Dam Emergency Spillway Side Profile Plot Showing Erosion for 100% PMF and Normal Manning's Conditions .....	79
Figure 38: Cheakamus Dam Emergency Spillway Channel Invert Change for 100% PMF Scenario and Lower, Normal and Upper 100% Manning's Scenarios .....	81
Figure 39: Cheakamus Dam Emergency Spillway Channel Invert Change for 70% PMF Scenario and Lower, Normal and Upper 100% Manning's Scenarios .....	82
Figure 40: Cheakamus Dam Emergency Spillway Channel Invert Change for 40% PMF Scenario and Lower, Normal and Upper 100% Manning's Scenarios .....	83
Figure 41: Cheakamus Dam Emergency Spillway Difference in Manning's Scenarios for Channel Invert Change for 100% PMF Scenario .....	84
Figure 42: Cheakamus Dam Emergency Spillway Difference in Manning's Scenarios for Channel Invert Change for 70% PMF Scenario .....	84
Figure 43: Cheakamus Dam Emergency Spillway Difference in Manning's Scenarios for Channel Invert Change for 40% PMF Scenario .....	85
Figure 44: Cheakamus Dam Emergency Spillway Eroded Material Sensitivity to Manning's Range at 90% Size .....	86

Figure 45: Cheakamus Dam Emergency Spillway Eroded Material Sensitivity to Manning's Range at 100% Size .....	86
Figure 46: Cheakamus Dam Emergency Spillway Eroded Material Sensitivity to Manning's Range at 110% Size .....	87
Figure 47: Cheakamus Dam Emergency Spillway Eroded Material Sensitivity to Manning's Vegetation Size Change at Lower Range .....	87
Figure 48: Cheakamus Dam Emergency Spillway Eroded Material Sensitivity to Manning's Vegetation Size Change at Normal Range.....	88
Figure 49: Cheakamus Dam Emergency Spillway Eroded Material Sensitivity to Manning's Vegetation Size Change at Upper Range.....	88
Figure 50: Cheakamus Dam Emergency Spillway Shear Stress Map for 100% PMF and Lower Manning's Scenario.....	90
Figure 51: Cheakamus Dam Emergency Spillway Velocity Map for 100% PMF and Lower Manning's Scenario .....	91
Figure 52: Cheakamus Dam Emergency Spillway Shear Stress Map for 100% PMF and Normal Manning's Scenario.....	92
Figure 53: Cheakamus Dam Emergency Spillway Velocity Map for 100% PMF and Normal Manning's Scenario .....	93
Figure 54: Cheakamus Dam Emergency Spillway Shear Stress Map for 100% PMF and Upper Manning's Scenario .....	94
Figure 55: Cheakamus Dam Emergency Spillway Velocity Map for 100% PMF and Upper Manning's Scenario .....	95

## List of Appendices

Appendix 1: Meyer-Peter Muller Sample Calculation (Brunner, 2016).....	106
Appendix 2: Toffaleti Fall Velocity Tables (Brunner, 2016) .....	108
Appendix 3: Thomas Mixing Method Algorithm (Brunner, 2016) .....	109

# Chapter 1

## 1 Introduction

This chapter will begin with an overview of the project and how it fits into ongoing research, then define the problem and the objectives of the work. A literature review will present the state of the art. A case study of Cheakamus Dam will also be introduced. Finally, the thesis organization will be described.

### 1.1 Systems Approach to Dam Safety

Hydroelectric dams are complex engineering systems. Although they are extremely useful to society for power generation and water management, they require a high level of safety due to the vast amount of water retained behind the dam. When designed, dams are built to withstand extreme events such as a flood of a given return period or a seismic event of certain intensity. This engineering practice of simply meeting the design criteria has become insufficient; history has shown that dams can in fact fail from “an unlikely combination of common events”. Extreme loads are rarely causing the failure of these complex structures; it is often interactions between system components that work together to lead to failures (Regan, 2010). As such, a new approach to dam safety risk assessment must be investigated, taking into consideration potential failures occurring within the design envelope. Systems approach, especially systems simulation presents a promising method for analysis of a multitude of scenarios taking into account how different system components function individually and together. By simulating a dam system, a wide variety of failure modes, both within and outside of the design envelope, can be generated.

#### 1.1.1 System Simulation Model of a Hydropower Dam

King et al (2017) present a system dynamics simulation model that incorporates both physical and nonphysical components of a hydropower dam system. Under various operating conditions, the simulation model can determine system performance and safety changes that occur from physical and functional component failures. The objective of King et al’s research is to utilize a system dynamics simulation model to observe the

systems response to various operating scenarios. King et al also aims to define performance measures in order to assess the system safety.

King et al explains that in system dynamics simulation, the system structure is directly linked to the behavior of the system. The system structure encompasses the relationships of components, feedbacks, and delays. King modelled the structure of the system dynamics model after Leveson's generic control system structure (Leveson, 2011)

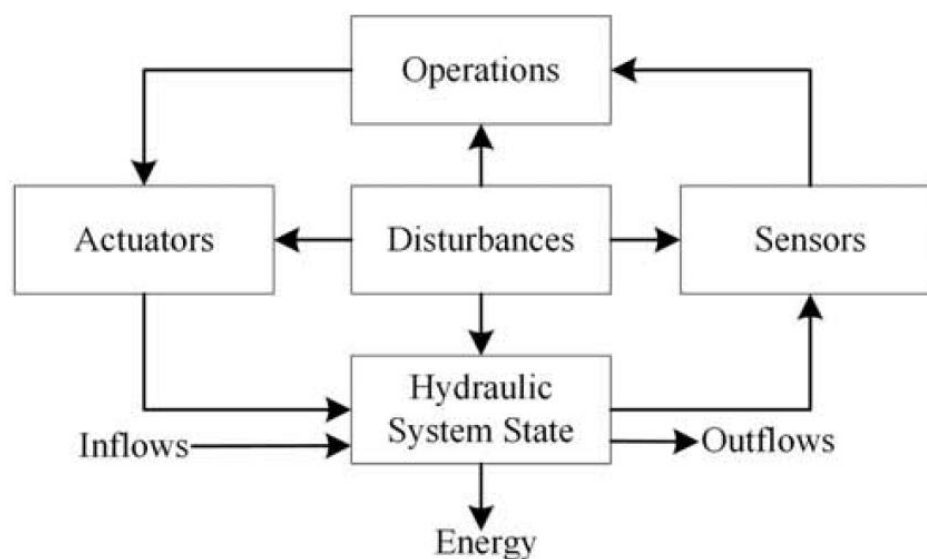


**Figure 1: Hydropower System Control Loop (King et al, 2017)**

Figure 1 shows King's control loop. This is the highest level of system and each box within this figure represents a system in its own. The hydraulic system state describes the system in terms of water retention and conveyance. Earthen and concrete dams retain the water, while controlled conveyance of water occurs in flow passages such as gated spillways, power outlets, and emergency spillways.

The hydraulic system state also represents the physical state of critical infrastructure and presents an opportunity for modelling the physical state. This research will pursue that opportunity that King has presented; providing a piece to the overall system dynamics puzzle. When referring to the system dynamics model in this thesis, it will be referring to the one King proposed.

### 1.1.2 Systems Approach to Dam Safety

Engineers and dam safety specialists are faced with the responsibility of predicting and preventing potential failure modes of dam systems. Loss of human life, serious financial impacts, and ecosystem destruction are all possibilities when a high consequence dam fails. Through the latter half of the twentieth century, numerous dams were constructed for sources of hydropower, water management, agricultural and recreational uses. Regan (2010) analyzed a database composed of dam failures and their respective timelines and causes, finding that roughly one third of all dam failures in the study happened either during construction or before the dam reached five years of age. Many experts in the industry believe that if a dam were to fail, it would occur relatively close to its infancy. However, the research of Regan (2010) showed that another one third of dam failures occurred after 50 years of age, indicating the importance of the whole life cycle asset management and consideration of infrastructure aging in dam safety assessments.

Dams are very complex structures. Because of this, there are many risks that can lead to the demise of a dam. Indiana's dam safety inspection manual categorizes these risks into four categories: operating factors, human factors, natural factors, and structural factors (Department of Natural Resources Indiana 2007). The importance of considering the interactions between physical and nonphysical system components are apparent to engineers and dam safety specialists, however traditional methods of dam safety evaluation may not be able to predict such interactions. Regan discusses the necessity of taking a systems approach to dam safety, discussing the current state of dam safety practice and limitations associated with certain methodologies (Regan, 2010). A detailed analysis of decision making in the dam safety community is provided and the author gives special focus to case studies where traditional methodologies were unable to predict the potential failure modes that ultimately resulted in dam failure. These case studies support the argument for a shift toward systems thinking in the dam safety community.

A systems engineering approach to dam safety aims to achieve a holistic, top-down view of the system that considers all physical and nonphysical system components. Regan

(2010) notes that systems engineering advocates argue that safety and reliability are different properties of a system that are often in conflict. With the increased use of Supervisory Control and Data Acquisition (SCADA) systems, this distinction between safety and reliability becomes more important. Measures to improve system reliability (e.g. multiple methods of control) can lead to increased complexity, and in turn lead to more opportunities for unforeseen component interactions (Regan 2010; Leveson 2003; and Leveson 2011). Systems thinking can help in understanding these complex non-linear relationships, leading to an overall increase in dam safety. Leveson (2003) and (Regan 2010) note that increasing system complexity increases the number of ways for components to interact in unforeseen and potentially unsafe ways.

Leveson (2003) discusses the potential of Systems Theoretic Accident Modelling and Process (STAMP). It is explained that systems are composed of three main sections: constraints, hierarchal levels of control, and process models. Leveson (2003) suggests that instead of viewing accidents as if they were caused by a root cause, that accidents should be viewed as results from interactions between components. Many accidents are found to occur when there is an inconsistency between the model used by the controller and the actual process state (Leveson 2003; Leveson 2011). Any overlap where two controllers can control the same process may also lead to accidents. Leveson uses the STAMP methodology to assess the Walkerton drinking water accident, using the concept of asynchronous evolution, which occurs when one part of a system changes without the related necessary changes in the other parts of the system. In the case of Walkerton, the contaminant (*E. coli*) concentration in the source water increased without the necessary increase in chlorination to ensure safe drinking water. Leveson's discussion does not refer to hydropower dams, however this line of thinking could be applied to improve understanding of potential failure modes for hydropower dam systems.

Komey (2015) applies systems thinking in dam safety assessment, demonstrating that systems modeling is a promising method for assessment of potentially unsafe operating scenarios. Komey (2015) and Baecher (2013) propose that accidents do not occur from severe loadings on a dam, but rather from an "uncommon combination of mishaps". Interactions between natural, engineered, and human systems are considered complex.



For example, if a dam's instrumentation misperforms, the reservoir level rises while ice has formed on the spillway gates and the operator in turn misperceives the danger at hand. Komey explains that dam safety specialists and engineers cannot simply analyze individual components against a prescribed standard, but must understand the complex interactions to determine the emergent system behaviour. Simulation provided an opportunity to investigate this further. An Ontario Power Generation (OPG) system of 4 cascading dams was modelled using GoldSim, a basic simulation software package (Komey, 2015). A variety of different disturbances were propagated through the system, demonstrating that accidents resulted from loss of remote control, incorrect operational decisions, loss of power supply, loss of access to the dam site, lack of qualified personnel on site, gate failure, excessive weather, common cause disruptions and failure to control instrumentation. Komey's research indicates that simulation is a promising approach to model complex systems and their interactions under a variety of operating conditions, however it is unclear whether component interactions and feedbacks were included in the system model.

### 1.1.3 Oroville Dam Safety Incident

Oroville Dam is the largest earthen embankment dam in the United States, impounding the Feather River near Oroville, California. In February of 2017, the main concrete spillway experienced significant erosion after a hole had formed. As the eroded material deposited downstream, it created a blockage along the river and forced the closure of the power generation station (Oroville Dam Spillway Incident Independent Forensic Team, 2017). This is an excellent example of system feedback and demonstrates how feedbacks can be modelled within a dam safety perspective. As the erosion increases, so does the size of the blockage. This in turn reduces the amount of allowable outflow from the power generation station, causing the reservoir elevation to rise. As reservoir elevation increase, as does the outflow from the concrete spillway, leading to an increase in erosion. This loop increases until the generation station is completely turned off. The Oroville Dam incident not only shows the importance of how much material will be eroded, but also where the material will deposit and how that could influence the safety of the dam.

The Oroville Dam safety incident provides insights on how the physical state of critical infrastructure may cause system feedbacks. With a systems approach to dam safety, modelling the critical infrastructure to investigate how different hydraulic loading conditions could have caused damage or negative system feedbacks may have lead to a better understanding of the system safety. The Oroville Dam safety incident will be discussed further in this chapter.

## 1.2 Problem Definition

System dynamics simulation modelling presents a challenge with defining the state of components through time. Some components are easily modelled; for example, a low-level outlet gate may either be open, closed, or partially closed. Any damage or loss of control can easily be modelled by changing the state of the component in the model. To best represent the dam system, the system dynamics simulation model presented by King must be able to describe different states of each component. Some components require more effort to model. An emergency spillway is one case of a component that requires further effort.

An emergency spillway provides additional outflow capacity to a dam system. A diagram of an emergency spillway can be seen in Figure 2. There are various designs of emergency spillway. A common design is to have the water freely spill over a structure that is at a lower elevation than the crest of the dam. The water then flows freely along the emergency spillway, which can be in various areas depending on the design of the dam. They are intended as a last resort overflow method to reduce reservoir levels so that the dam does not overtop; causing a breach. Emergency spillways typically have minimal protection against erosion, unlike main spillways (U.S. Department of the Interior Bureau of Reclamation, 2014). This is due to the infrequent use of the emergency spillway and as a cost reduction method; lining the emergency spillway in concrete would be an expensive endeavor. However infrequent the use of the emergency spillway is, its use is within the design envelope of the dam. As the aim of the system dynamics simulation

model is to model system performance within the design envelope (King, Simonovic, & Hartford, 2017), usage of the emergency spillway must be incorporated into the model.

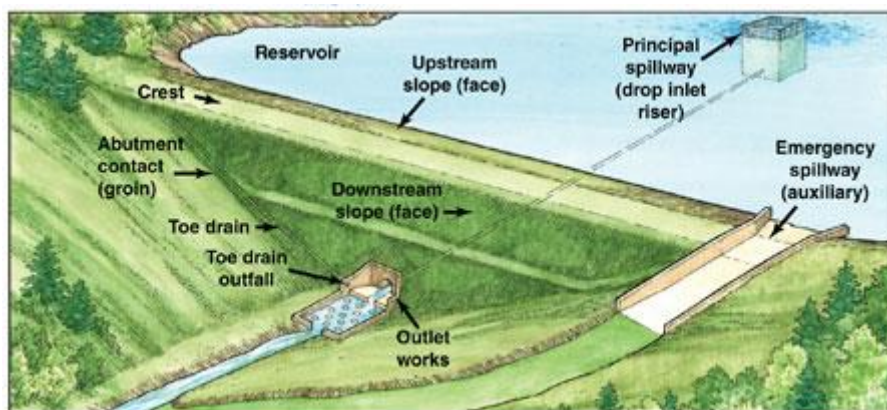


**Figure 2: Diagram of an Emergency Spillway (Groenier, 2012)**

Most emergency spillways flow uncontrolled, so as the reservoir elevation rises as does the overflow into the emergency spillway. As flows increase, as does the potential for erosion within the emergency spillway. Because the inflow is directly related to the reservoir elevation, which can be affected by a number of other components, the flow over the spillway and in turn erosion is directly dependent on the reservoir elevation. This proposes a problem as there are many different scenarios and inflow events that could alter the water spilling into the emergency spillway. One way to model the emergency spillway as a component within the dam system simulation model is to have erosion as a damage state. An emergency spillway can be completely damaged, otherwise known as failure, or the damage could range between damaged and undamaged as the level increases or decreases. For the system dynamics model to represent this correctly, the model cannot simply assume a damage state for a given inflow event as data on erosion from previous inflow event does not exist. A method must be devised to represent the damage occurring in the emergency spillway from various overflow events. The method must be easily repeatable for other dam systems. The method does not have to be highly accurate, however it must be able to predict where and roughly how much erosion and deposition will occur.

## 1.3 Research Objective

This absence of a damage state relationship for various flow events in the emergency spillway has presented a clear objective to the problem. The objective of this research is to develop a model that describes the flow passing through the emergency spillway and damage that could occur in the form of erosion. The model must satisfy the following criteria:

1. The model must be computationally simple.
2. The model must be able to be recreated for other dam systems.
3. The model must be able to test various inflow conditions.

The model must be tested using the Cheakamus Dam in British Columbia, which is the hydropower system used in King's research. This model will then be utilized by King's system dynamics simulation model to provide a representation of the physical state of the emergency spillway during system simulations.

The model developed in this research must be recognized as a qualitative tool to judge damage to an emergency spillway and not a quantitative tool. Without comparable data, there is no way to accurately determine the level of uncertainty of such an application of these models. Without a level of uncertainty, there can be little confidence with the quantitative results.

## 1.4 Literature Review

The following sections present the relevant literature and set the stage for the research.

### 1.4.1 Hydraulic Modelling of Open Channel Flow

The principles used in 1-dimensional steady flow modelling date back to the year 1738, when Bernoulli applied the conservation of linear momentum to an incompressible steady flow. The Bernoulli equation has had a tremendous impact on the study of fluid mechanics. With several limitations, the equation allowed for a simplification of various

fluid mechanics problems (Cengal et al, 2008). Although the equation is only an approximation, it can serve as a helpful tool when modelling hydraulic problems.

A further simplification came into the world of hydraulics when Robert Manning created his famous Manning's equation in 1891. Without the use of a weir or measuring device, it is very difficult to estimate the velocity within an open channel. Manning created an equation that allowed for the calculation of flows within an open channel. Equation 1 shows the Manning equation (Manning, 1891). Hydraulic engineers have used the equation since it was created as it is a simple empirical relationship that requires little information. Manning created the equation by averaging the velocities calculated by alternative equations (Fischenich, 2000). The equation takes into consideration the slope of the channel, the bed roughness, and the hydraulic radius. Initially, Manning had proposed the use of a different equation, to avoid the computational time required to solve a cubic root. In 1918, Horace King had written on the recommendation of Manning's equation over Kutter's formula, which had an inverse value of the roughness coefficient. King also included a table of computed values of the cubic root, allowing an engineer with the table to quickly compute velocities using Manning's original formula (Fischenich, 2000).

$$Q = \frac{1}{n} AR^{2/3} S_f^{1/2} \quad (1)$$

$Q = \text{flow rate (m}^3/\text{s)}$

$n = \text{Manning's roughness coefficient (s/m}^{1/3}\text{)}$

$A = \text{flow area (m}^2\text{)}$

$R = \text{hydraulic radius (m}^2/\text{m)}$

$S_f = \text{friction slope (m/m)}$

The Manning equation describes the flow of water in an open channel. The equation can be used to calculate flow rates in an open channel, or if the flow rates and channel

geometry are known, the equation can be used to calculate the friction slope. The friction slope is useful to calculate the energy headloss through an open channel, as seen in Equation 2. With the use of Bernoulli's equation, Equation 3, the headloss can be utilized to calculate downstream water surface elevations. Both Equations 2 and 3 derive from Bernoulli's principles, and have been documented in many texts (Te Chow, 1959).

$$h_e = L\bar{S}_f + C \left| \frac{a_2 V_2^2}{2g} - \frac{a_1 V_1^2}{2g} \right| \quad (2)$$

$h_e$  = energy head loss (m)

$L$  = Reach length (m)

$\bar{S}_f$  = friction slope between two sections (m/m)

$C$  = expansion or contraction loss coefficient (unitless)

(2 annotates upstream value where 1 annotates downstream value)

$$Z_2 + Y_2 + \frac{a_2 V_2^2}{2g} = Z_1 + Y_1 + \frac{a_1 V_1^2}{2g} + h_e \quad (3)$$

$Z_2$  and  $Z_1$  = elevation of invert (m)

$Y_2$  and  $Y_1$  = water surface elevation (m)

$V_2$  and  $V_1$  = average velocities (m/s)

$a_2$  and  $a_1$  = velocity weighting factors (unitless)

$g$  = gravity (m/s<sup>2</sup>)

$h_e$  = energy head loss (m)

(2 annotates upstream value where 1 annotates downstream value)

The combination of these equations allows for the calculation of water surface elevations through an open channel. In order to calculate the water surface elevations through a channel, the following parameters need to be known or assumed; steady flow rate, known

channel geometry, known channel roughness, and a downstream boundary condition, typically set as the friction slope.

In many modelling scenarios, the flow is not steady and is varying in time. If flow is unsteady, Bernoulli's steady state equation becomes inapplicable and the problem becomes much more complex. The Navier-Stokes equations must be used to model the hydrodynamics. If the Navier-Stokes equations are integrated over the cross-sectional surface of the flow, then the St. Venant equations are found and can be used to model 1-dimensional unsteady flow (Neelz & Pender, 2009). To further increase the accuracy of the model, the Navier-Stokes equations could be integrated over the flow depth to arrive at the 2-dimensional St. Venant equations. Instead of having velocities range only in the downstream direction, the velocities would range in the lateral direction as well, which is more accurate to what is occurring in an open channel (Neelz & Pender, 2009). In order to achieve a higher level of accuracy than what 1-dimensional modeling provides, the model must add another dimension and become more complex. As the level of model complexity increases, so does the computational time and the time required to build the model. 2-dimensional models can range from hours to days to fully run, while 1-dimensional models take minutes to run (Neelz & Pender, 2009). Although 2-dimensional modelling provides much more accurate results, engineers still widely use 1-dimensional model due to its simplicity and ease of application.

There are many commercial and open source software packages that allow users to compute water surface elevations. Practicing engineers in North America are often using the HEC-RAS and Telemac-Mascaret software packages that perform the same tasks with no financial cost to the user. The United States Army Corps of Engineers created a software package in 1968 called HEC-2, which eventually evolved into HEC-RAS (Maeder, 2015). In 1984 the program was modified for compatibility with personal computers. As the years progressed, HEC-RAS grew in its capabilities; initially starting out as a simple water surface calculation of a cross section, to having the capabilities of modelling steady and unsteady flow, various flow regimes, 1 and 2-dimensional modelling, sediment transport modelling, and various other features (Maeder, 2015). The

software has grown to be widely accepted by the engineering community and continues to maintain its widespread use by constantly providing updates with added features.

## 1.4.2 Sediment Transport

As water flows over the river bed, sediment can be transported downstream and deposited. As velocities increase, sediment is suspended in the water and as velocities slow the sediment may fall out of suspension. This phenomenon has been of importance to hydraulic engineering for a long time. The earliest bed load transport equation was created by the French engineer DuBoys in 1879 (Hager, 2005). Although it is not used in applications today, the structure of the formula is very similar to current bed load transport formulas; the actual force multiplied by the actual force less the entrainment force.

Through the twentieth century, various bed load equations were developed with either different data sets from rivers or within flume experiments. One of the most commonly used equations was developed in 1948 by Meyer-Peter and Muller at the Swiss Federal Institute of Technology. Equation 4 derives from an extensive number of experiments that were performed with steady and uniform flow (Meyer-Peter & Muller, 1948). Various sediment properties were tested to derive the final formula. The relationship is based on the excess shear.

$$\frac{Q_s}{Q} \left( \frac{k_s}{k^r} \right)^{3/2} \gamma_w h J = 0.047(\gamma_s - \gamma_w) d_m + 0.25 \left( \frac{\gamma_w}{g} \right)^{1/3} g_s^{2/3} \quad (4)$$

$$g_s = \text{unit sediment transport rate in } \left( \frac{\text{tonnes}}{\text{m} \cdot \text{s}} \right)$$

$$k_s = d_{90} \text{ the bed roughness height (m)}$$

$$k^r = \text{Manning - Strickler Roughness Coefficient } \left( \frac{\text{m}^{1/3}}{\text{s}} \right)$$

$$\gamma_w = \text{unit weight of water (tonne/m}^3\text{)}$$

$$\gamma_s = \text{unit weight of sediment (tonne/m}^3\text{)}$$



$$g = \text{gravity } \left(\frac{m}{s^2}\right)$$

$$d_m = \text{mean particle diameter (m)}$$

$$h = \text{depth of water (m)}$$

$$J = \text{slope of energy line } \left(\frac{m}{m}\right)$$

The dimensionless form of Equation 4 has been presented as Equation 5. The dimensionless form of the Meyer-Peter and Muller Equation was proposed by (Chien 1954).

$$q^* = 8 \left[ \frac{q^{w'}}{q^w} \left(\frac{k_b}{k_r}\right)^{3/2} \tau^* - 0.047 \right]^{3/2} \quad (5)$$

$$q^* = \text{dimensionless sediment transport rate}$$

$$q^{w'} = \text{flow of water per unit width including sidewall effects } \left(\frac{m^3}{s}\right)$$

$$q^w = \text{flow of water per unit width } \left(\frac{m^3}{s}\right)$$

$$k_b = \text{Manning - Strickler Coefficient for bed region } \left(\frac{m^3}{s}\right)$$

$$k_r = \text{Manning - Strickler Coefficient associated with skin friction } \left(\frac{m^3}{s}\right)$$

$$\tau^* = \text{dimensionless shear stress}$$

The Meyer-Peter Muller equation has undergone several proposed modifications. The original formula proposed by Meyer-Peter and Muller was only deemed applicable to slopes ranging from 0.04% to 2% (Wong & Parker, 2006). As many rivers have smaller sections of steep slopes, an opportunity to further Meyer-Peter and Muller's work presented itself. In 1984, Smart ran a series of flume experiments that ranged up to a 20% slope. From these experiments he provided a modified equation, that better predicted bed

transport in steep slopes. The original Meyer-Peter Muller equation had a correlation coefficient of  $r = 0.6$  when predicting the steep slope rates, whereas the new proposed equation had  $r = 0.93$  (Smart, 1984). The equation can be seen as Equation 6.

$$\phi = 4 \left[ \left( \frac{d_{90}}{d_{30}} \right)^{0.2} S^{0.6} C \theta^{0.5} (\theta - \theta_{cr}) \right] \quad (6)$$

$\phi$  = dimensionless sediment transport

$d_{90}$  = grain diameter for which 90% weight is finer

$d_{30}$  = grain diameter for which 30% weight is finer

$S$  = channel slope  $\left( \frac{m}{m} \right)$

$C$  = flow resistance factor (dimensionless), where  $C = v/(gHS)^{0.5}$

$v$  = velocity  $\left( \frac{m}{s} \right)$

$g$  = gravity  $\left( \frac{m}{s^2} \right)$

$H$  = depth of flow (m)

$\theta$  = dimensionless shear stress =  $HS/((s - 1) * d)$

$s$  = ratio of sediment density to water density (dimensionless)

$\theta_{cr}$  = dimensionless critical shear stress

This modification allowed hydraulic modelers to better predict sediment transport rates within steeper slopes. Hunziker and Jaeggi investigated how graded material eroded versus how a uniform material eroded as the original experiments in the Meyer-Peter Muller had outlined. A fraction wise calculation method was proposed to accommodate for the grain sorting processes (Hunziker & Jaeggi, 2002).

In 2006, Wong and Parker reexamined the Meyer-Peter Muller equation and experiments. It was found that the equation had a form drag coefficient within it to correct the data and account for flow resistance (Wong & Parker, 2006). Wong and Parker removed this coefficient and rederive the formula to hold true to the experimental data. The result is a

simplified equation. The dimensionless form of Wong and Parker's equation can be seen as Equation 7.

$$q^* = 3.97 \left[ \frac{q^{w'}}{q^w} \left( \frac{k_b}{k_r} \right)^{3/2} \tau^* - 0.0495 \right]^{3/2} \quad (7)$$

$q^*$  = dimensionless sediment transport rate

$q^{w'}$  = flow of water per unit width including sidewall effects  $\left( \frac{m^3}{s} \right)$

$q^w$  = flow of water per unit width  $\left( \frac{m^3}{s} \right)$

$k_b$  = Manning – Strickler Coefecient for bed region  $\left( \frac{m^3}{s} \right)$

$k_r$  = Manning – Strickler Coefecient associated with skin friction  $\left( \frac{m^3}{s} \right)$

$\tau^*$  = dimensionless shear stress

Calculating the sediment transport rate is import, but in order to model sediment transport across the profile of an open channel, a continuity equation must be utilized to balance the sediment entering and exiting each cross section of the open channel. The Exner continuity equation in 1-dimensional format can be seen in Equation 8. The original paper was published in German in 1920, and introduced to English language in 1955 by Leliavsky (Leliavsky, 1955).

$$(1 - \lambda_p) B \frac{\partial \eta}{\partial t} = - \frac{\partial Q_s}{\partial x} \quad (8)$$

$B$  = channel width (m)

$\eta$  = channel elevation (m)

$\lambda_p$  = active layer porosity (unitless)

$t$  = time (s)

$x$  = distance (m)

$$Q_s = \text{transported sediment load (m}^3\text{/s)}$$

The Exner equation takes the sediment transport rate calculated by Equation 4 and converts it into a change in channel elevation. This allows for sediment transport modelers to calculate the erosion through a profile of an open channel. Many programs utilize both Equation 4 and Equation 8 to aid in the calculation of erosion within an open channel. One such program is HEC-RAS.

As the capabilities of HEC-RAS continued to grow, the idea of incorporating sediment transport into the software was developed by Thomas and the package called HEC-6, which was released to the public in 1990 (Maeder, 2015). The program applied the sediment transport calculations to open channels under steady, gradually varied flow. The program included several other developments to sediment transport modelling, including temporal deposition and erosion. The amount of erosion is also limited by the sorting and armouring methods built into the program. Modifications and improvements were made until the current release, HEC-RAS Version 5, was released in 2016 (Brunner & CEIWR-HEC, 2016). The current release includes the Wong and Parker correction; however, it does not include the Smart modification to widen the applicability to steep slopes. Without the modification, the current version of HEC-RAS will underpredict the erosion when modeling a steep sloped channel.

## 1.5 Oroville Dam Incident of 2017

Oroville Dam is the largest earthen embankment dam in the United States, impounding the Feather River near Oroville, California. The dam is approximately 230 m tall and has a maximum storage of approximately  $4.317 \times 10^9 \text{ m}^3$ . Outlet features include a controlled concrete spillway with a maximum of  $4247 \text{ m}^3\text{/s}$  discharge, a bypass valve with a maximum of  $150 \text{ m}^3\text{/s}$  discharge, a power generation station with a maximum of  $480 \text{ m}^3\text{/s}$ , and an emergency spillway with a crest that is 6.4 m below the crest of the

main dam. The dam was built in 1968 and the power plant has a total capacity of 762 Megawatts (State of California Department of Water Resources, 2005).

On February 7, 2017, engineers noticed unusual flow patterns along the concrete spillway during a spill of 1543 m<sup>3</sup>/s. The flow was stopped, and a large area of erosion was found halfway down the concrete spillway (Oroville Spillway Incident Timeline). On the 11<sup>th</sup> of February, the reservoir elevation reached the emergency spillway weir, and water began to flow over the emergency spillway. Erosion occurred at a much faster rate than anticipated and a mandatory evacuation of the downstream area was ordered. On the 12<sup>th</sup> of February the concrete spillway gates were opened further to increase outflow to 2831 m<sup>3</sup>/s in order to reduce the reservoir elevation and prevent further erosion of the emergency spillway (California Data Exchange Center, 2017). As the flow was increased in the concrete spillway, the erosion along the concrete spillway grew further, causing the eroded material to deposit and block the power generation outlet, resulting in the closure of the power generation outlet. The emergency spillway underwent immediate repairs as the reservoir elevation continued to drop. The evacuation was downgraded to a warning, and the incident luckily did not lead to a collapse of the structure (California Data Exchange Center, 2017).

The Oroville Dam spillway incident of 2017 was investigated, and the final report was published (France, et al., 2018). The large area of erosion that was found on the concrete spillway was caused by the removal of a concrete slab (Oroville Dam Spillway Incident Independent Forensic Team, 2017). The slab was likely upheaved by the water uplift pressure underneath the slab. When the upstream edge of the slab had angled into the high velocity flow, the pressure underneath would have surged and caused failure of the slab. When the slab was removed, erodible material was exposed, and the hole propagated as the flow increased over top (Oroville Dam Spillway Incident Independent Forensic Team, 2017). There are several factors hypothesized as to why the slab failed. It is possible that there were small cavities below the slab, which could have allowed the slab to tilt. Another possibility is that the slab anchors failed from potential erosion underneath the slab or the anchors failed from rusting (Oroville Dam Spillway Incident Independent Forensic Team, 2017). Failure of the anchor would have allowed the

upheaval form to become greater than the anchoring force, resulting in the upheaval of the slab (Oroville Dam Spillway Incident Independent Forensic Team, 2017). Although these two potential causes of failures are only hypotheses, it is important to know that both small cavities and rusting of anchors could lead to potential failure of a concrete spillway. These two consequences could become apparent if water became present underneath the slabs; rusting could occur from the presence of water and small cavities could form if water flowed underneath the slab. The Oroville Dam incident shows the importance of not having water reach the underside of a concrete spillway.

The investigation has also identified some of the physical factors which lead to significant damage along the emergency spillway. Although erosion was expected with the use of the emergency spillway, the level of erosion that occurred was far larger than anticipated. This can be attributed to several factors. The geometry of the channel lead to flows being focused into smaller regions instead of spreading out across the hill, leading to higher shear stress values (Oroville Dam Spillway Incident Independent Forensic Team, 2017). There was also a considerable depth of erodible material along the emergency spillway, which allowed for a rapid headcut to the crest of the emergency spillway (Oroville Dam Spillway Incident Independent Forensic Team, 2017). The Oroville Dam incident shows the importance of channel geometry within an emergency spillway and how it can potentially lead to a higher level of erosion.

The lessons learned from the Oroville Dam incident have guided this research. Channel geometry, concrete slab anchoring integrity, and location of eroded material all played a serious role in the Oroville Dam incident, and therefore will be given a special focus in this research.

## 1.6 Cheakamus Dam Case Study

Cheakamus Dam is a BC Hydro power generation and water management dam. It impounds Daisy Lake reservoir, which receives inflow from Cheakamus River,

contributing approximately 590 GWh/year to BC Hydro (BC Hydro, 2005). The site includes four flow control systems: gated spillway with concrete chute, low level outlet gate, power generation and saddle dams that pass water when reservoir levels are dangerously high.

The system dynamics simulation model that King et al (2017) developed has been applied to Cheakamus Dam. Cheakamus Dam was chosen because it is an extreme-consequence dam, meaning that loss of life is possible in the case of a dam safety accident. King's system dynamics simulation model does not have a representation of the physical state of the emergency spillway. This thesis will develop a model that can be used to fill that void. This will be discussed further in Chapter 3.

## 1.7 Thesis Organization

This thesis report will be broken down into several chapters. Chapter 1, the current chapter, has introduced the problem, discussed the relevant literature, and stated the objectives of this research. Chapter 2 will explain the methodology used to achieve the objectives and solve the problem stated in the introduction. Chapter 3 will demonstrate how the methodology is applied to the case study of Cheakamus Dam. Chapter 4 will conclude the research and discuss future work.

## Chapter 2

### 2 Methodology for 1-Dimensional Modelling of an Emergency Spillway

The following section will outline the methodology required to fulfill the research objective set out in Chapter 1.

#### 2.1 Introduction

This section will reiterate the objective and demonstrate how the methodology will achieve the objective. The software used and the overall research process will be outlined as well, allowing the reader to follow the hierarchy of the methodology application and how each step leads to achieving the objective.

##### 2.1.1 Research Objective

The objective of this research is to combine existing models in a way that describes the flow passing through the emergency spillway and damage that could occur in the form of erosion. The model must satisfy the following criteria:

1. The model must be computationally simple.
2. The model must be able to be recreated for other dam systems.
3. The model must be able to test various inflow conditions.

After evaluating available software, a combination of software packages was selected to build a model that would satisfy the research objective. To keep the model both computationally simple and repeatable for other dam systems, a 1-dimensional model was selected. Although 1-dimensional models do not provide as accurate results as 2-dimensional models, they are computationally simpler. The 1-dimensional model utilizes the principles of steady, gradually varied flow to describe the surface water elevation. The 1-dimensional model uses the principles of sediment transport to model the erosion and damage occurring in the emergency spillway. In order to test the various inflow and outflow conditions that change over time, a separate reservoir routing model is created to allow for any inflow scenario to be modelled.



## 2.1.2 Software Utilized

This section will briefly explain the software packages used and provide justification for their selection.

### 2.1.2.1 HEC-RAS

The software used largely governs the procedure and the methodology has been based off the available literature provided with the software packages. The hydraulic and sediment transport analyses were performed in HEC-RAS version 5 (Brunner & CEIWR-HEC, 2016). HEC-RAS is a free software package created by the U.S. Army Corps to model 1-dimensional open channel flow (Brunner & CEIWR-HEC, 2016). The software was selected due to its simplicity and its ability to model both open channel hydraulics and sediment transport.

### 2.1.2.2 ArcGIS and HEC-GeoRAS

For the spatial data preprocessing, ArcGIS and the HEC-GeoRAS extension were used (Ackerman, 2009). ArcGIS is an Esri software that requires a significant financial cost, however other preprocessing options may be available to a modeler. This software package was selected to perform the preprocessing of spatial data as it has an extension, HEC-GeoRAS, that links to the HEC-RAS software package. Mandatory features for HEC-RAS can be built within ArcGIS using the HEC-GeoRAS extension (Ackerman, 2009). ArcGIS was selected because of the connection to HEC-RAS and the efficiency that would result in building the model.

### 2.1.2.3 Vensim

Vensim system dynamics simulation package was used for the development of the reservoir routing model (Ventana Systems, 2017). Vensim allows the user to model using graphical objects of stocks, flows and relationships (Ventana Systems, 2017). Stocks describe the state variables and go up and down; very similar to the water in a reservoir. Flows, which represent an amount of something moving over time and changing stocks,

allow for a perfect representation of reservoir inflow and outflow features such as emergency spillways. Vensim allows the user to build in the hydraulic relationships and simulate various inflow events and operating conditions of a hydropower system with ease.

### 2.1.3 Research Process

A methodology must be developed to achieve the objective that were set out in Chapter 1. A large portion of the methodology derives from the literature provided by HEC-RAS and HEC-GeoRAS (Ackerman, 2009; Brunner, 2016). By following the methodology from the HEC-RAS User Manual, the process of sediment transport analyses is applied to an emergency spillway. The overall process of the research methodology can be viewed in the process diagram in Figure 3.

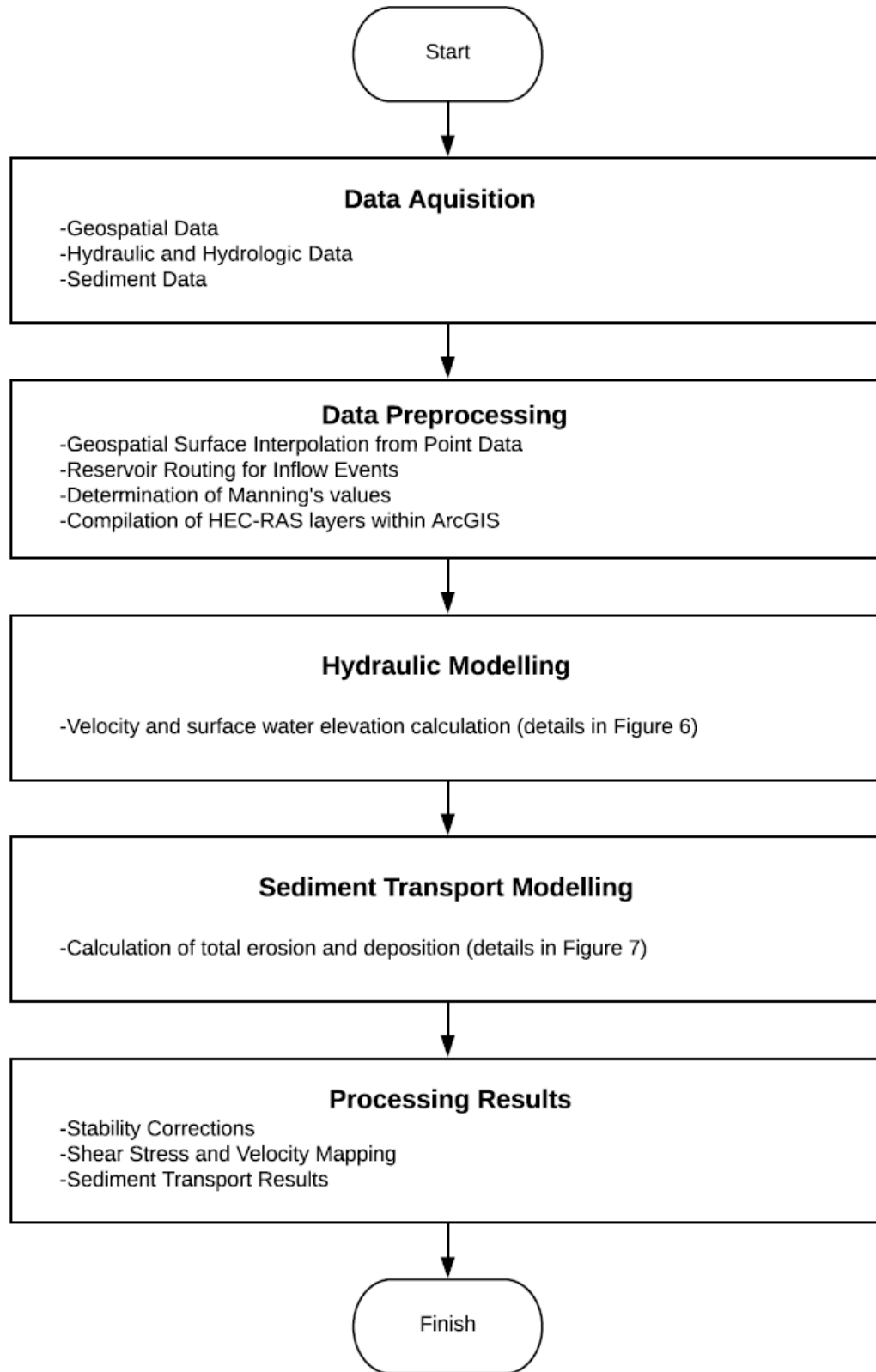


**Figure 3: Research Process Flow Chart**

The methodology is broken down into 5 main steps. The first being Data Acquisition, where the user collects the highest quality data available. Once the raw data are collected, the second step of Data Preprocessing commences. This step is where the raw data is prepared in a way that is required for use with HEC-RAS. The third step is the 1-dimensional hydraulic modelling. This is when HEC-RAS calculates water surface elevations and velocities within the emergency spillway. The fourth step is the sediment transport modelling. HEC-RAS approximates the eroded and deposited material with equations and methods that will be discussed further. The fifth and final step is processing of the results. This section of methodology is where the objective is achieved, and the hydraulic and sediment transport results are viewed.

The following sections of the methodology will describe in detail each of the five steps shown in Figure 3.

## 2.2 Data Acquisition

The first step of the process as seen in Figure 3 is data acquisition. Before a sediment transport analysis can be performed, geospatial, hydraulic and sediment data must be collected and prepared for the model. The accuracy and quality of each data type largely affects the overall accuracy and quality of the results.

### 2.2.1 Required Data for Hydraulic and Sediment Modelling

The mandatory data required for this methodology are listed below:

1. Geospatial Data in the form of elevation point data of the study area
2. Hydraulic and Hydrologic Data for the reservoir:
  - a. Reservoir Storage-Elevation relationship
  - b. Reservoir Outflow-Elevation relationships for any outflow features (such as emergency spillway, controlled gated spillway, power generation, and low-level outlet)
  - c. Inflow Probable Maximum Flood (PMF) or any inflow events that are selected

3. Sediment Data in the form of Bed Gradation and Manning's roughness coefficients

After the data have been acquired, they must then be preprocessed as shown in Figure 3.

## 2.3 Data Preprocessing

The second step in the methodology is data preprocessing, as seen in Figure 3. The main purpose of this step is to prepare the raw data in a format that is compatible with the HEC-RAS software. ArcGIS is utilized as well as the HEC-GeoRAS extension. Hydraulic data is used to create an inflow hydrograph with the use of Vensim. The following sections will describe in detail each step of the data preprocessing.

### 2.3.1 Geospatial Elevation Data Interpolation

An emergency spillway can be described as an open channel. To best represent the physical geometry of an open channel, the channel must be surveyed if the dimensions are not already known. Upon surveying the channel, elevation data of the spillway can be used with a data preprocessing software. Elevation data is typically stored in point data format, which is a series of points representing different elevations. This format must be converted into a digital terrain model. GIS software packages allow the user to quickly convert point data into a triangular irregular network (TIN). By creating a TIN, the elevation point data has now been converted into a 3-dimensional surface. This 3-dimensional surface can now be deconstructed into equally spaced cross sections. The cross sections are utilized by the hydraulic modelling software to represent the emergency spillway geometry (Ackerman, 2009).

Before the triangular irregular network surface can be created, the regions without data must be interpolated if the data in any regions being modelled is not sufficient. It is recommended that the Kriging method be utilized, as it is best suited for data sets that have spatially correlated distance bias (Esri, 2016). In an emergency spillway, there may be some areas that have a dense region of point data and other areas that do not, suggesting less of a drastic change in topography within the less dense area. Kriging takes this into account, and is the preferred method for interpolating the TIN surface.

### 2.3.2 Preparing the Geospatial Data with HEC-GeoRAS

By using the HEC-GeoRAS extension, the user can convert the triangular irregular network into cross sections that will be utilized by HEC-RAS. During this process, the user adds features such as river reach, bank stations, and cross sections (Ackerman, 2009). This is where the user can define the study area. Additional features such as blocked obstructions and Manning's values can be added as well. When the process is complete, the cross sections are ready to be imported into HEC-RAS.

### 2.3.3 Reservoir Routing with Vensim

In order to model sediment transport within an emergency spillway, the hydraulic data must be determined. By determining the hydraulic conditions within the dam system, an inflow hydrograph can be created for the water spilling through the emergency spillway.

A dam system can be simplified hydraulically into the continuity equation seen in Equation 9. Inflow is described as the water flowing into the reservoir. Outflow is the water flowing out of the reservoir. Change in storage is the volume change of the water behind the dam.

$$I(t) - O(t) = \frac{dS(t)}{dt} \quad (9)$$

$$I(t) = \text{the inflow of water into the reservoir} \left(\frac{m^3}{s}\right)$$

$$O(t) = \text{the outflow of water from the reservoir} \left(\frac{m^3}{s}\right)$$

$$\frac{dS(t)}{dt} = \text{the change in storage divided by the change in time} \left(\frac{m^3}{s}\right)$$

By routing the flow hydrograph through the reservoir, the known hydraulic parameters can be used to calculate the discharge hydrograph through the emergency spillway for a given inflow event. Selection of an inflow event is case dependent, however, emergency spillways are not designed to frequently pass flow, and so the probable maximum flood (PMF) is modelled as this inflow hydrograph is typically known for dams. Outflow can

be subdivided into various sections depending on the dam. For example, a typical dam may have outflows in the form of power generation flow, controlled spillway, emergency spillway, overtopping flow, and a low-level outlet flow. Each outflow feature must have a corresponding elevation-discharge relationship that is known. This allows for the combination of each outflow to find the total outflow for the current reservoir elevation. The reservoir elevation-storage relationship must be known as well, and the user must decide upon the initial condition of reservoir level. When these parameters and features have been determined, the user may proceed with the reservoir routing technique to calculate the outflow hydrograph for the emergency spillway. This method is best done with aid of software, and it is recommended that the software Vensim be utilized for its overall stock and flow structure and ease of use, however this method may be applied within spreadsheets.

In Figure 4, an example routing of the inflow through the reservoir of a hydropower dam is modelled within Vensim. The large arrows represent inflows and outflows ( $\text{m}^3/\text{s}$ ), the blue arrows represent direct relationships, specifically the reservoir elevation corresponding to each specific discharge variable. Vensim will calculate the total volume added to the reservoir over a specified time step and apply the Runge-Kutta explicit numerical method to perform the integration of the continuity equation (Ventana Systems, 2017).

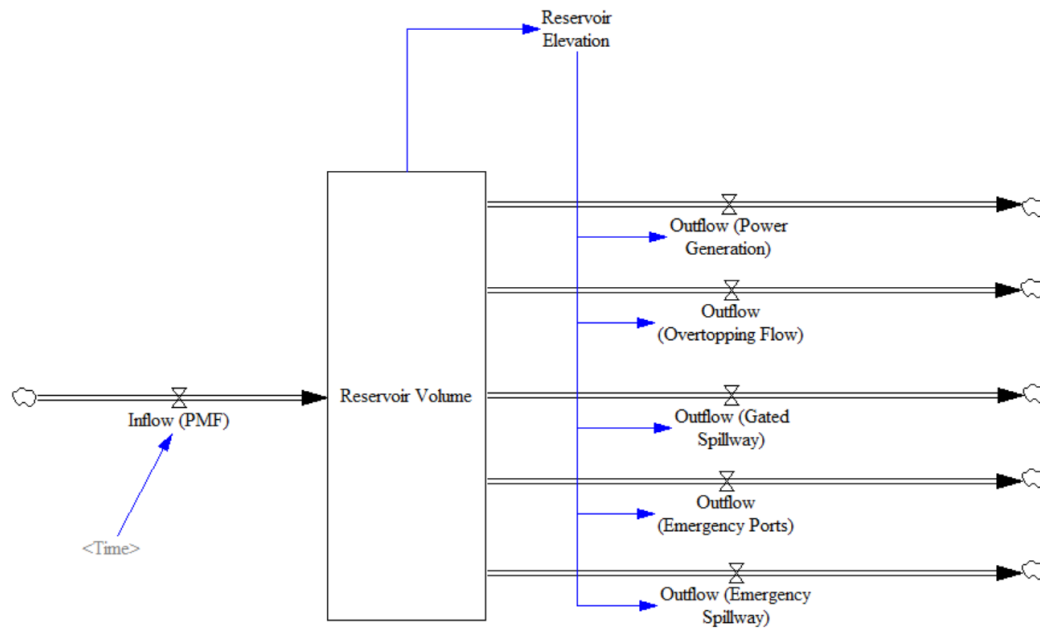


**Figure 4: Reservoir Routing Model**

The outflow hydrograph for the emergency spillway must now be converted from an unsteady flow hydrograph to a quasi-unsteady flow hydrograph. This must be done for model stability purposes, as having a dynamic flow event coupled with a dynamic sediment transport process leads to a very unstable model (Brunner, 2016). The solution to this is to create a quasi-unsteady flow hydrograph. A quasi-unsteady flow hydrograph is a regular hydrograph partitioned into steady flows for a specified amount of time (Brunner, 2016). A comparison of a quasi-unsteady hydrograph and an unsteady hydrograph can be seen in Figure 5. This allows for steady flow simulation but still representing the original hydrograph shape.



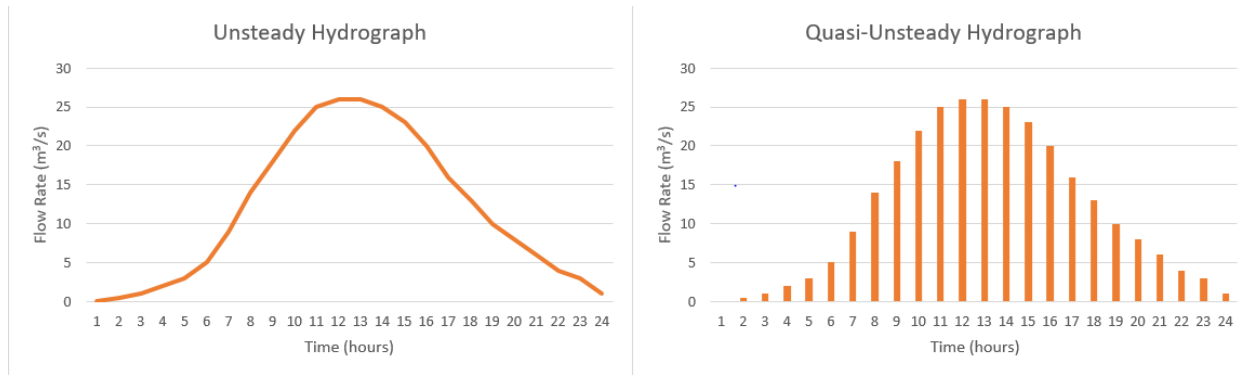


**Figure 5: Comparison of Unsteady and Quasi-Unsteady Hydrographs**

### 2.3.4 Sediment Data and Manning's Values

In order to model sediment transport, several sediment parameters must be known or estimated. The overall accuracy of the model can hinge on the accuracy of the sediment data. Typically, sediment transport models are calibrated using historical changes, however emergency spillways are rarely used, and it is very uncommon for this calibration data to exist. The user is then at the mercy of the available data. The specific gravity and shape factor must either be known or assumed to utilize a sediment transport method (Brunner, 2016). The bed gradation of the sediment within the emergency spillway must be known as well. If it is not, users could estimate based on known local sediment gradations and adjust accordingly. The bed gradation is the percent finer vs. grain size relationship and is calculated in a laboratory using a sieve analysis. If bedrock is present, or there is a maximum depth at which erosion does not occur, then the user must calculate the maximum erodible depth for each geometry cross section (Brunner & CEIWR-HEC, 2016).

Manning's roughness coefficient must be either calibrated or estimated. Manning's values range depending on the vegetation or roughness of the sediment. It is very common practice to calibrate a hydraulic model for the Manning's values, however, this cannot be done in an emergency spillway that does not have historical data. The user must make reasonable assumptions and test the model sensitivity to Manning's values.

Aerial photographs can aid in the location and size of vegetation regions. This spatial variation of different Manning's values can be applied with the HEC-GeoRAS extension as a layer, and then applied similarly to the cross sections. Standard Manning's values are given based on descriptions of vegetation, sediment, and topography (Brunner & CEIWR-HEC, 2016).

Now that the raw data have been converted into a format that is compatible with HEC-RAS, the Data Processing step is complete, and the user can progress to the next step, Hydraulic Modelling as seen in Figure 3.

## 2.4 Hydraulic Modelling of Open Channel Flow

This section will outline the third step in the research methodology as seen in Figure 3. The following sections will outline the purpose of the model, an overview of the computational process, and the issues with accuracy.

### 2.4.1 Introduction

In HEC-RAS, the hydraulic model and the sediment transport model are run in unison, however it is important to view them as two separate processes that are coupled. The hydraulic model aims to calculate the surface water elevation and velocity for each given cross section. These values are a crucial input into the sediment transport model.

### 2.4.2 Overview of Computational Process of Hydraulic Model

For one-dimensional steady flow, the overall water surface elevation computation process can be seen in Figure 6. This flow diagram aims to explain the computational process that HEC-RAS uses to arrive at a surface water elevation for each cross section during each steady flow rate. This section will explain in detail the process.

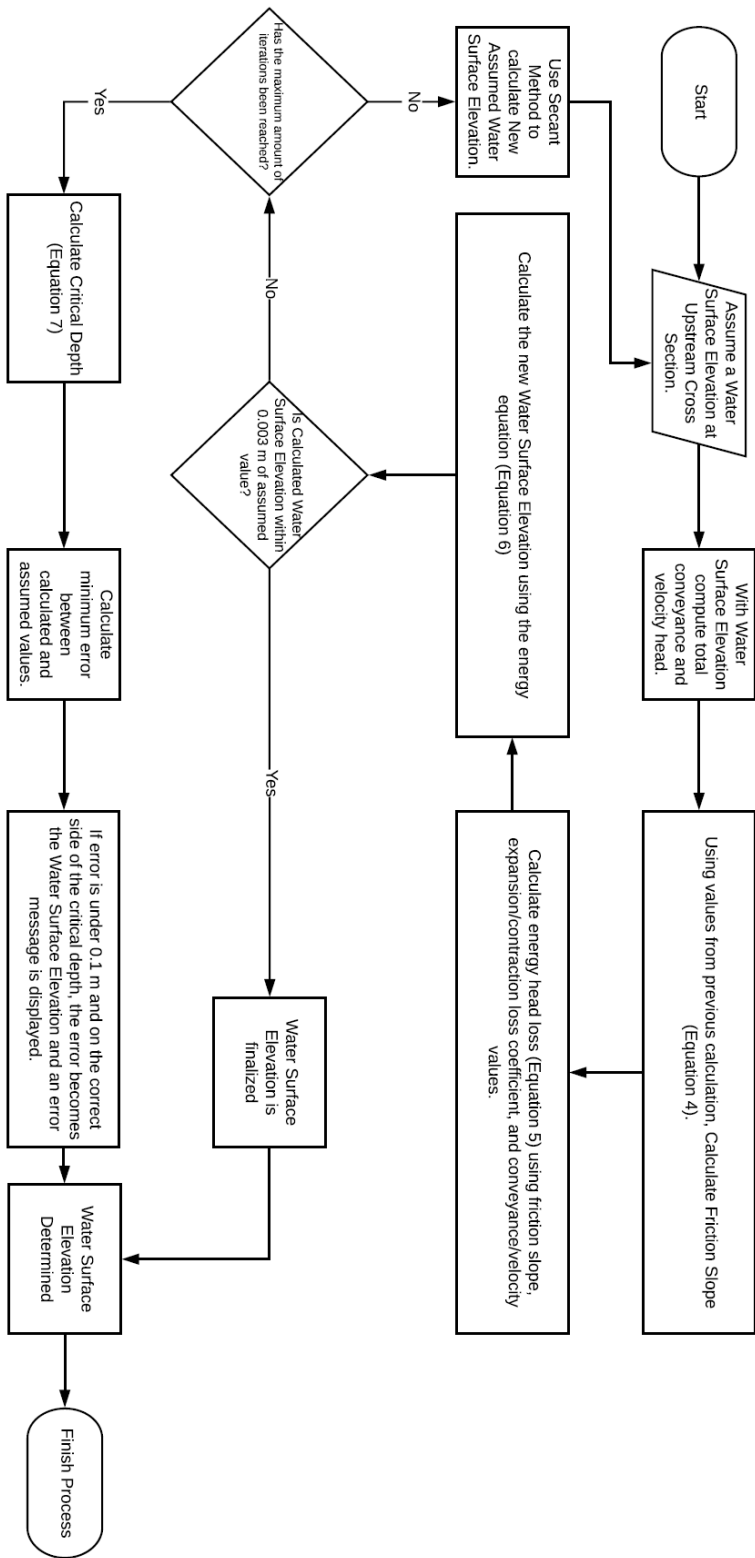


Figure 6: Flow Chart of HEC-RAS Quasi-Unsteady Flow Calculation

The process begins by initially assuming a water surface elevation for the first cross section (Brunner, 2016). The cross section is split into different regions based on where the Manning's values change. The flow is inputted for each region in the cross section using Manning's equation, as seen in Equation 1. The flows are then summed and then used to calculate the friction slope (Brunner, 2016).

When the friction slope has been calculated, the energy head loss can be found by using the energy head loss equation as seen in Equation 2 (Te Chow, 1959).

The final step is to solve the energy equation for the downstream water surface elevation. The energy equation can be seen in Equation 3.

If the maximum number of iterations is reached and a water surface has not yet been determined, then the program proceeds to calculate the critical depth. Critical depth occurs when the energy head is at its minimum value (Brunner, 2016). This is calculated by utilizing an iterative method to solve for the total energy head using Equation 10.

$$H = WS + \frac{av^2}{2g} \quad (10)$$

$H = \text{total energy head (m)}$

$WS = \text{water surface elevation (m)}$

$\frac{av^2}{2g} = \text{velocity head (m)}$

If the water surface is below the critical depth, then the regime is determined to be supercritical. Transitioning from subcritical to supercritical would mean that the flow is not gradually varied, and therefore the energy equation is not applicable and the momentum equation would have to be applied. Typically, HEC-RAS applies the

momentum equation when the user selects a mixed flow regime, which encompasses a transition from subcritical or supercritical flow. However HEC-RAS does not allow for a mixed flow regime simulation to occur within sediment transport modelling, so solutions that have supercritical values are not valid solutions. If the solution is supercritical, the model will display an error message and set the water surface to the critical depth (Brunner & CEIWR-HEC, 2016).

Now that the surface water elevations and velocities have been calculated for each steady flow rate, the third step of the research methodology is completed, and the sediment transport modelling may begin as seen in Figure 3.

### 2.4.3 Hydraulic Accuracy Issues

There are several pitfalls within the HEC-RAS model. Assumptions, default settings and the lack of customization all lead to inaccuracy when modelling an emergency spillway. These features simplify the program and lead to reduced computational efforts; however, they sacrifice the ability to accurately apply HEC-RAS to various conditions.

When deriving the energy equation HEC-RAS makes an assumption of the vertical pressure head. The true formula can be seen in Equation 11. However the pressure head is just assumed to be equal to the depth of the water perpendicular to the channel bottom (Brunner, 2016). Slopes less than 10% are barely affected by this assumption, with a 10% slope yielding 99.5% of the true value. However steeper slopes, such as 20% yield values of 98.1% of the true value (Brunner, 2016). Although this is a minimal error, these errors can compound when applied to a dynamic process such as sediment transport modelling.

$$H_p = d \cos \theta \quad (11)$$

$H_p$  = vertical pressure head (m)

$d$  = perpendicular water depth (m)

$\theta$  = channel bottom slope angle (degrees)

In the computational process of calculating the water surface profile, a maximum of 20 iterations can be performed before the water surface elevation is set to the minimum error value (Brunner, 2016). Although 20 iterations may be sufficient when using the secant method for most conditions, not allowing the user to specify the maximum number of iterations leads to inaccurate water surface elevations when the maximum iteration value is reached.

Although most sediment transport analyses are performed where the flow is gradually varied, allowing the option to model supercritical flow regimes would be a great benefit. When the program sets the water surface profile to the critical depth after reaching the maximum number of iterations, it is likely because the solution is below the critical depth. Seeing critical depth values within the model suggests that the application of the energy equation is not valid in the critical regions.

## 2.5 Sediment Transport Modelling

This section will introduce the sediment transport model within HEC-RAS and explain the computational process. This is the fourth step of the research methodology as seen in Figure 3. Some of the shortcomings of the process will be discussed throughout.

### 2.5.1 Introduction

The sediment transport model aims to compute the erosion or deposition that occurs at each cross section. It is a highly dynamic process that runs alongside the hydraulic model; using the surface water elevation and velocities calculated in step 3 of Figure 3 as inputs.

## 2.5.2 Computational Process of Sediment Transport Model

This section will explain the computational process performed in a sediment transport analyses in detail. The flow diagram seen in Figure 7 shows the process for 1-dimensional sediment transport modelling using HEC-RAS. The end goal of the sediment transport calculation is to determine the level of erosion or deposition at each cross section.

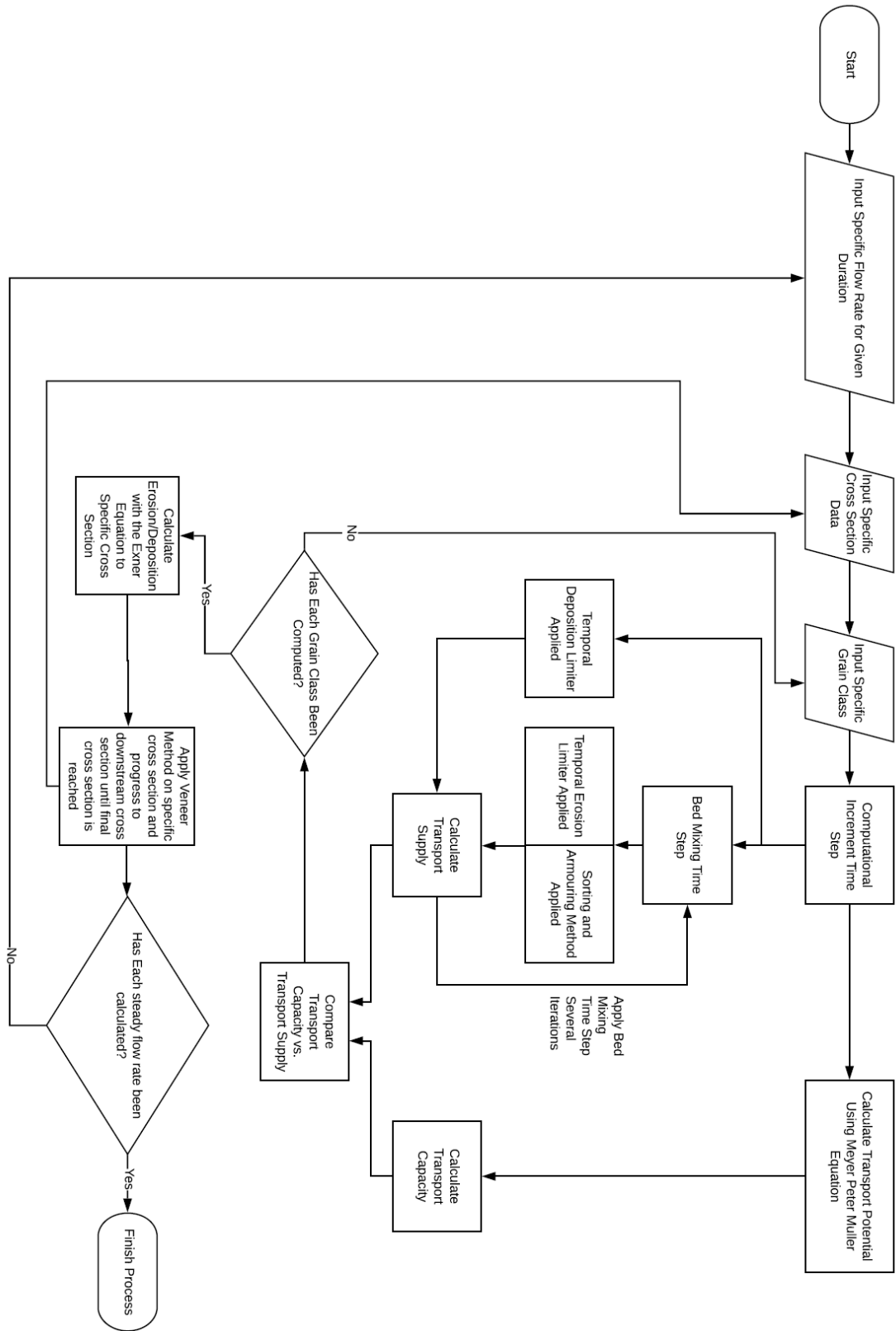


Figure 7: Flow Chart of HEC-RAS Sediment Transport Calculation



Understanding the breakdown of time steps in a sediment transport model is important to arriving at a stable solution. Quasi-Unsteady flow allows for a simplified approach and maintains stability. Each time step flow that occurs has a steady flow rate, and when the time step changes, so does the flow rate. Stage, sediment, and temperature are constant during each time step. Within the flow duration are computational increments. In each computational increment, the bed geometry changes within the bed mixing time step (Brunner, 2016).

Within each computational increment, the sediment transport capacity and the sediment transport supply are calculated, compared, and then applied to the Exner equation to determine the total amount eroded or deposited in each cross section (Brunner, 2016). Each process is explained in detail below, and the flow chart in Figure 7 shows how the computational process is performed.

### 2.5.2.1 Sediment Transport Potential

The first value calculated is the sediment potential, which is simply the mass of a certain grain class that can be transported from the given cross section and current hydraulic conditions. There are many sediment transport functions to select, however the most applicable to gravel beds is the Meyer-Peter Muller function (Brunner, 2016).

The Meyer-Peter Muller equation was developed in laboratory flume experiments in 1948. It is an excess shear relationship that calculates bed load transport (Meyer-Peter & Muller, 1948). Various modifications have been made to the equation. The modification in HEC-RAS is the Wong and Parker adjustment (Brunner, 2016). Unfortunately, HEC-RAS has yet to include the modification for steep slopes as Smart proposed (Smart, 1984). Until that is available, the user must note that the values of bed load transport may be lower than what actually would occur when modelling steeper slopes typically found in emergency spillways. It must also be noted that Meyer-Peter and Muller equation is only applicable for steady and gradually varied flows (Meyer-Peter & Muller, 1948). The Meyer-Peter Muller equation can be seen in Equation 4 and sample calculations from the HEC-RAS user manual can be found in Appendix 1. The sediment transport potential is calculated with Equation 4.

### 2.5.2.2 Sediment Transport Capacity

After the transport potential has been calculated for a grain class, the transport capacity is then calculated by multiplying the transport potential by the mass ratio of the computed grain class to the entire bed gradation, as seen in Equation 12 (Brunner, 2016).

$$T_c = \sum_{j=1}^n B_j T_j \quad (12)$$

$T_c$  = total transport capacity (tonnes/day)

$n$  = number of grain classes

$B_j$  = percentage of active layer composed of grain class (percentage)

$T_j$  = transport potential computed for the material in grain class (tonnes/day)

Equation 12 simply allows for the program to subdivide each grain class.

### 2.5.2.3 Temporal Deposition

HEC-RAS limits the potential of deposition by applying a deposition efficiency coefficient to each grain class. The coefficient is calculated as a ratio of the fall velocity multiplied by the time step, divided by the effective depth as seen in Equation 13 (Brunner, 2016).

$$C_d = \frac{V_s(i)\Delta t}{D_e(i)} \quad (13)$$

$C_d$  = deposition efficiency coefficient (m/m)

$V_s(i)$  = Toffaleti fall velocity for grain class (m/s)

$\Delta t$  = time step (s)

$D_e(i)$  = effective depth of water (m)

The fall velocity can be determined using the Toffaleti method (Toffaleti, 1968). The Toffaleti method looks up a fall velocity from an empirical set of tables which can be found in Appendix 2. Each grain size and temperature range have a specific fall velocity associated with them. The shape factor is set to 0.9 and specific gravity is set to 2.65, however this empirical relationship is easily used to represent different velocities for different grain sizes (Brunner, 2016). The deposition efficiency coefficient is a ratio that is applied to the sediment depositing within the cross section.

#### 2.5.2.4 Temporal Erosion

Physical processes can limit the amount of erosion in a river bed. These processes are difficult to model, so empirical relationships have been developed and can be applied to various conditions. An entrainment coefficient is calculated using Equation 14 and ranges from 0.368 to 1.0 (Brunner, 2016). The entrainment coefficient is then multiplied by the sediment transport capacity calculated in Equation 12 to calculate the total erosion.

$$C_e = 1.368 - e^{-\left(\frac{L}{30D}\right)} \quad (14)$$

$C_e$  = entrainment coefficient (m/m)

$D$  = flow depth (m)

$L$  = length of flow depth (m)

#### 2.5.2.5 Sorting and Armoring

Erosion is also limited by the ratio of sediment readily available to be eroded, as river beds typically have a coarse armored layer on the surface (Brunner, 2016). Various algorithms are available, however the default method is the Thomas Mixing Method (Thomas, 1982).

In the Thomas Mixing Method, the active layer is split into two layers. The first being the cover layer, is a smaller coarse layer which limits erosion. Underneath is the second layer, which encompasses the rest of the soil gradation (Brunner, 2016). The active layer can change each time step and is determined by calculating the equilibrium depth as seen in Figure 8. The Thomas Method calculates equilibrium depth by combining Manning's equation, Strickler's roughness equation, and Einstein's transport intensity equation (Brunner, 2016). Equation 13 shows the formula for equilibrium depth. Each grain class is computed and the largest depth is set to the active layer. The algorithm of the Thomas Method can be seen in Appendix 3.

$$D_{eq} = \left( \frac{q}{10.21d_i^{1/3}} \right)^{6/7} \quad (15)$$

$D_{eq}$  = equilibrium depth for particle size (m)

$q$  = water discharge ( $\frac{m^3}{m}$ )

$d_i$  = particle diameter (m)

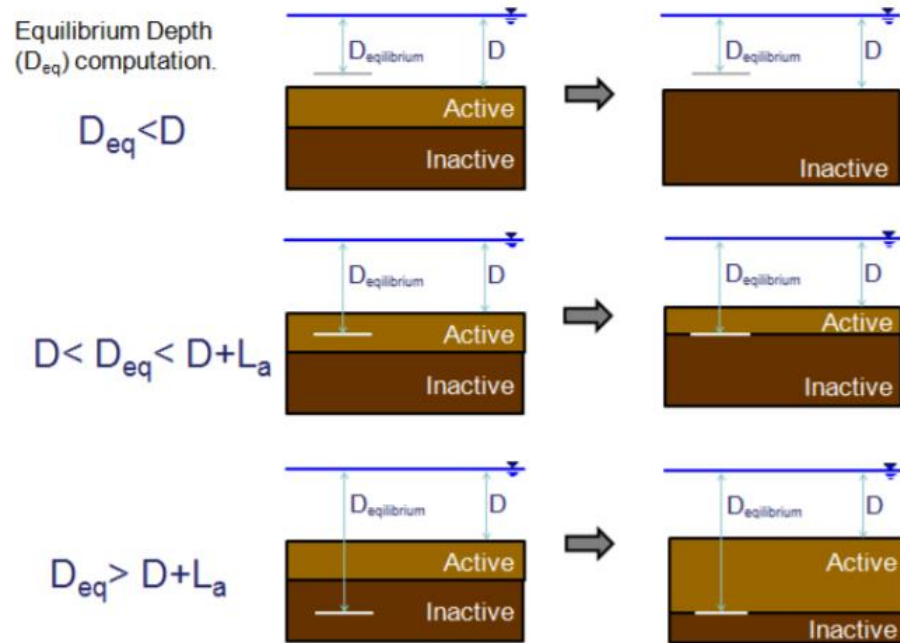


**Figure 8: Equilibrium Depth Scenarios (Brunner, 2016)**

### 2.5.2.6 Sediment Continuity

After sediment capacity and supply have been computed, they are compared. If capacity exceeds supply then erosion occurs, whereas if supply exceeds capacity then deposition occurs (Brunner, 2016). Both values of either erosion or deposition have their respective limiter equations applied to them. The Exner equation, which is a sediment continuity equation, is shown in Equation 8. Once the inflow and outflow of sediment have been calculated, as discussed in the previous steps, Equation 8 is applied and the change in channel elevation is computed.

### 2.5.2.7 Bed Change

After the amount of soil to be eroded or deposited has been calculated, the cross section must be adjusted to the change in channel elevation calculated with Equation 8. The

Veneer method is applied, which simply erodes or deposits the wetted base to an equal amount (Brunner, 2016). The erosion or deposition is also spread in the formation of a triangle, as shown in Figure 9. As a triangular bump will occur at each cross section, the changes in between cross sections could superimpose to create sawtooth formations.

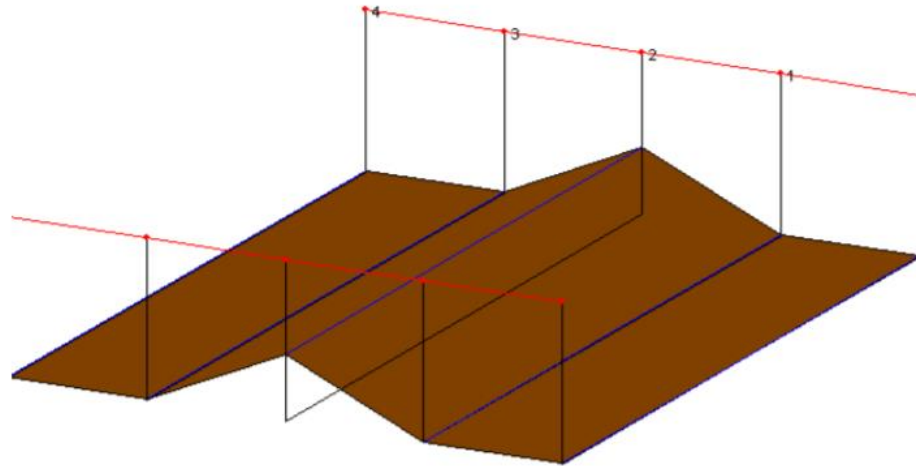


**Figure 9: Distribution of Eroded or Deposited Material (Brunner, 2016)**

The process is repeated for each steady flow. This process is very dynamic and difficult to perform over shorter periods of time. The sediment transport process is normally used to model years of flow data, however with a well-built model, the process can successfully be applied to shorter inflow events.

Now that the amount of erosion or deposition has been estimated for each cross section for the entire inflow event, the fourth step as outlined in Figure 3 has concluded. The final step is outlined in the next section.

## 2.6 Processing Hydraulic and Sediment Transport Results

The final step of the research methodology involves processing the results, as can be seen in Figure 3. The following section will explain some potential ways to view the results obtained through the process. Making sure that the model is stable before processing the results is a key requirement. Both hydraulic results and sediment transport results will be processed.

### 2.6.1 Stability

There are several factors which could cause model instability or create oscillations within the sediment transport model. If this is occurring, users have several options to create a more stable solutions. Users can modify the weighting factors for hydraulic values applied to the adjacent upstream and downstream cross sections. In lower flow events, giving a 25% weight to the upstream and downstream cross sections will reduce the sawtooth formations observed in the results, whereas in high flow events the upstream and downstream cross sections may be given zero weighting (Brunner & CEIWR-HEC, 2016). Users may also reduce the computational increment to a shorter period. This would increase the overall computation time of the simulation as more computation increments would have to be performed, however it can greatly aid in smoothing out any model instabilities (Brunner & CEIWR-HEC, 2016).

### 2.6.2 Hydraulic Open Channel Flow Results

After the model has been deemed robust and stable, the results can be viewed within HEC-RAS. The program will list any errors that have occurred in the model, such as setting the water surface to the critical depth, which occurs whenever the program cannot calculate a subcritical water surface. Hydraulic results such as velocity, depth, and shear stress can be exported back into ArcGIS to create maps (Ackerman, 2009). Shear stress is calculated using the shear stress equation, Equation 16, as presented in many texts (Wolman et al. 1964).

$$\tau = \gamma R S_f \quad (16)$$

$\tau =$  *shear stress* (kN/m<sup>2</sup> or kPa)

$\gamma =$  *unit weight of water* (kN/m<sup>3</sup>)

$R =$  *hydraulic radius* (m<sup>2</sup>/m)

$S_f =$  *friction slope* (m/m)

As the data is only 1-dimensional, an interpolation must be used to create the velocity and shear stress maps. These maps are useful for observing any trends that might be occurring within the emergency spillway.

### 2.6.3 Sediment Transport Results

Sediment transport results can be viewed in various ways. In order to view the overall deposition and erosion patterns it is best to look at the profile plot. To look more specifically into certain areas, a cross section can be observed with the changes through the inflow event. Users have the option to view various output parameters at different flow profiles, with either the cross section or profile plot. If comparing various models, it is recommended that the total amount of material eroded be viewed. Tables and graphs are available to be saved after the simulations have run.

## 2.7 Conclusion

This concludes the methodology outlined in Figure 1. The methodology insures that the data is collected and then preprocessed for compatibility within HEC-RAS. Then the hydraulic and sediment transport models are built and executed. And finally, the results are viewed and exported for the modeler to use. The presented methodology provides for meeting the research objective and a model that describes the relationship between various inflows and damage in the form of erosion can be developed.



## Chapter 3

### 3 Case Study: Cheakamus Dam

This chapter will utilize the methodology discussed in Chapter 2 and apply it to Cheakamus Dam Case Study.

#### 3.1 Introduction

This section will briefly outline the case study specifics.

##### 3.1.1 Site Specifics of Cheakamus Dam

Cheakamus Dam is a BC Hydro power generation and water management dam. It impounds Daisy Lake reservoir, which receives inflow from Cheakamus River, contributing approximately 590 GWh/year to BC Hydro (BC Hydro, 2005). The site includes four flow control systems: gated spillway with concrete chute, low level outlet gate, power generation and saddle dams that pass water when reservoir levels are dangerously high. Figure 10 is an image of the entrance to the gates of the spillway facing downstream. Figure 11 outlines the site layout, surrounding landmarks and key locations. Figure 12 shows an aerial view of the gated spillway and low-level outlet. Cheakamus Dam was chosen as a Case Study because it is an extreme-consequence dam, meaning that loss of life is possible in the case of a dam safety accident. This site was chosen to model specifically because of the existing research and previous system dynamics modelling performed by King et al (2017).



**Figure 10: Cheakamus Dam (photo taken by Ryan Weise on August 11, 2015)**

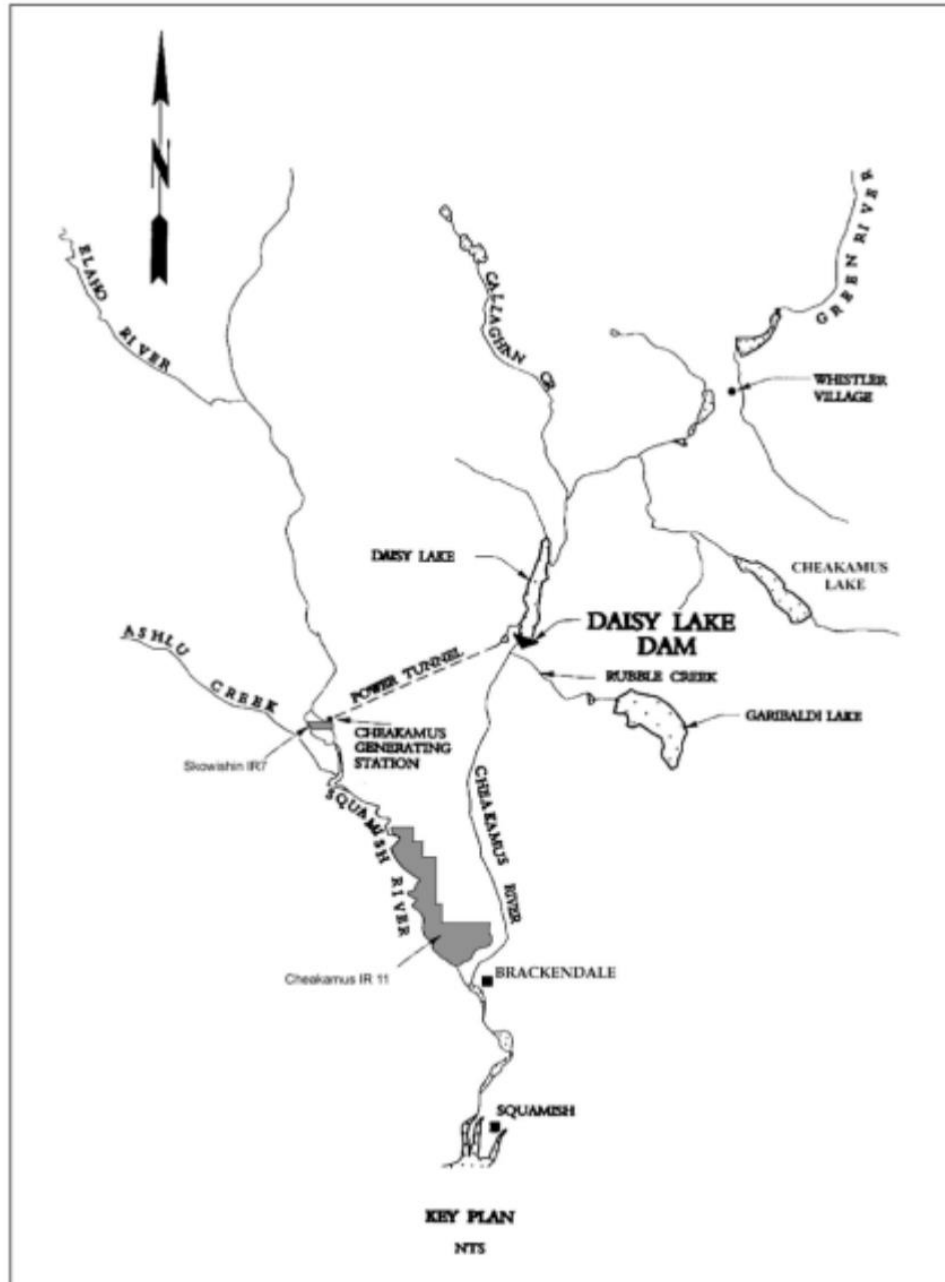
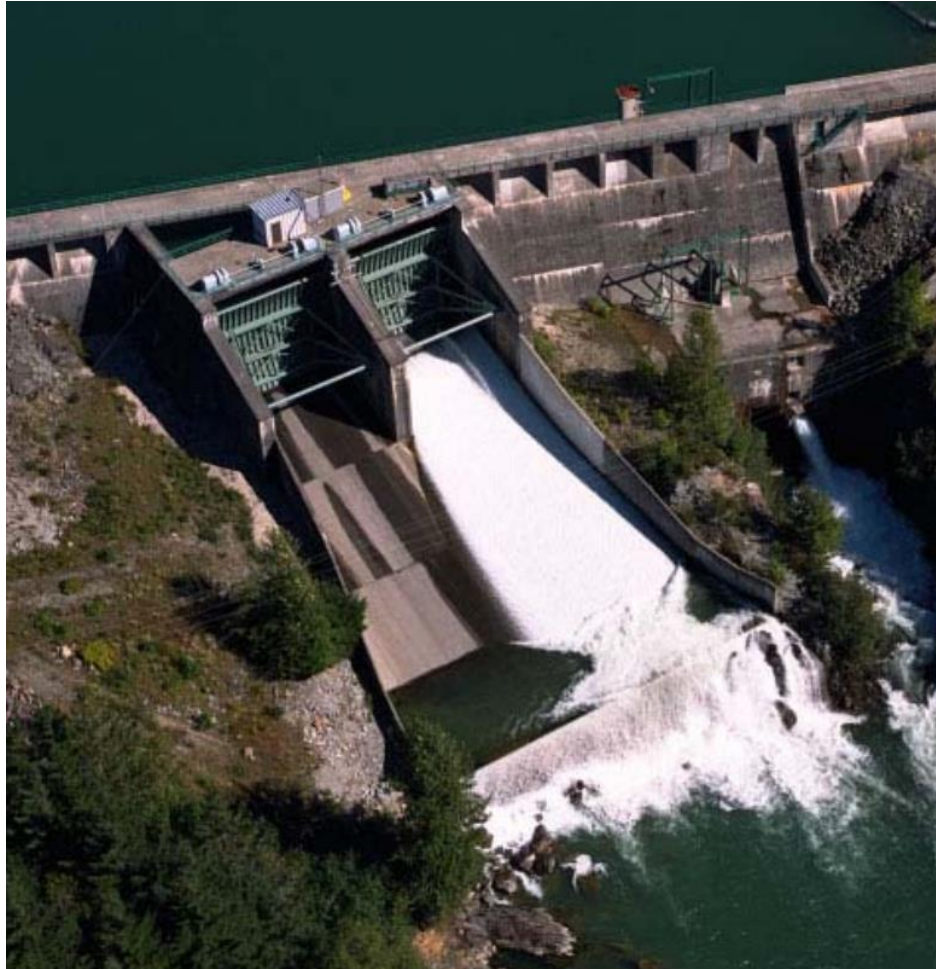


Figure 11: Map of the Cheakamus Dam System (BC Hydro, 2005)



**Figure 12: Aerial Photograph of Concrete Spillway and Emergency Spillway (BC Hydro, 2005)**

### 3.1.2 Overview of the Case Study

Special focus will be given to a 50-meter-long section along the concrete spillway as seen in Figure 12. This region could have water flowing against the edge of the concrete wing walls and potentially lead to the underside of the concrete slabs becoming wet. Special focus will also be given to where the eroded material is depositing and how that could potentially lead to any impacts similar to what happened in the Oroville incident. And finally, the patterns of shear and velocity will be studied to see which regions of the spillway are likely to erode and how that could affect the safety of the dam.

Various Manning's values will be tested. By evaluating the erosion for different flow events, the damage to the emergency spillway can be quantified. This data could then be utilized by the systems dynamic simulation model of King et al (2017).

## 3.2 Analyses for the Cheakamus Dam

This section will go through the application of the first four steps of the methodology presented in Figure 3 to the Cheakamus Dam.

### 3.2.1 Geometry Data

With the use of an aerial drone and LIDAR, the area surrounding Cheakamus Dam was easily surveyed. The data was presented in point format, with key areas having a higher density of point data as seen in Figure 13.

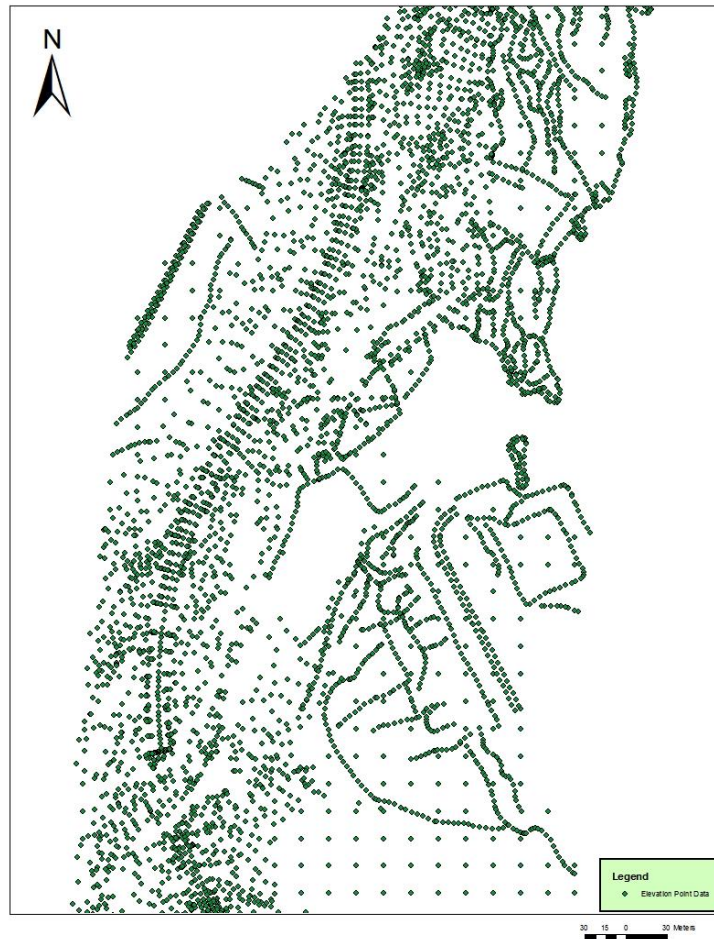


**Figure 13: Map of the Cheakamus Dam Elevation Point Data**

Drawings of the location of the highway, saddle dams and main concrete dams were also available.

### 3.2.2 Processing of Hydraulic Data and Reservoir Routing

As with most emergency spillways, the emergency spillway at Cheakamus was designed to be used during infrequent high flow events. Although the probable maximum flood is at the edge of the design envelope, it is an appropriate flow event to consider as it represents the worst-case scenario. The PMF can be seen below in Figure 14.

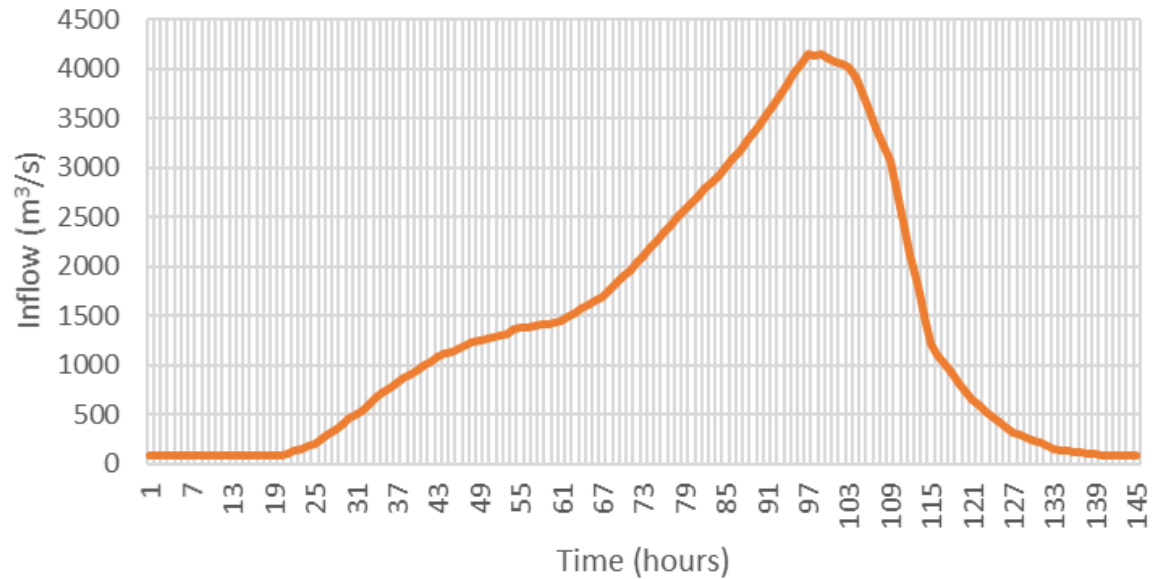


**Figure 14: Probable Maximum Flood for the Cheakamus Dam Reservoir (BC Hydro, 2013)**

To model lower flow events, the PMF was scaled down from 100% to 10% in 10% intervals as seen in Figure 15. This keeps a consistent shape of the hydrograph while modelling lower flow events. These scaled PMF inflow events are used with the hydraulic routing model to determine the corresponding overflow events within the emergency spillway.

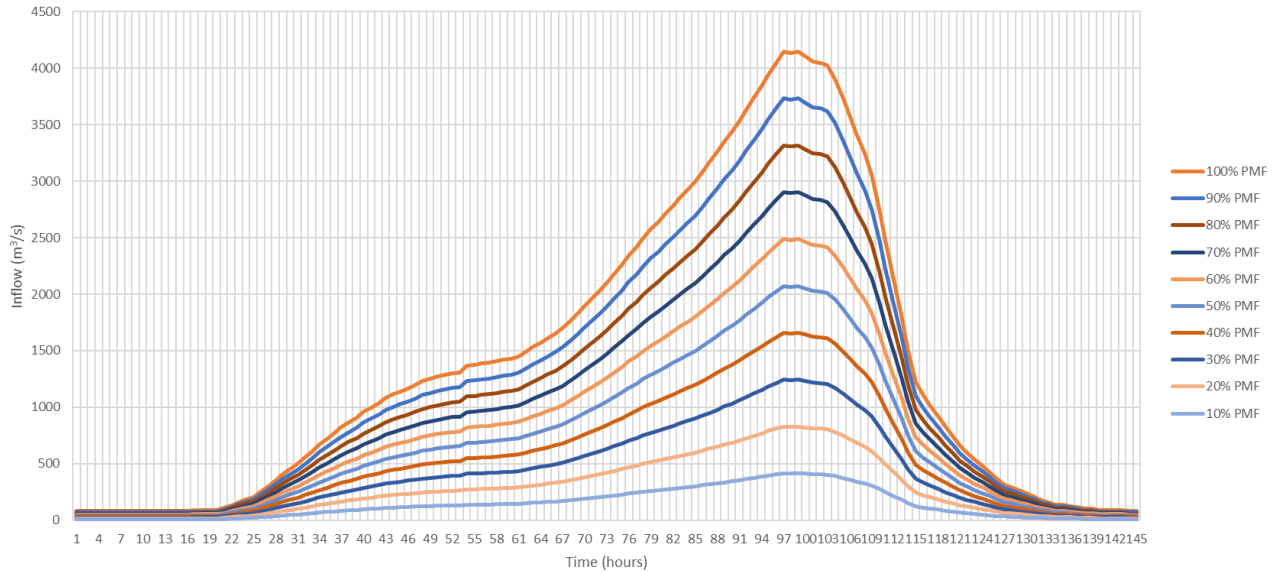


**Figure 15: Scaled Down Probable Maximum Flood for the Cheakamus Dam**

To build a routing model, several relationships must be known. The first relationship is the Reservoir Elevation-Storage relationship as seen in Figure 16. Cheakamus's Reservoir Elevation-Storage relationship is fairly linear. The relationship begins at zero, where the elevation of the radial spillway gate invert aligns. The relationship ends at the highest elevation of the dam. The user can define the initial conditions of the reservoir storage, but in this analysis the reservoir is assumed to be initially empty.



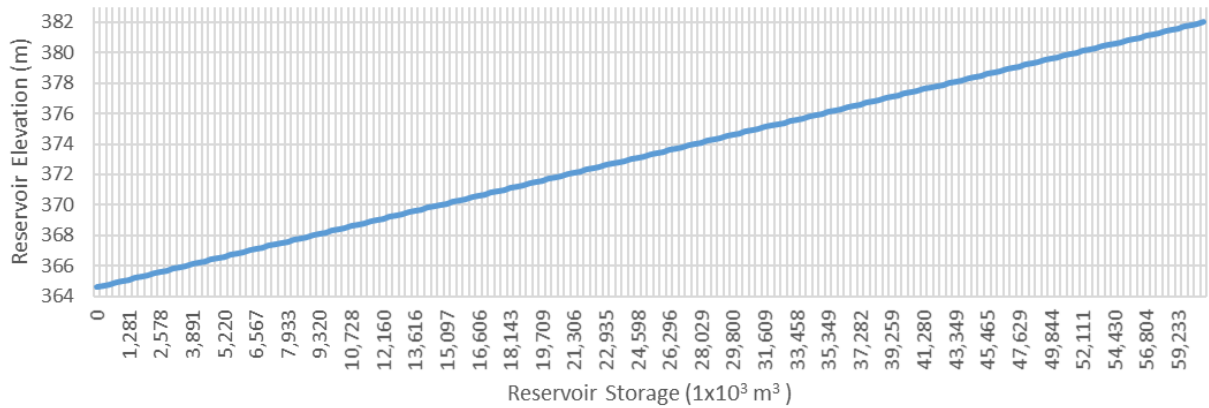


**Figure 16: Reservoir Elevation-Storage Relationship for the Cheakamus Dam (BC Hydro, 2013)**

Cheakamus Dam has various outflow options. Each outflow feature has a specific elevation-discharge relationship (BC Hydro, 2013). Figure 17 was taken from a BC Hydro report and shows the elevation-discharge relationships for the emergency ports, the saddle dams, and the overtopping of the main dam. The emergency ports and saddle dams begin discharging at elevation 378.5 m, whereas the dam doesn't begin to overtop until the reservoir reaches an elevation of 380.5 m.

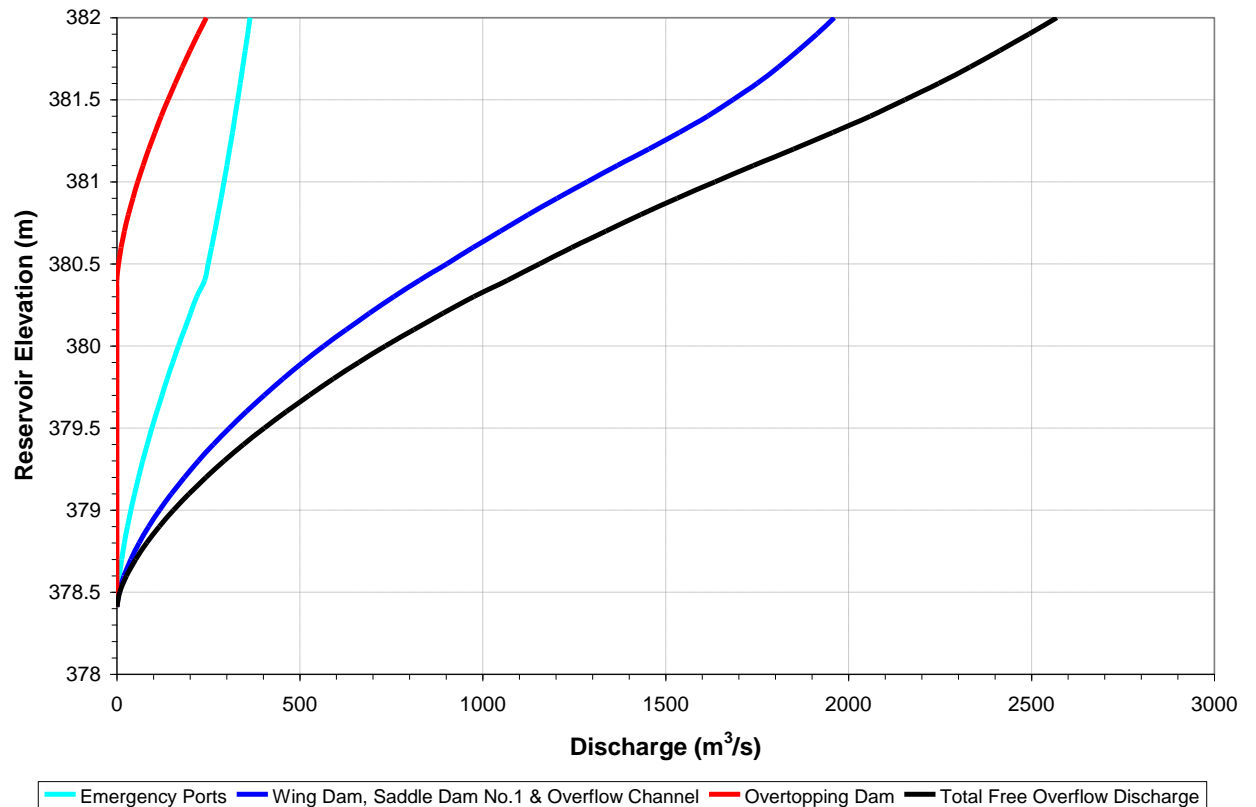


**Figure 17: Reservoir Elevation-Discharge Relationships for Various Outflow Structures of the Cheakamus Dam (BC Hydro, 2013)**

In addition to the above outflow features, Cheakamus Dam also has two radial spillway gates that have an elevation-discharge relationship for each gate position. The positions range from 0 m (closed) to 10 m (fully open). In a high inflow event, the gates would be fully open to maximize discharge. The gate discharge relationship used in the model was set to the fully open position and can be seen in Figure 18. Various gate positions could easily be tested and modelled to demonstrate a closed or stuck gate.

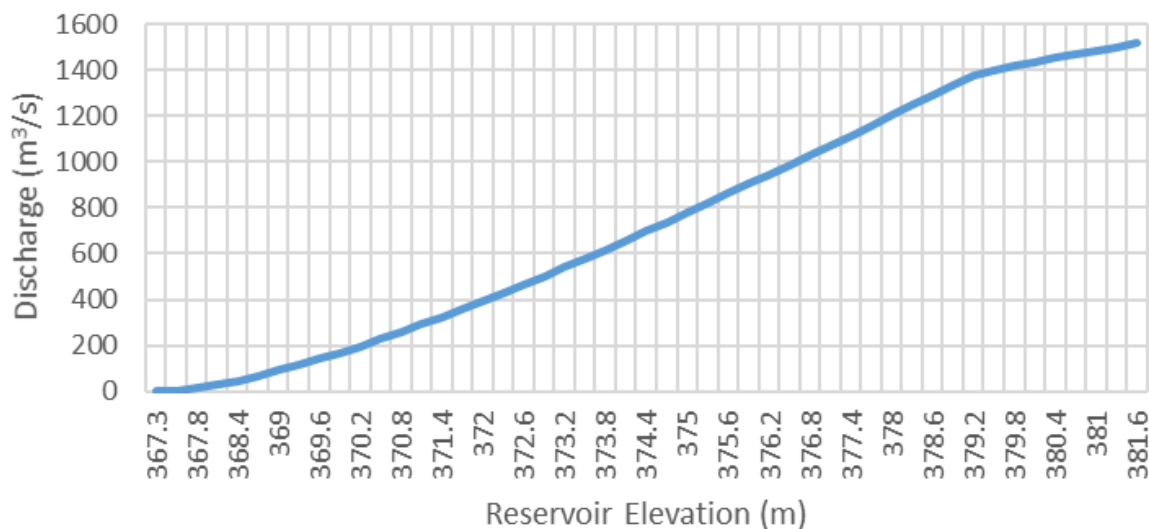


**Figure 18: Cheakamus Dam Concrete Spillway Elevation-Discharge Relationship (BC Hydro, 2013)**

Cheakamus has two other outflow features as well. Power generation has an elevation-discharge relationship with a penstock that can open fully to pass a maximum of 30 m<sup>3</sup>/s and a low-level outlet gate intended to pass 5 m<sup>3</sup>/s to sustain minimum fish flows during summer months (BC Hydro, 2005). The model assumes that both of these are operating at their maximum capacity, however it must be noted that the low-level outlet gate could be closed, and the power generation penstock could be shut if power demand is not present. Both can easily be modified to represent either situation.

Now that the inflow hydrograph, reservoir elevation-storage, and various elevation-discharge relationships are known, the routing model can be built. The model is built in Vensim, with a 1-hour time step and 4<sup>th</sup> order Runge-Kutta interpolation method. The routing model structure can be seen in Figure 4.

After running the 10 scaled down versions of the PMF through the routing model, the overflow hydrographs were created for the emergency spillway. Figure 19 shows the 100% PMF down to the 30% PMF. At 30% PMF and below, the emergency spillway does not have any flow passing through, so 40% PMF is the minimum flow event to be modelled. A maximum of 1960 m<sup>3</sup>/s is observed in the 100% PMF scenario.

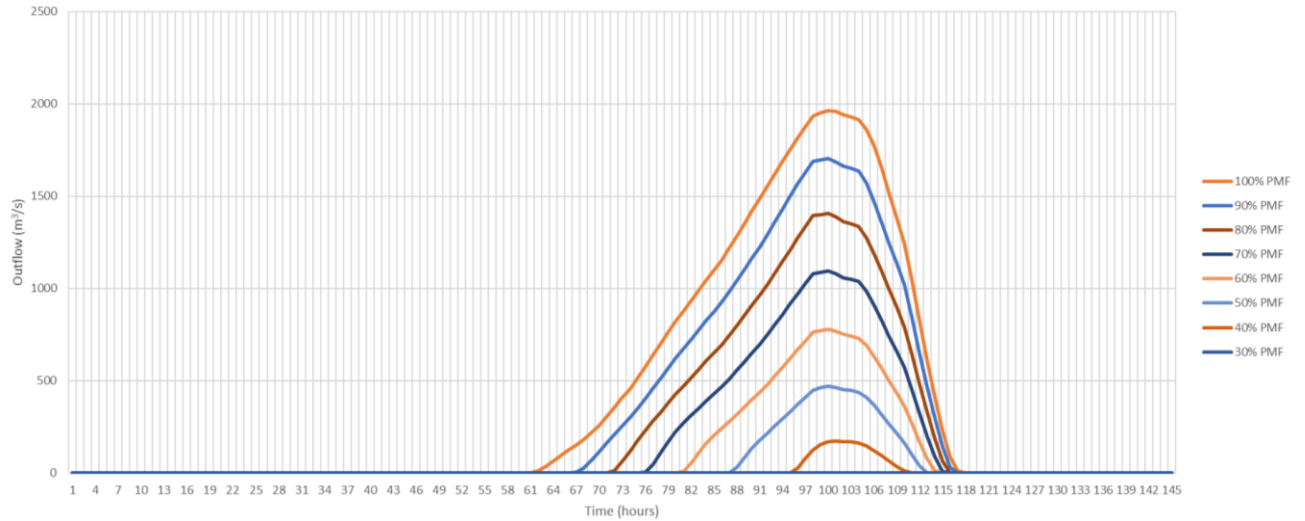


**Figure 19: Cheakamus Dam Emergency Spillway Overflow Hydrographs for Probable Maximum Flood Scenarios**

As explained in the methodology, the hydrographs must be in the form of a quasi-unsteady hydrograph. Figure 20 shows the 100% PMF quasi-unsteady hydrograph for the emergency spillway with hour long increments.

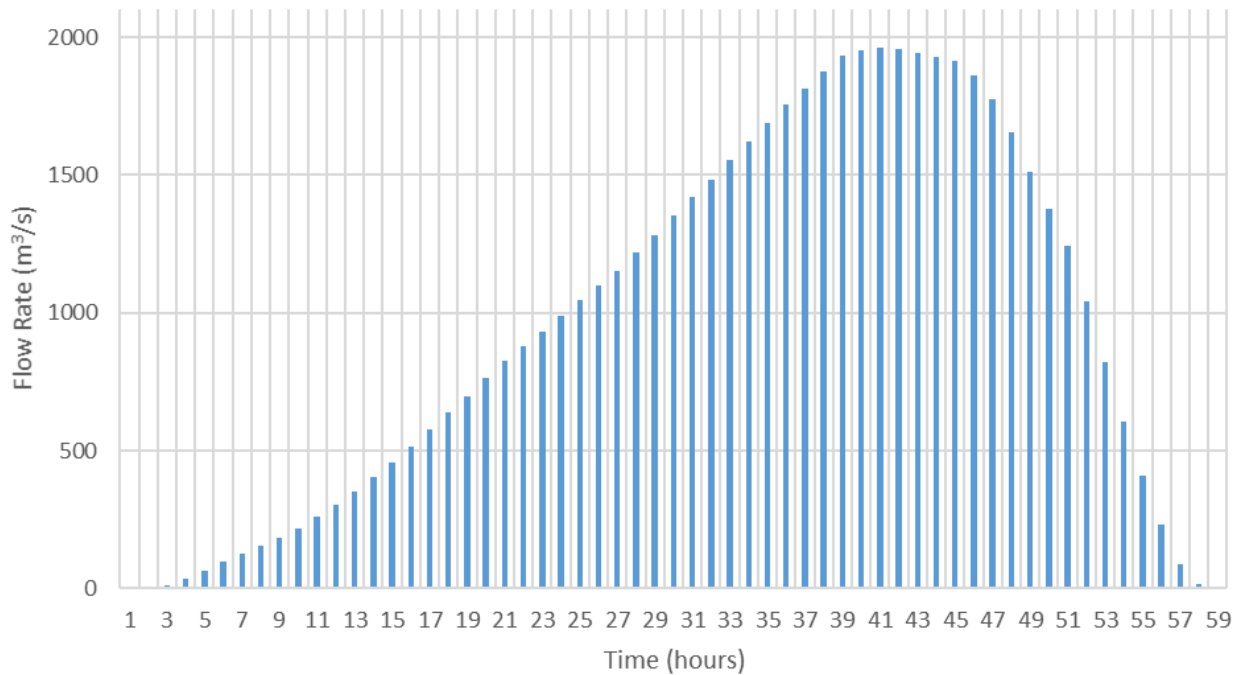


**Figure 20: Cheakamus Dam Emergency Spillway Overflow Quasi-Unsteady Hydrograph**

### 3.2.3 Processing of Sediment Data for the Cheakamus Dam

Various sediment and roughness parameters are required for hydraulic and sediment transport analyses. The hydraulic modelling process requires Manning's values to represent the roughness of the bed. With the use of an aerial photograph, Figure 21, and a site visit, different regions of the emergency spillway were classified based on the HEC-RAS user manual. The different regions were classified and can be seen in both, Table 1 and Figure 22.



**Figure 21: Aerial Photograph of the Cheakamus Dam Emergency Spillway  
Vegetation (after Google Maps January 2018)**

<i>Manning's Number Legend</i>				
<b>Area</b>	<b>Description</b>	<b>Lower Limit</b>	<b>Normal</b>	<b>Upper Limit</b>
1	Medium to dense brush, in summer	0.07	0.1	0.16
2	Light brush and trees, in summer	0.04	0.06	0.08
3	Light brush and trees, in summer	0.04	0.06	0.08
4	Dense willows, summer, straight	0.11	0.15	0.2
5	Corase River deposits with boulders	0.04	0.05	0.07

**Table 1: Cheakamus Dam Emergency Spillway - Manning's Coefficients for Various Areas**

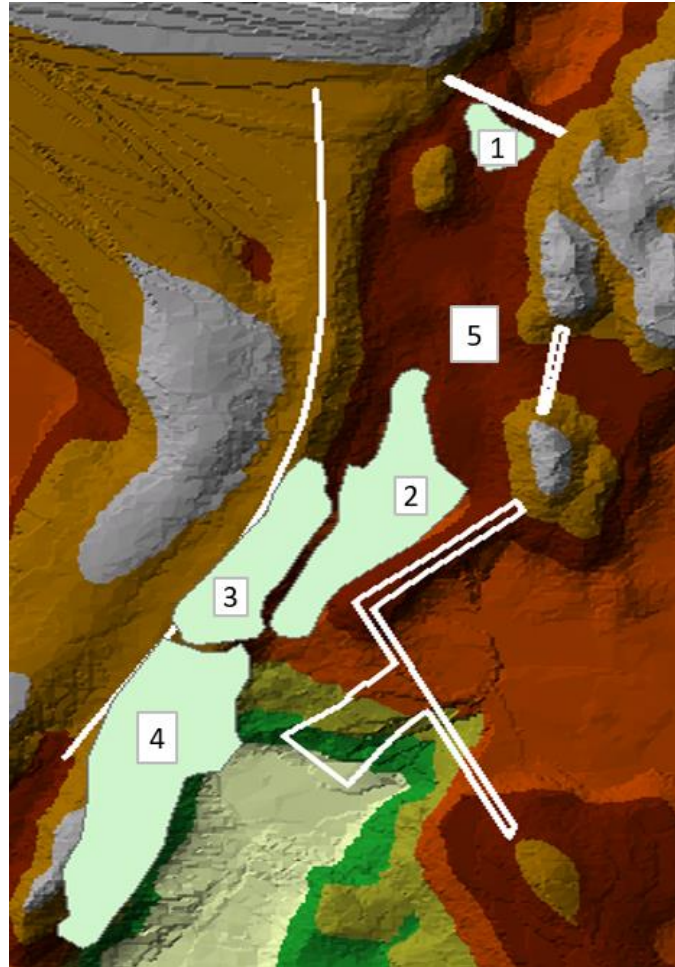


**Figure 22: Cheakamus Dam Emergency Spillway Map of Different Manning's Areas**

The sediment transport modelling process also requires the soil gradation. Although the soil gradation of the emergency spillway is not known, a similar material close by was used to best represent the bed gradation. Figure 23 shows the gradations of the local material. TP07-3 was used as it has the largest gradation and best aligned with what was visually observed in the site visit. It must be noted however that because the modelling process is sensitive to gradation change, an unknown error is associated with the results as the actual bed gradation of the emergency spillway was not used.



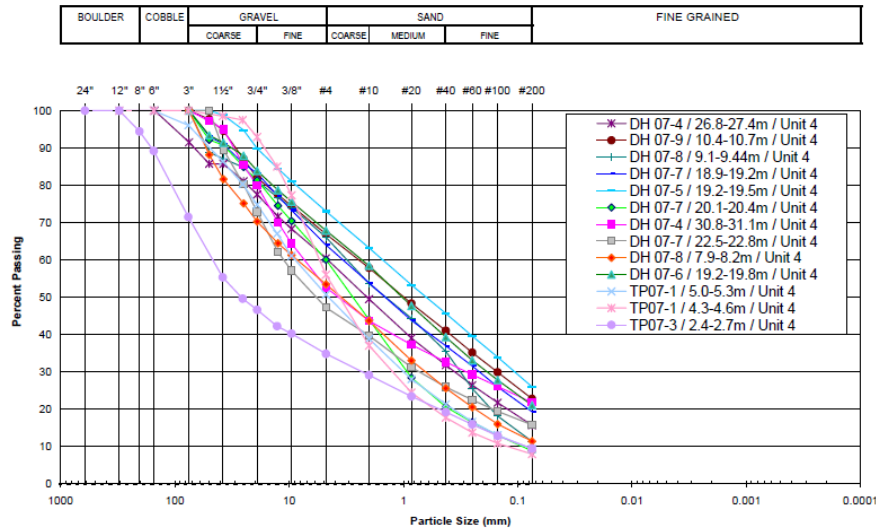


**Figure 23: Cheakamus Dam Sample of Soil Gradations (BC Hydro, 2008)**

### 3.2.4 HEC-GeoRAS Preprocessing of the Cheakamus Dam Data

As explained in the methodology section, the preprocessing phase is critical in performing a sediment transport study for an emergency spillway. The process is broken down into three phases; the formation of a triangular irregular network (TIN), the addition of site specific features, and the creation of HEC-RAS required features. The GIS processing phase begins with the formation of the surface from the point data.

Point data is converted and interpolated into a TIN using the Kriging interpolation method.

Now that a surface has been created, additional features can be added to the model. Engineering drawings provided by BC Hydro showed the location of the saddle dams, main concrete dam, concrete spillway, and highway, all from an aerial perspective. The engineering drawings were converted from PDF to a DWG file using AutoCAD. Now that the engineering drawings were in DWG format, they could be converted into a SHP file to allow compatibility within ArcGIS. Without the use of georeferencing, the shape file had to be manually positioned onto the TIN surface. The highway location can be

seen on the TIN surface, and by aligning the curve of the TIN with the drawings the shape file was positioned. This is not an entirely accurate method and is bound to have some degree of error, however it was the best available method.

Figure 24 shows the TIN surface with the concrete dam and emergency spillway in the southeast corner. The saddle dams can be seen in the east and north sections of the drawing, while the highway can be seen in the west section.

The next feature added was the Manning's values. Aerial photographs were imported into AutoCAD, where the vegetation bounds were drawn and converted into a DWG file and scaled to 100% size. The drawing was then converted into a SHP file and imported into ArcGIS.

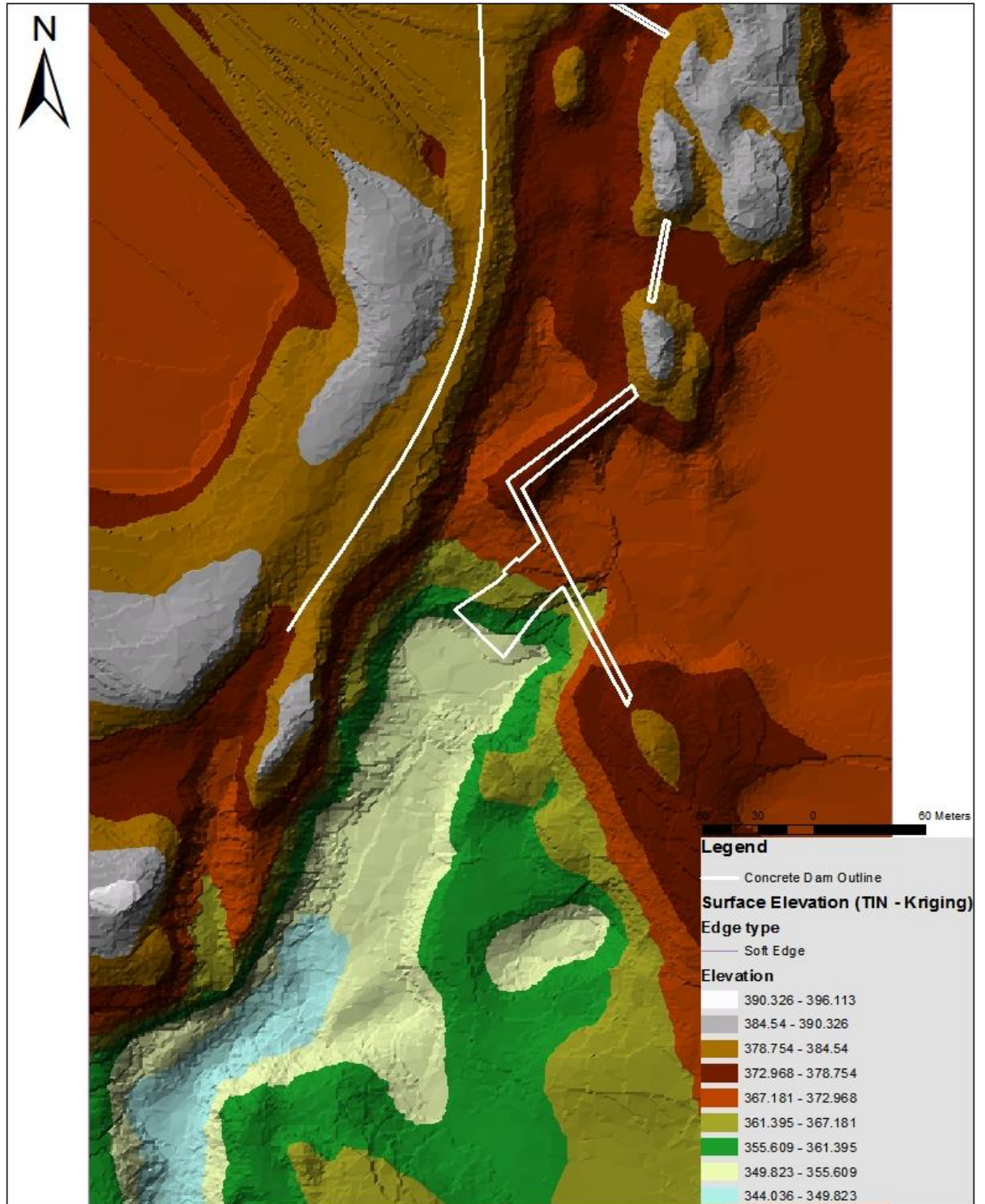


**Figure 24: Cheakamus Dam Triangular Irregular Network Including Outline of Main Concrete Dam and Spillway, Highway, and Saddle Dams**

The next phase in GIS preprocessing is the addition of the required features for HEC-RAS. By using the HEC-GeoRAS tool, these features are easily added to the model. The first feature drawn onto the map is the river. This sets the length of the reach to be modelled and can be seen in Figure 25 as the blue line. For simplicity of modelling and to avoid model stability issues, the river reach begins at the corner of the concrete dam and finishes at a sufficient distance downstream of the study area. The banks are then drawn and added to the model as the black lines. This feature is more important for inundation studies and less so for this case, however HEC-RAS requires bank stations (Ackerman, 2009). The cross section cut lines are then added to the model at a specified interval and width. In this model a width of 150 meters was chosen to fully cover the extent of the flooding and an interval of 1 meter was chosen to best capture the surface and to avoid instability issues and large errors that occur when the elevation changes too much from one cross section to another. The cross section cut lines can be seen as the red extent in Figure 26; the cross sections cannot be individually seen in this figure due to the 1-meter spacing.

After the mandatory HEC-RAS features have been created and added to the model, the optional features are added. The Manning's shape file is added to the model and corresponding Manning's values are provided. These values are pulled and added to the cross-section data. To model the concrete dam and the concrete spillway, a blocked obstruction must be added. HEC-RAS models blocked obstructions as zero flow zones (Brunner & CEIWR-HEC, 2016). The concrete outline is then converted to a blocked obstruction and set to an elevation that will not be overtopped. In reality, the concrete spillway could potentially have water spilling over the wing walls, however the complexity of the model would increase significantly.

After all the features have been added, the file is prepared to be exported for use by HEC-RAS.

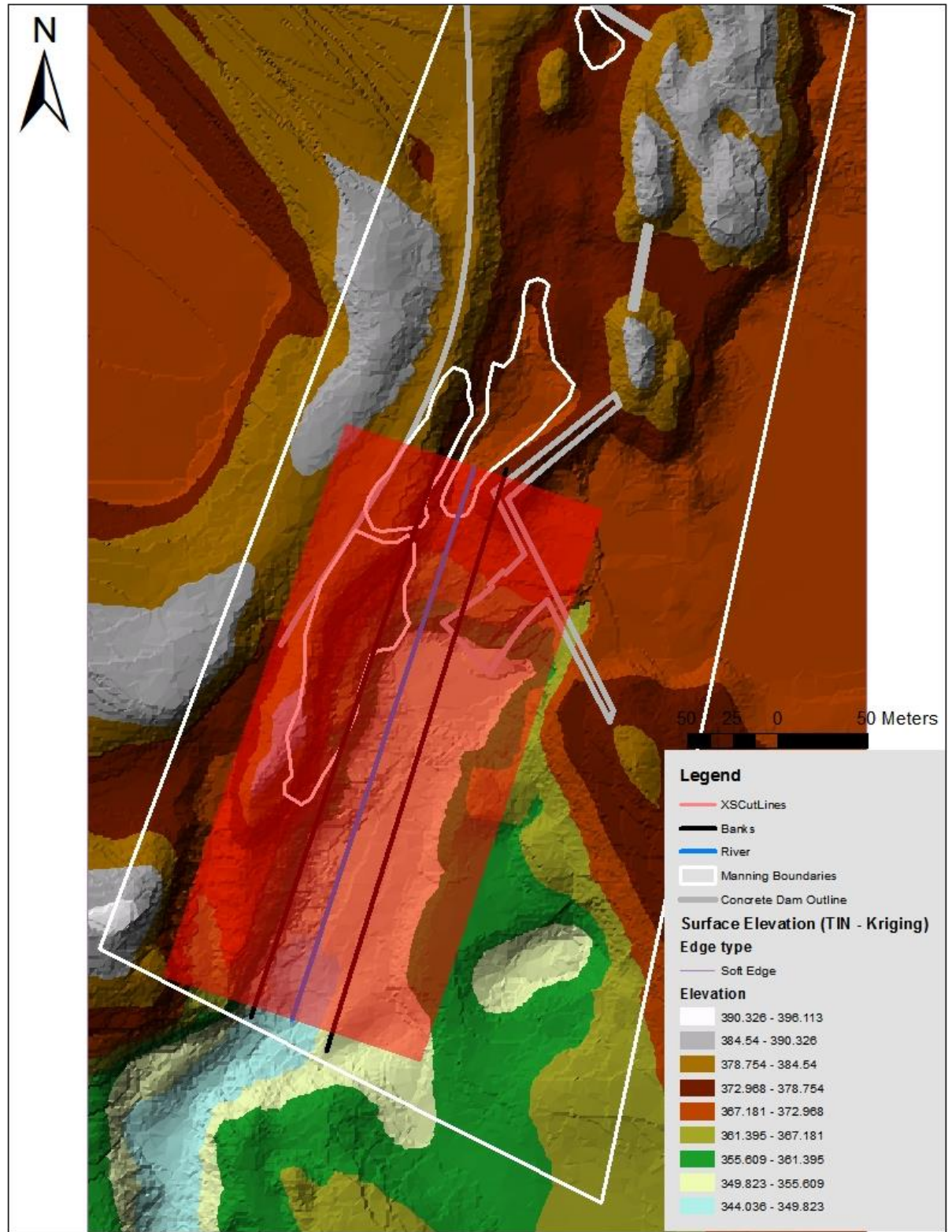


**Figure 25: Cheakamus Dam Emergency Spillway with HEC-GeoRAS Layers**

### 3.2.5 HEC-RAS Model Preparation for the Cheakamus Dam

There are three main data files required for HEC-RAS to run a sediment transport study. The first being the geometry file, which was preprocessed in ArcGIS, the second being the hydraulic data, which was created using the routing model, and the third being the sediment data. When these files have been created and the boundary conditions set, the model can be executed.

The geometry file was created, and the GIS data imported into HEC-RAS. Figure 26 shows the aerial view of the model and the cross sections. It is important to inspect the cross sections to ensure that Manning's values and elevation data have correctly been imported. This can be done with the cross-section editor tool.

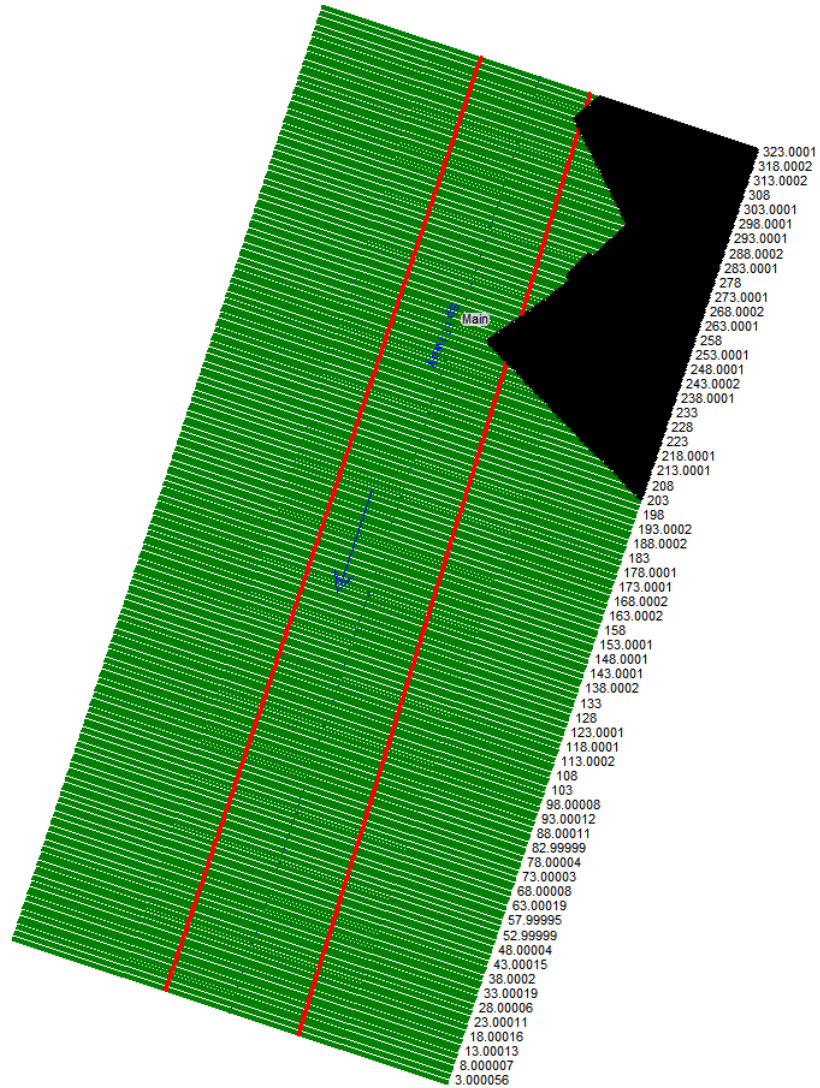


**Figure 26: Cheakamus Dam Emergency Spillway Aerial View of HEC-RAS Model  
Cross Sections with the Concrete Spillway as a Blocked Obstruction**

Figure 27 shows the cross section at station 250. In table format the elevation data is presented alongside Manning’s values in tabular and graphical forms, showing the concrete spillway as a blocked obstruction.

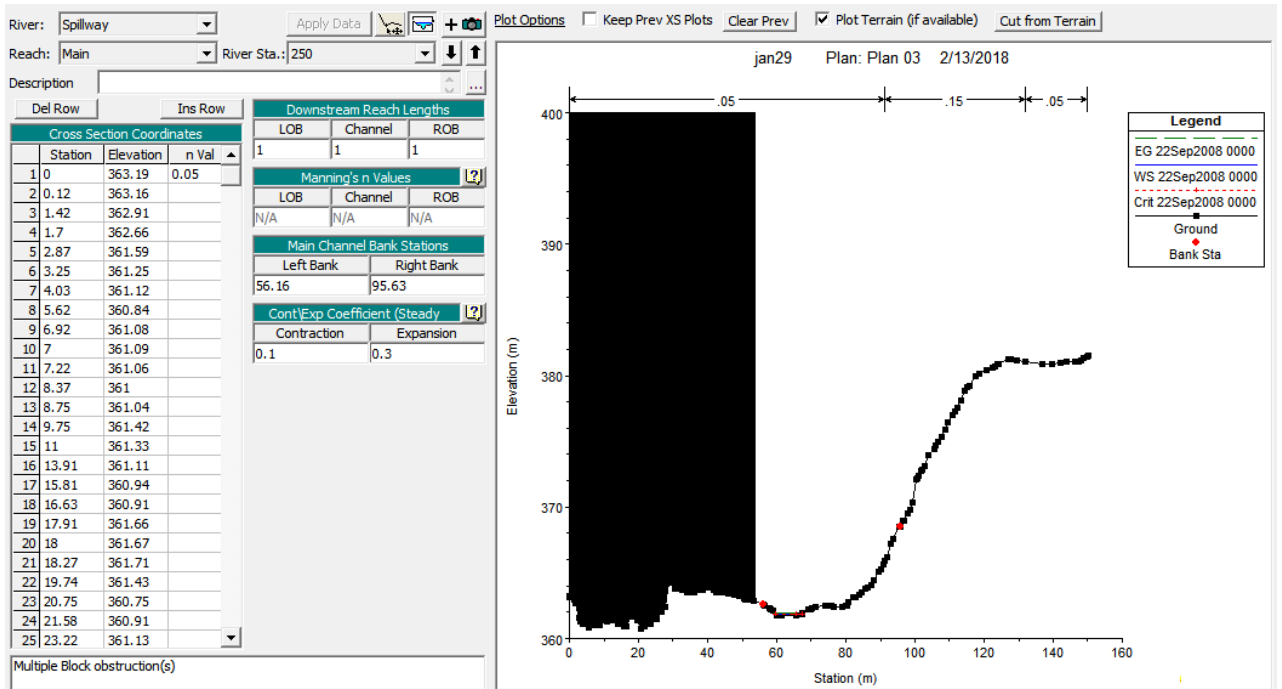


**Figure 27: Cheakamus Dam Emergency Spillway Cross Section at Station 250**

After the geometry data is finalized the hydraulic data can now be added. Hydraulic data is added to the most upstream cross section and the most downstream cross section. The upstream boundary condition is set to an inflow hydrograph. The outflow hydrograph obtained by reservoir routing is added with hourly increments. The computation increment is set to 6 minutes, allowing for 10 computation steps to occur for each steady flow value, as explained in the methodology section. The downstream boundary is set to the normal depth, which is the friction slope. The lowest slope was tested as well as the highest slope, and the most stable solution was found to be the average slope, 0.08. This value was set far enough downstream that it did not affect the study area along the concrete spillway. The file is then saved and ready to be used in the simulation.

The sediment data is then added to the model. The first step is to add the sediment bed gradation. Figure 28 shows the bed gradation data obtained from the BC Hydro Report E591 (BC Hydro, 2008). The data is entered in the percent finer method, which is standard among most engineering disciplines. After the bed gradation has been specified,



each cross section must be set to the specific bed gradation, as the user has the option to have multiple bed gradations for different regions. In this case only one bed gradation is used.

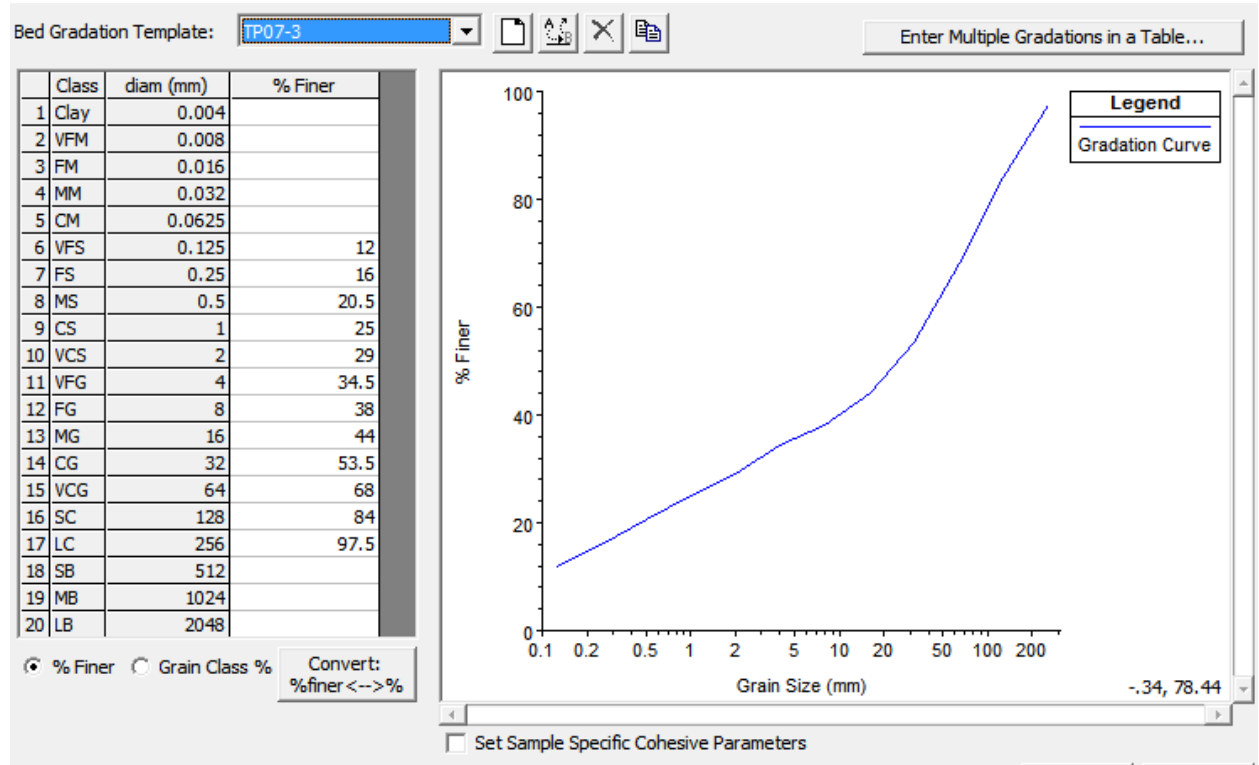


**Figure 28: Cheakamus Dam Emergency Spillway HEC-RAS Soil Gradation Editor**

The maximum depth of erosion must be set too. Upon inspection of the bedrock depths within the emergency spillway, an average of 2 meters was selected as the maximum depth of erosion. This can be seen in Figure 29. If a higher level of detail was desired, users could input the actual maximum depth for each cross section. However this data was not available. The user has the option to choose the transport function, sorting method, and fall velocity method. In this case the Meyer Peter Muller method, Thomas (Ex5), and Toffaleti are chosen respectively.

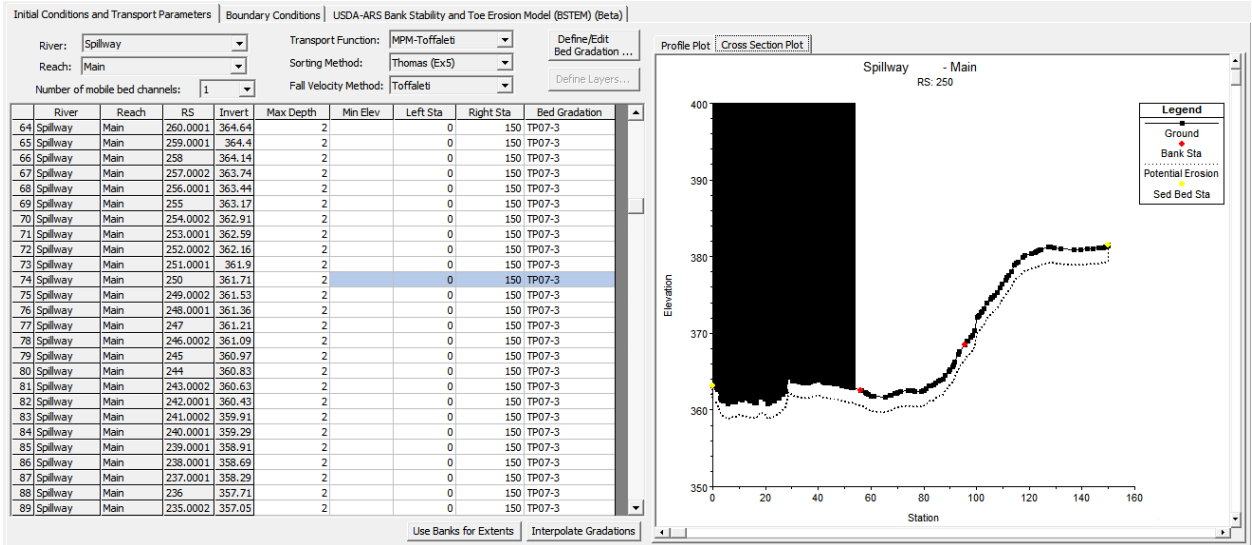


**Figure 29: Cheakamus Dam Emergency Spillway Cross Section at Station 250  
Showing Maximum Erodible Depth**

The upstream boundary condition must also be set within the sediment file. As there is no data available on the sediment entering the upstream cross section, the value was set to zero. In reality this value would not be zero and there would be some sediment entering the upstream cross section. This was the only option available, but to best model the reach, the upstream cross section was placed where the channel invert begins to raise slightly when heading downstream for a small distance, as seen in Figure 30. This increase in elevation would likely reduce the sediment being transported into the upstream cross section, thereby reducing the error associated with setting the value to zero. The sediment data is then complete and ready to be utilized within the simulation.

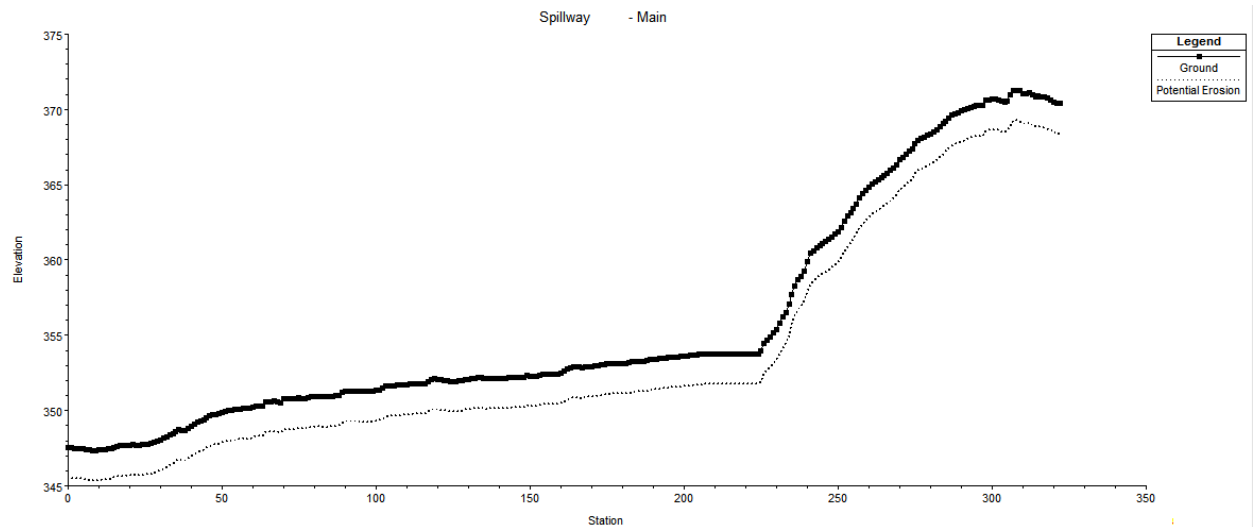


**Figure 30: Cheakamus Dam Emergency Spillway Side Profile Plot Showing Maximum Erodible Depth**

### 3.3 Results for the Cheakamus Dam 1-Dimensional Model

This section will outline the fifth step of the methodology as shown in Figure 3.

#### 3.3.1 Hydraulic Results

The HEC-RAS model was executed with the 100% PMF scenario. The geometry file used was the normal Manning's case with no size change to the various areas. The peak flow of  $1963 \text{ m}^3/\text{s}$  occurs at the 45<sup>th</sup> of 57 hours. Various output results are presented below, ranging from an individual cross section, the 2D and 3D water surface profiles, and velocity and shear maps.

In Figure 31, a side profile view of the emergency spillway can be seen. The firm black line shows the initial channel invert elevation. Below this line is the current channel invert elevation, at the peak flow time step. The blue section is the water surface profile. Critical depth sections are highlighted in red. These red sections show where the program could not achieve a solution and defaulted to the critical depth.

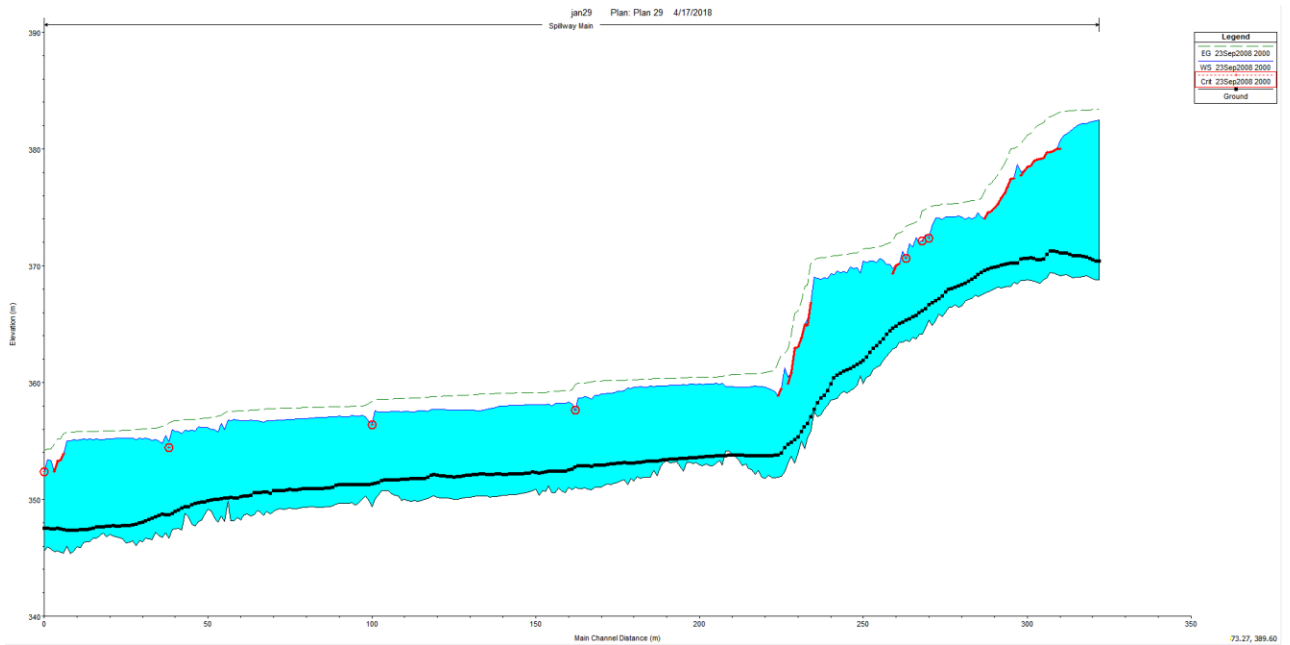


**Figure 31: Cheakamus Dam Emergency Spillway Side Profile Water Surface Elevation at Peak Outflow**

The peak flow is shown flowing through the emergency spillway in Figure 32. The 3D plot shows how narrow the passage is at the end of the concrete spillway.

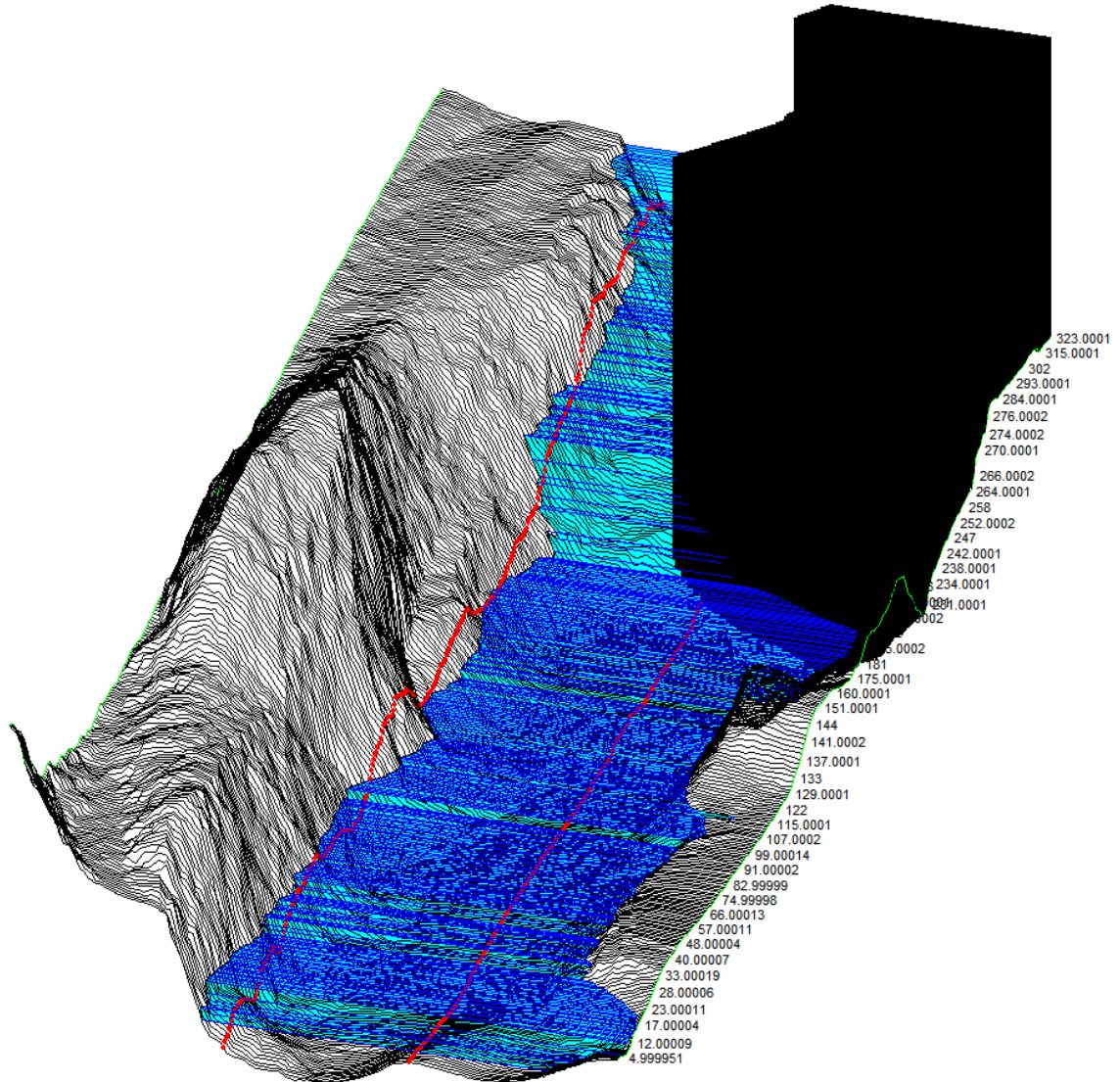


**Figure 32: Cheakamus Dam Emergency Spillway 3-Dimensional Water Surface Elevation at Peak Outflow**

During the peak flow the water surface elevation rises significantly through the narrow section along the end of the concrete spillway. In Figure 33, the cross section at station 236 is shown. The depth of water here is approximately 10 meters, due to the steep embankment on the right-hand side of the channel. In reality, the depth would be much lower as water would spill into the concrete spillway. This situation is not possible to model within HEC-RAS.

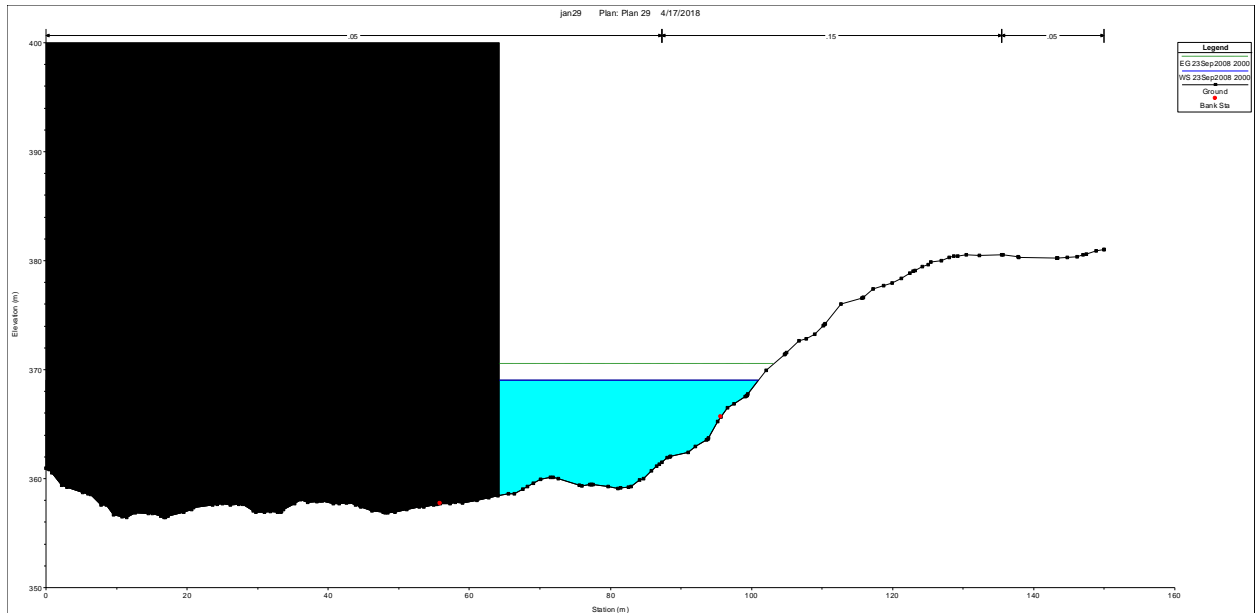


**Figure 33: Cheakamus Dam Emergency Spillway Cross Section at Station 236  
Showing Water Surface Elevation**

After the model has been run, the results can be exported into ArcGIS. Both shear stress and velocity maps are shown in Figures 34 and 35 respectively. The legends show the velocity and shear stress values on the maps. Shear stress reaches values of up to 3000 kPa, as shown in the red. This is occurring in the narrow section of the emergency spillway. A similar pattern for velocity can be observed as well. Velocities surpassing 9 m/s are seen in the dark purple and occur in the steep sections of the spillway. Where both velocity and shear stress are high, it is expected that erosion will also be highest in this region. These maps are an important tool in evaluating where potential erosion will occur. Both velocity and shear stress maps also show the extent of the inundation.

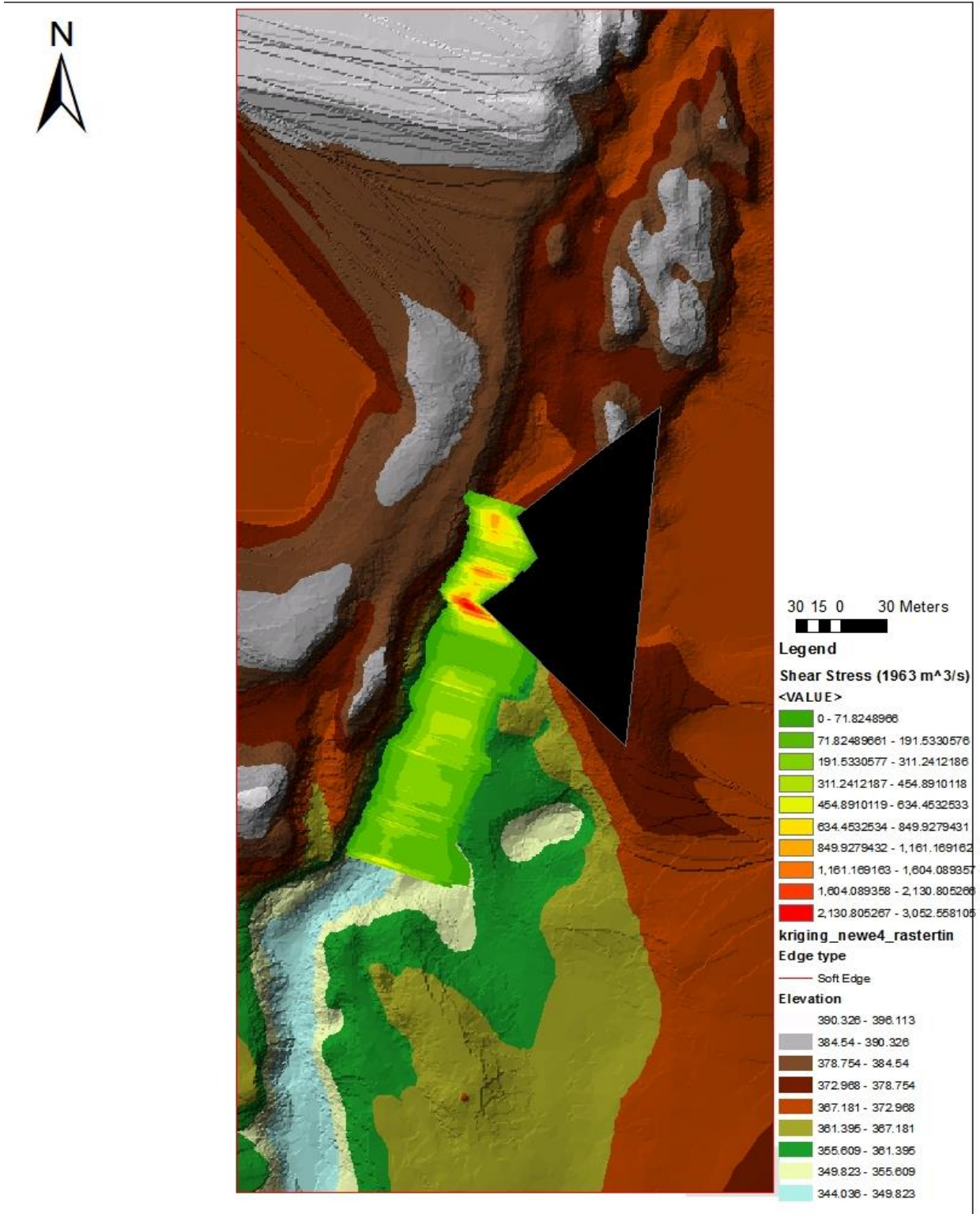


**Figure 34: Cheakamus Dam Emergency Spillway Shear Stress Map for 100% PMF and Normal Manning's Conditions**

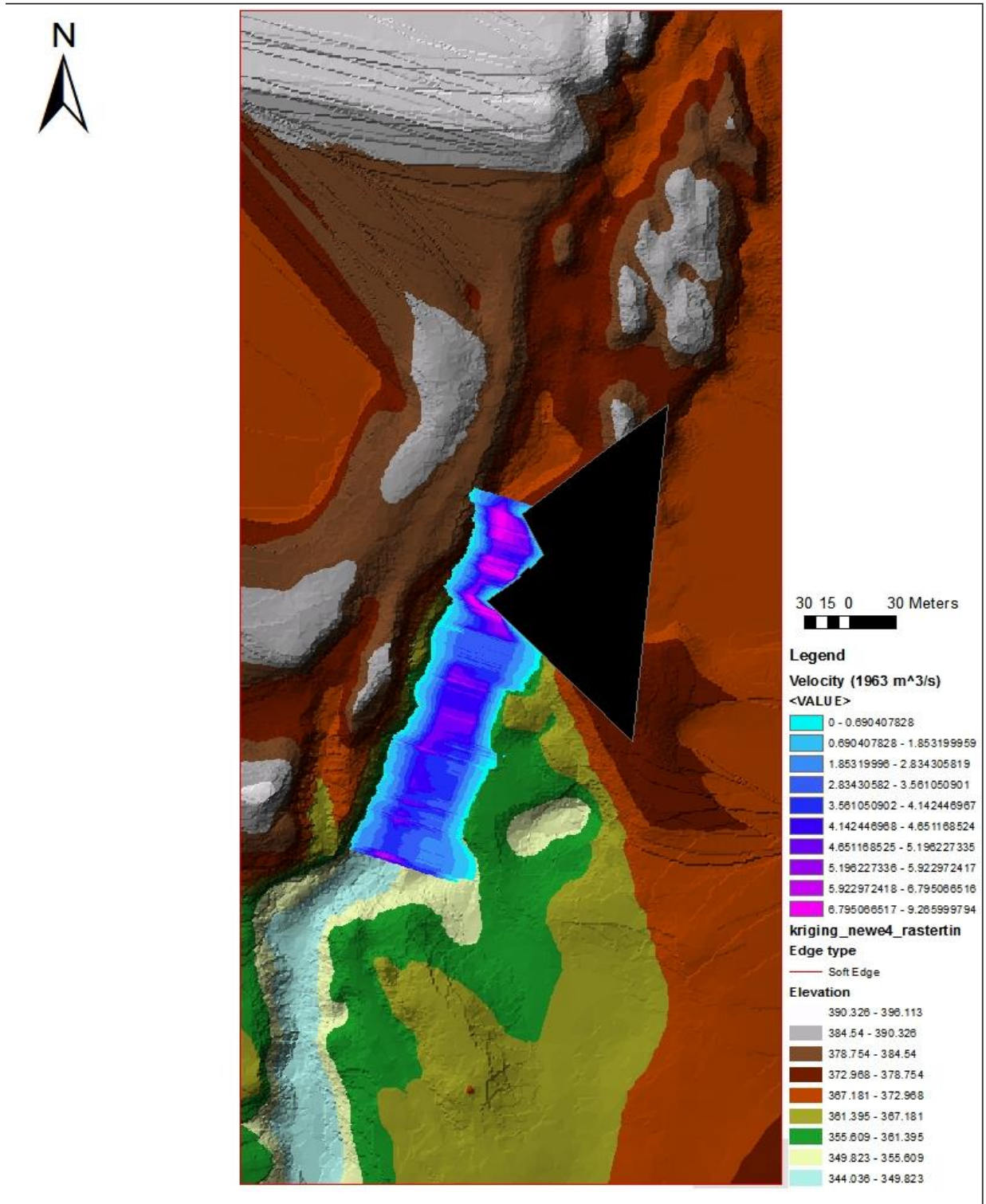


**Figure 35: Cheakamus Dam Emergency Spillway Velocity Map for 100% PMF and Normal Manning's Conditions**



### 3.3.1.1 Errors

After the model was run, it was observed that several errors occurred. The error that occurred several times was that HEC-RAS was unable to calculate a surface water profile and defaulted to the critical depth after the maximum number of iterations has been reached. In Figure 31, the error locations are in red.

These regions are where the flow is likely transitioning to supercritical flow.

Unfortunately, HEC-RAS can only perform sediment transport in gradually varied flow. The surface water values must be recognized to be incorrect, as they were set to the critical depth.

### 3.3.2 Sediment Transport Results

The hydraulic model is coupled with the sediment transport model, so the results for sediment transport are viewed in the same simulation that the hydraulic results were performed in. The results can be viewed in various ways, from a cross section to the side view plot.

Figure 36 is the same cross section shown in the hydraulic results, the narrow part of the emergency spillway at station 236. The blue line represents the new channel cross section after the inflow event of 100% PMF has passed through. Significant erosion occurs through the main channel. It can also be seen that erosion is occurring along the concrete spillway. Although at Cheakamus Dam the concrete spillway is anchored to bedrock, it is still important to acknowledge any potential damage areas (BC Hydro, 2008). If this were to occur to a similar dam, the erosion along the edge of the concrete spillway could lead to scouring underneath. This scouring could eventually cause enough erosion to potentially damage the concrete spillway, similarly to the Oroville Dam Incident.

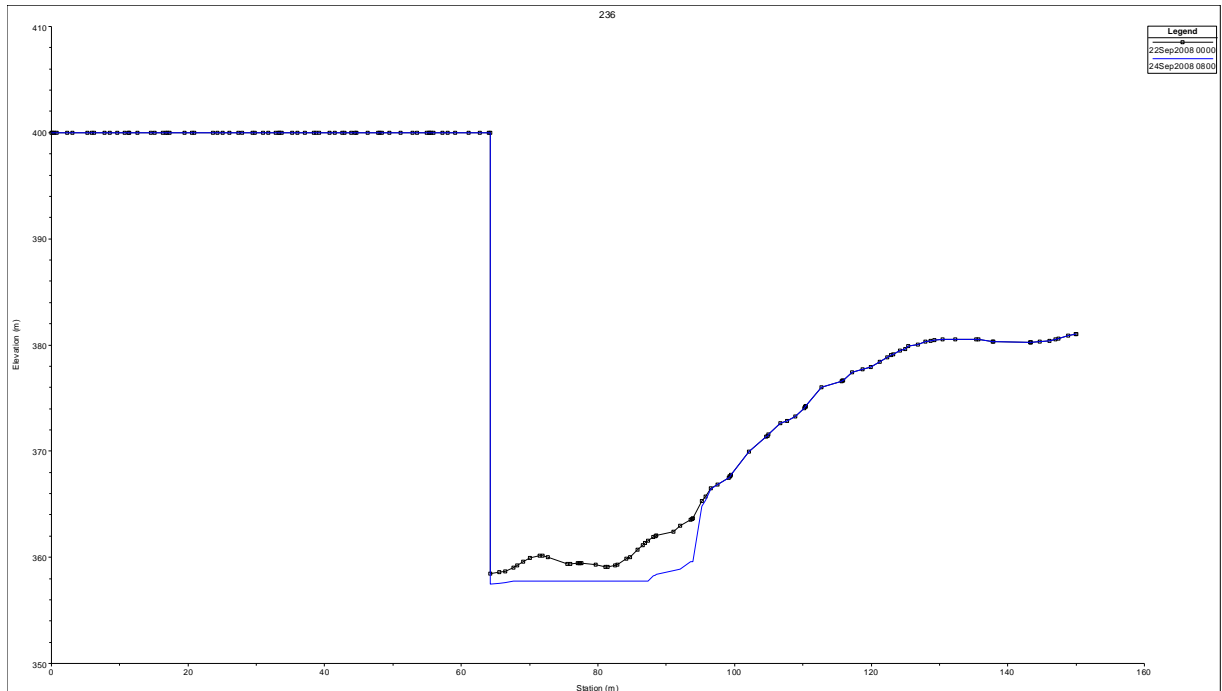


**Figure 36: Cheakamus Dam Emergency Spillway Cross Section at Station 236  
Showing Erosion for 100% PMF and Normal Manning's Conditions**

Further to individual cross section presentation, the side profile plot can also be generated. Figure 37 shows the original channel invert elevation in black and the post event channel inert elevation in blue. The emergency spillway flow direction is from the right side of the diagram to the left. It can be observed that significant erosion occurs in the steep segment of the emergency spillway. This is expected as the steep slopes create high velocities and shear stress values, resulting in a higher potential for erosion. Around station 225 a significant dip can be observed. The channel cuts deep and then rises. This occurs where the pre-erosion channel transitions from a steep slope to less steep slope. In this region large debris from the steep section deposits as the velocity decreases. The channel continues to erode further downstream. A sawtooth pattern can be seen

throughout the post-erosion channel plot. These oscillations are due to the HEC-RAS cross section weighting factors. Upstream and downstream weighting factors can cause erosion at one cross section and then deposition at the following cross section, resulting in the sawtooth patterns.

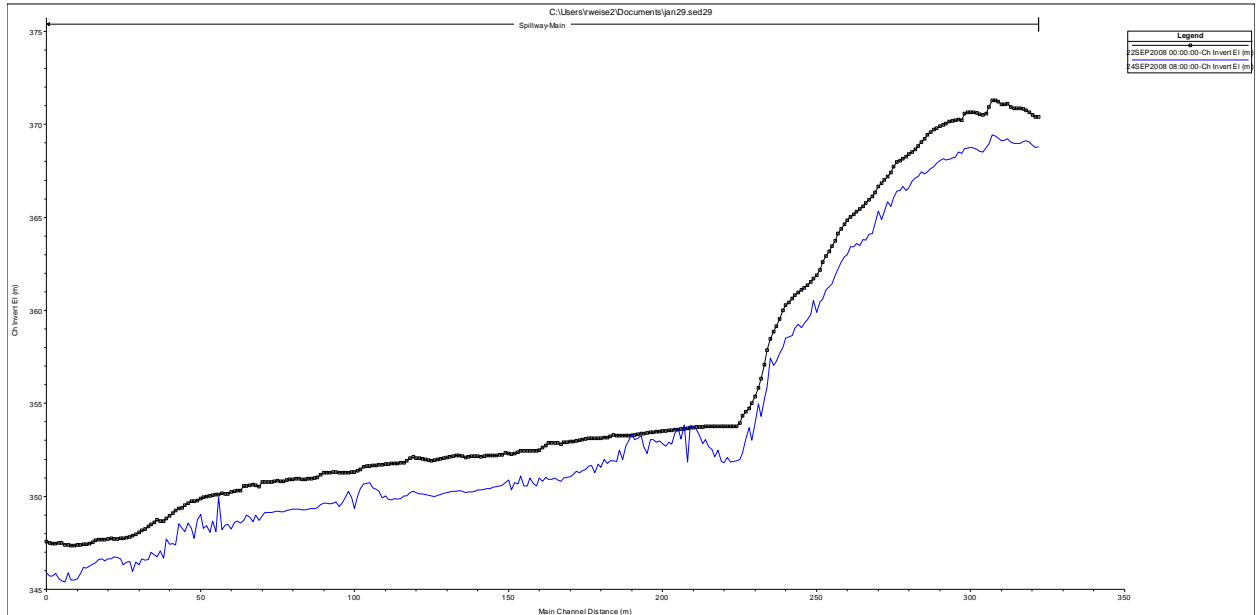


**Figure 37: Cheakamus Dam Emergency Spillway Side Profile Plot Showing Erosion for 100% PMF and Normal Manning's Conditions**

### 3.3.3 Manning's Sensitivity

This section will outline the changes in the results for the range of Manning's values tested.

#### 3.3.3.1 Introduction

Manning's roughness coefficients can have a drastic impact on a hydraulic model, and in turn a sediment transport model. Typically, Manning's values are calibrated to comply with historical data. As this downstream data does not exist for the emergency spillway, values must be estimated. When estimating, there are bound to be errors. It is prudent then to examine how a range of Manning's values may impact the simulation results. Lower, normal, and upper ranges of Manning's values are examined for each classification. A 10% increase and a 10% decrease in size of vegetation area is also examined. Table 2 outlines the list of simulation experiments performed to test the impact of Manning's roughness coefficients on the simulation results.

<b>Geometry File Name</b>	<b>Size</b>	<b>Manning's</b>
AL90	90%	Lower
AN90	90%	Normal
AU90	90%	Upper
AL100	100%	Lower
AN100	100%	Normal
AU100	100%	Upper
AL110	110%	Lower
AN110	110%	Normal
AU110	110%	Upper

**Table 2: Manning's Scenarios for the Cheakamus Dam Emergency Spillway**

### 3.3.3.2 Erosion Patterns

For the 100% Manning's size scenario, the channel invert elevation is plotted for the lower, normal, and upper Manning's values. Figure 38, Figure 39, and Figure 40 show the 100% PMF, 70% PMF, and 40% PMF cases respectively.

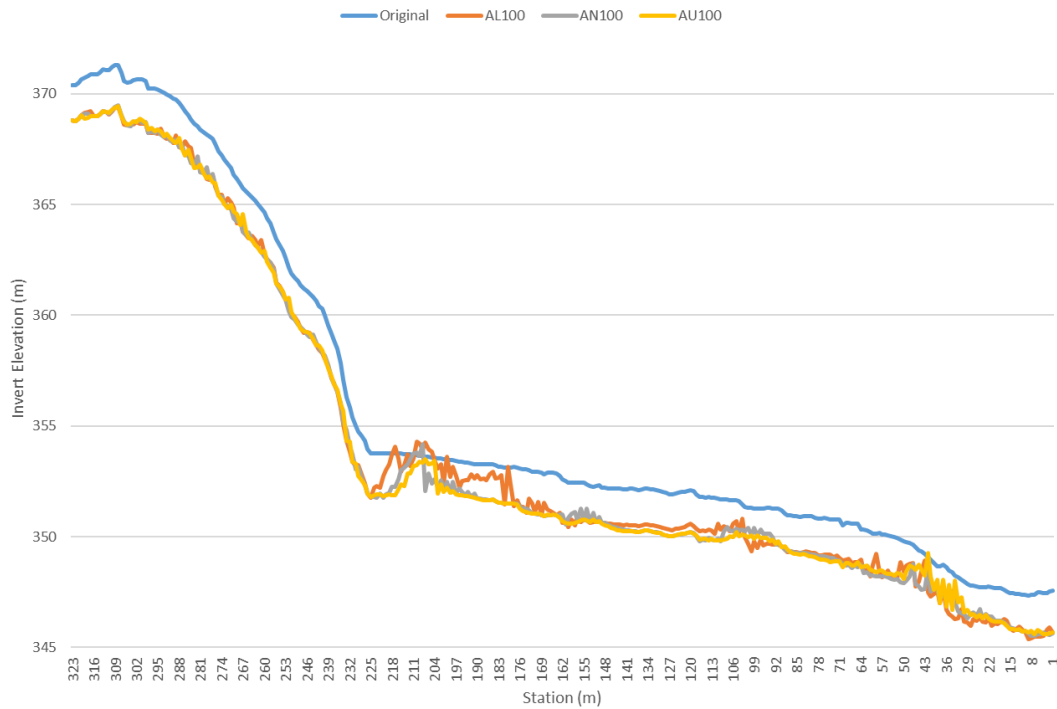


**Figure 38: Cheakamus Dam Emergency Spillway Channel Invert Change for 100% PMF Scenario and Lower, Normal and Upper 100% Manning's Scenarios**

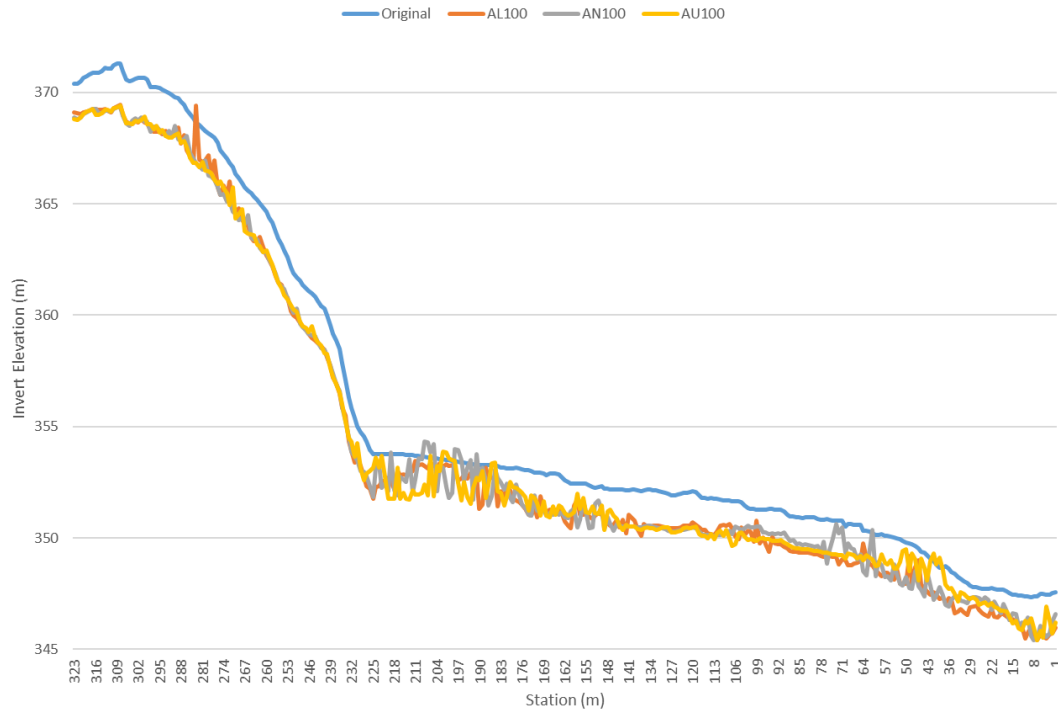


**Figure 39: Cheakamus Dam Emergency Spillway Channel Invert Change for 70% PMF Scenario and Lower, Normal and Upper 100% Manning's Scenarios**

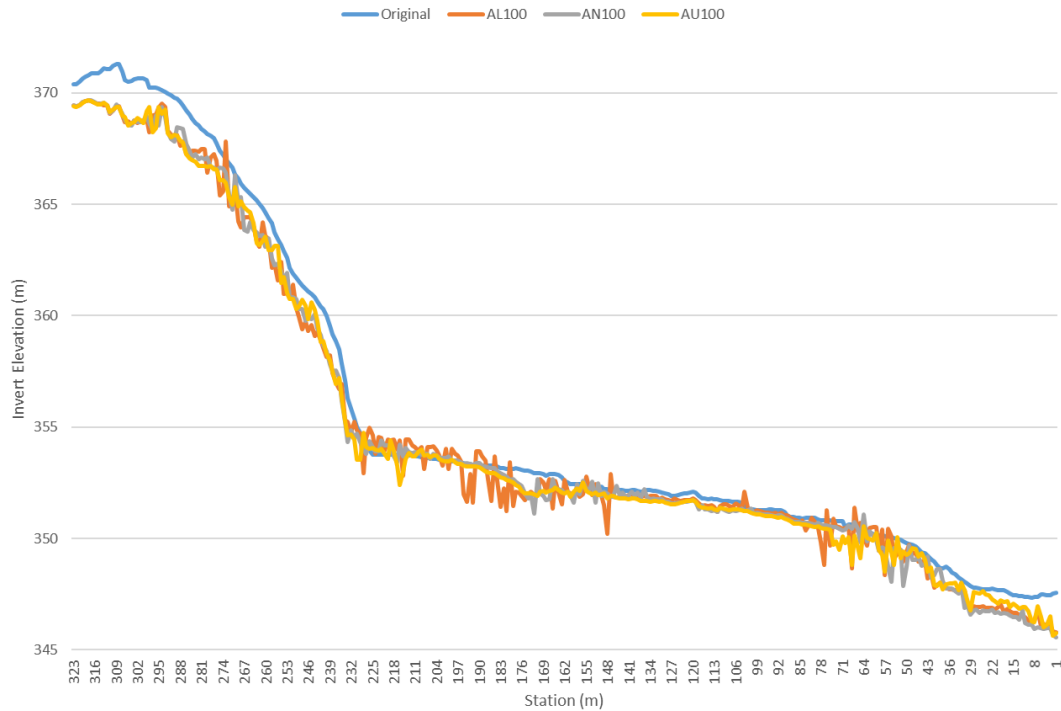


**Figure 40: Cheakamus Dam Emergency Spillway Channel Invert Change for 40% PMF Scenario and Lower, Normal and Upper 100% Manning's Scenarios**

In the 100% scenario, the pattern is apparent. For the most part, erosion stays constant through the steep section. Apart from some oscillations, erosion in the less steep downstream section also remains constant. The main change occurs in the transition zone, where the channel invert dips and then rises. It can be observed that as Manning's values increase, from AL100 (lower case Manning's) to AN100 (normal case Manning's) to AU100 (upper case Manning's), the location of the initial rise moves further downstream. The general shape of the bump stays the same but is shifted further downstream. This pattern can be seen up to a certain level in the 70% PMF scenario, however the oscillations mask the clarity of the pattern. No pattern can be seen for the 40% PMF scenario.

As Manning’s values increase, the velocity within that cross section decreases, and in turn the water surface elevation increases. As water surface elevation increases, so does the shear stress and in turn so does the potential for erosion.

The drastic changes that occur to the model when Manning’s values are adjusted can be seen in Figure 41, Figure 42, and Figure 43. No clear pattern can be observed from the change of Manning’s values.

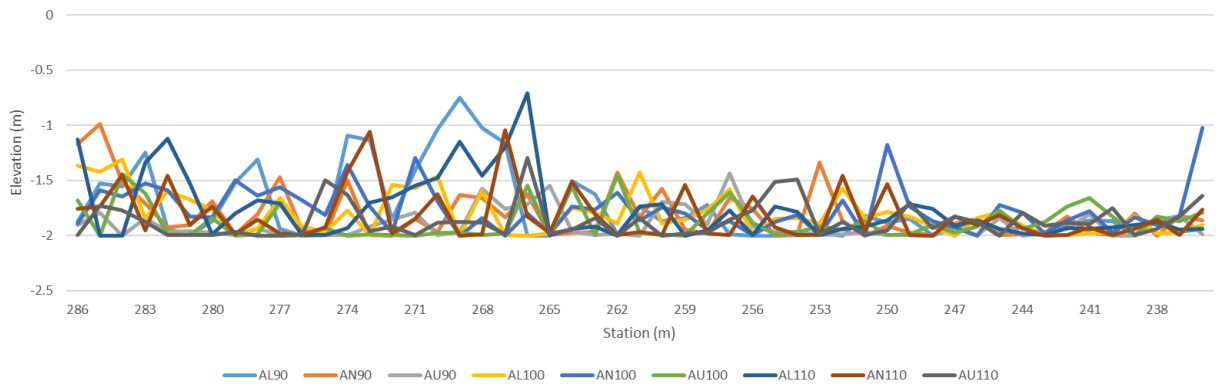


**Figure 41: Cheakamus Dam Emergency Spillway Difference in Manning’s Scenarios for Channel Invert Change for 100% PMF Scenario**

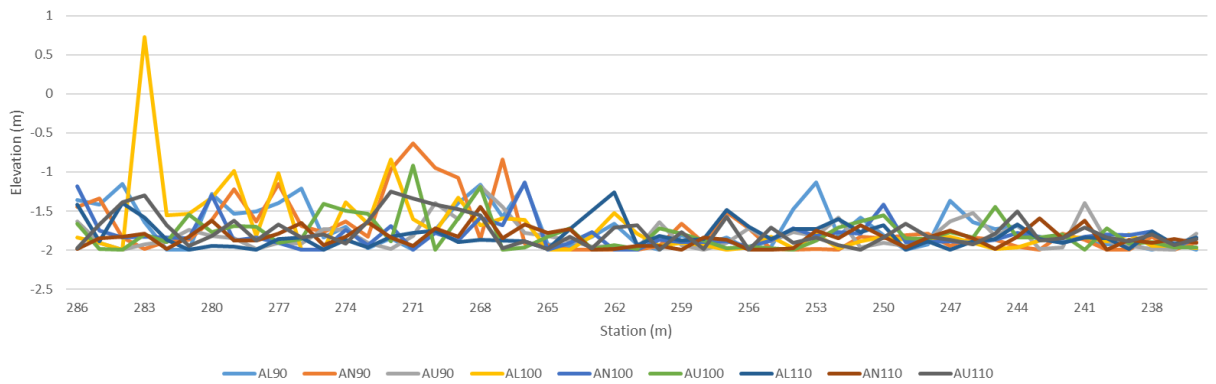


**Figure 42: Cheakamus Dam Emergency Spillway Difference in Manning’s Scenarios for Channel Invert Change for 70% PMF Scenario**



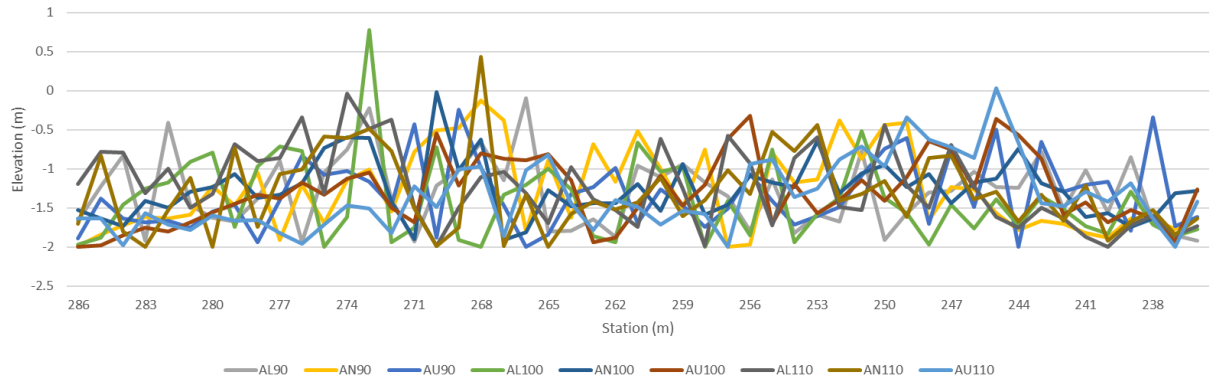


**Figure 43: Cheakamus Dam Emergency Spillway Difference in Manning's Scenarios for Channel Invert Change for 40% PMF Scenario**

### 3.3.3.3 Total Material Eroded

Figure 44, Figure 45, and Figure 46 show a comparison of results obtained using various Manning's values and the cumulative eroded material along the edge of the concrete spillway. Figure 44 shows the 90% sized Manning's area scenario, Figure 45 shows the 100% size, and Figure 46 shows the 110% size scenario. In the 40% and 80% PMF situations, there is very limited difference between lower, normal, and upper Manning's scenarios with regards to eroded material, whereas the opposite is true for the 70% and 90% PMF scenarios.

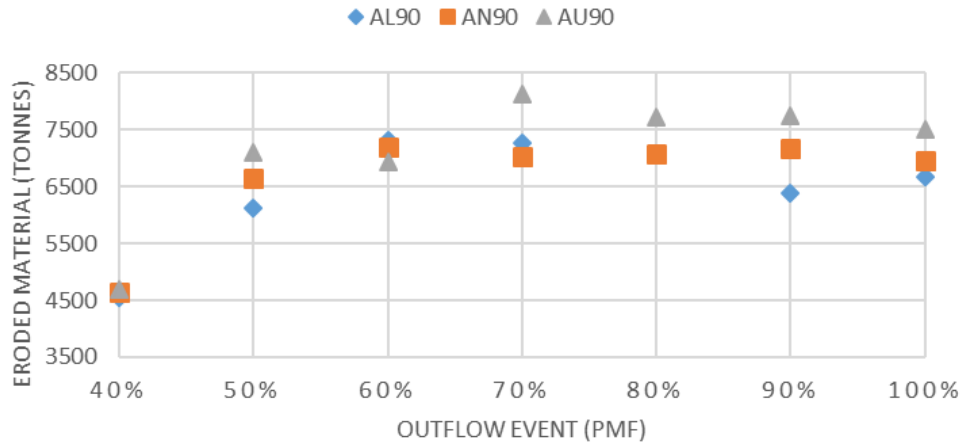


**Figure 44: Cheakamus Dam Emergency Spillway Eroded Material Sensitivity to Manning's Range at 90% Size**

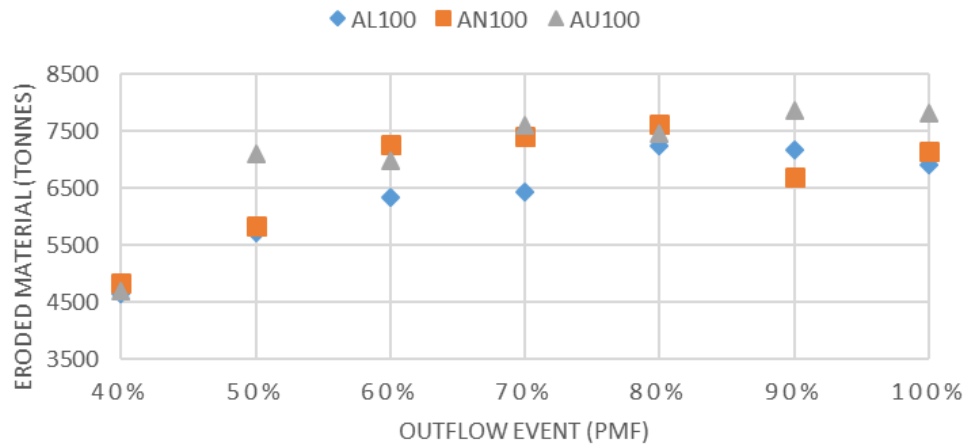


**Figure 45: Cheakamus Dam Emergency Spillway Eroded Material Sensitivity to Manning's Range at 100% Size**

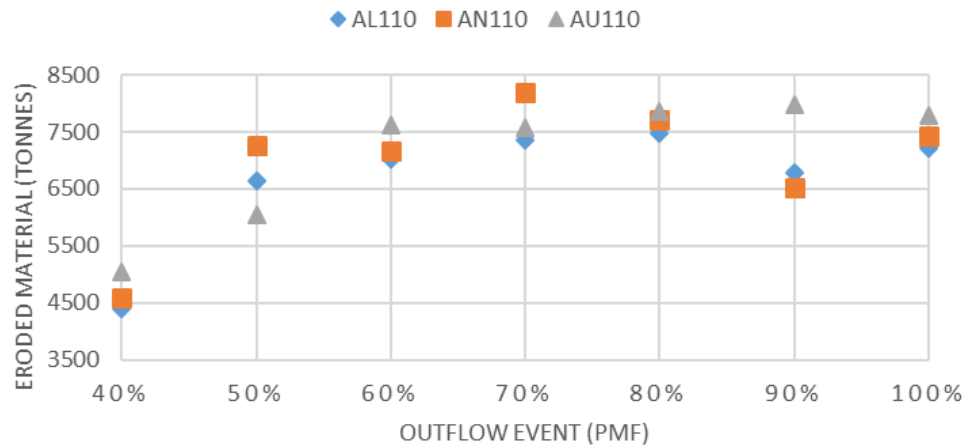


**Figure 46: Cheakamus Dam Emergency Spillway Eroded Material Sensitivity to Manning’s Range at 110% Size**

Figure 47 shows the lower Manning’s scenarios, Figure 48 shows the normal Manning’s scenarios, and Figure 49 shows the upper Manning’s scenario.

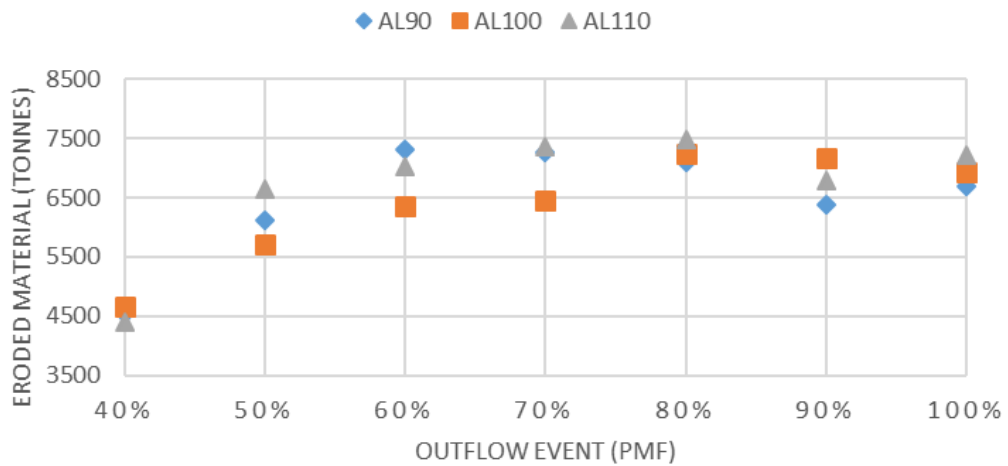


**Figure 47: Cheakamus Dam Emergency Spillway Eroded Material Sensitivity to Manning’s Vegetation Size Change at Lower Range**

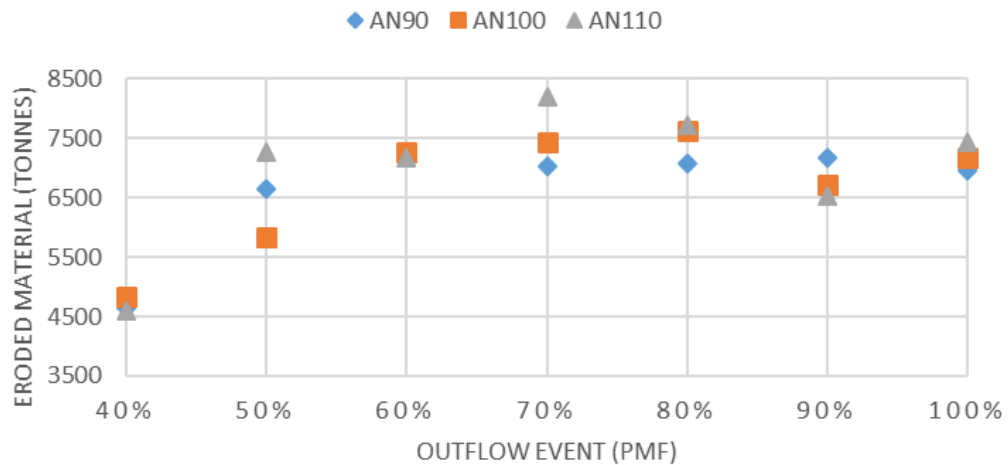


**Figure 48: Cheakamus Dam Emergency Spillway Eroded Material Sensitivity to Manning's Vegetation Size Change at Normal Range**

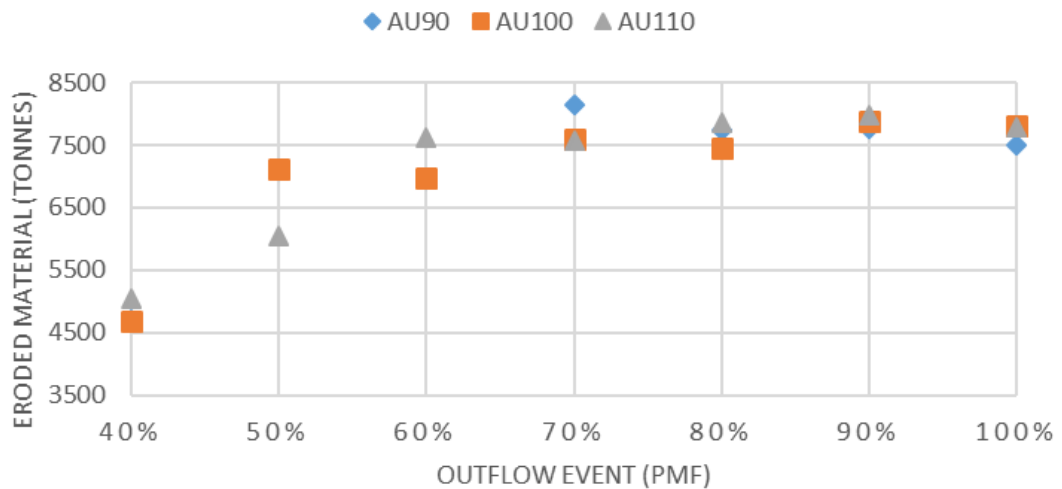


**Figure 49: Cheakamus Dam Emergency Spillway Eroded Material Sensitivity to Manning's Vegetation Size Change at Upper Range**

In theory, increase in Manning's values should result in decrease of eroded material, however the model is so dynamic and sensitive to change in Manning's values that this trend does not present itself, likely because model oscillations obscure it. An overall plateau pattern can be observed however with regards to increase in PMF. The eroded material increases consistently from 40% to 70% PMF but then plateaus to the 100%

PMF. This is likely due to the 2-meter maximum depth of erosion that limits the amount of erodible material.

#### 3.3.3.4 Velocity and Shear Stress Mapping

The hydraulic results are mapped for the 100% PMF scenario at the peak flow. Velocity is calculated with the Manning's equation, Equation 3, and shear stress is calculated using the shear stress equation, Equation 15. The values are interpolated and mapped within ArcGIS. Figures 50 and 51 show the shear stress and velocity for lower Manning's scenario, respectively. Figures 52 and 53 show the shear stress and velocity for normal Manning's scenario, respectively. Figures 54 and 55 show the shear stress and velocity for upper Manning's scenario, respectively.

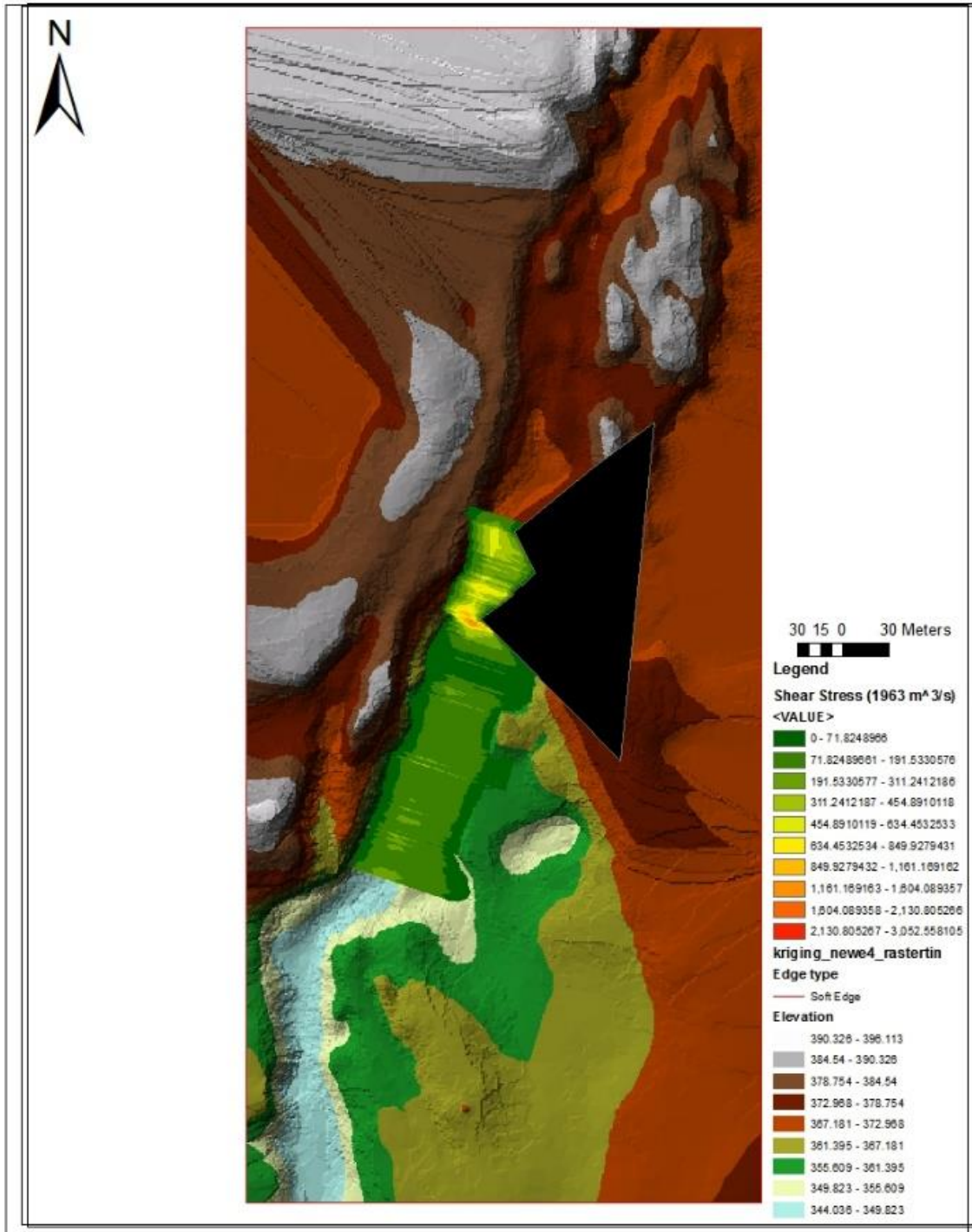


**Figure 50: Cheakamus Dam Emergency Spillway Shear Stress Map for 100% PMF and Lower Manning’s Scenario**

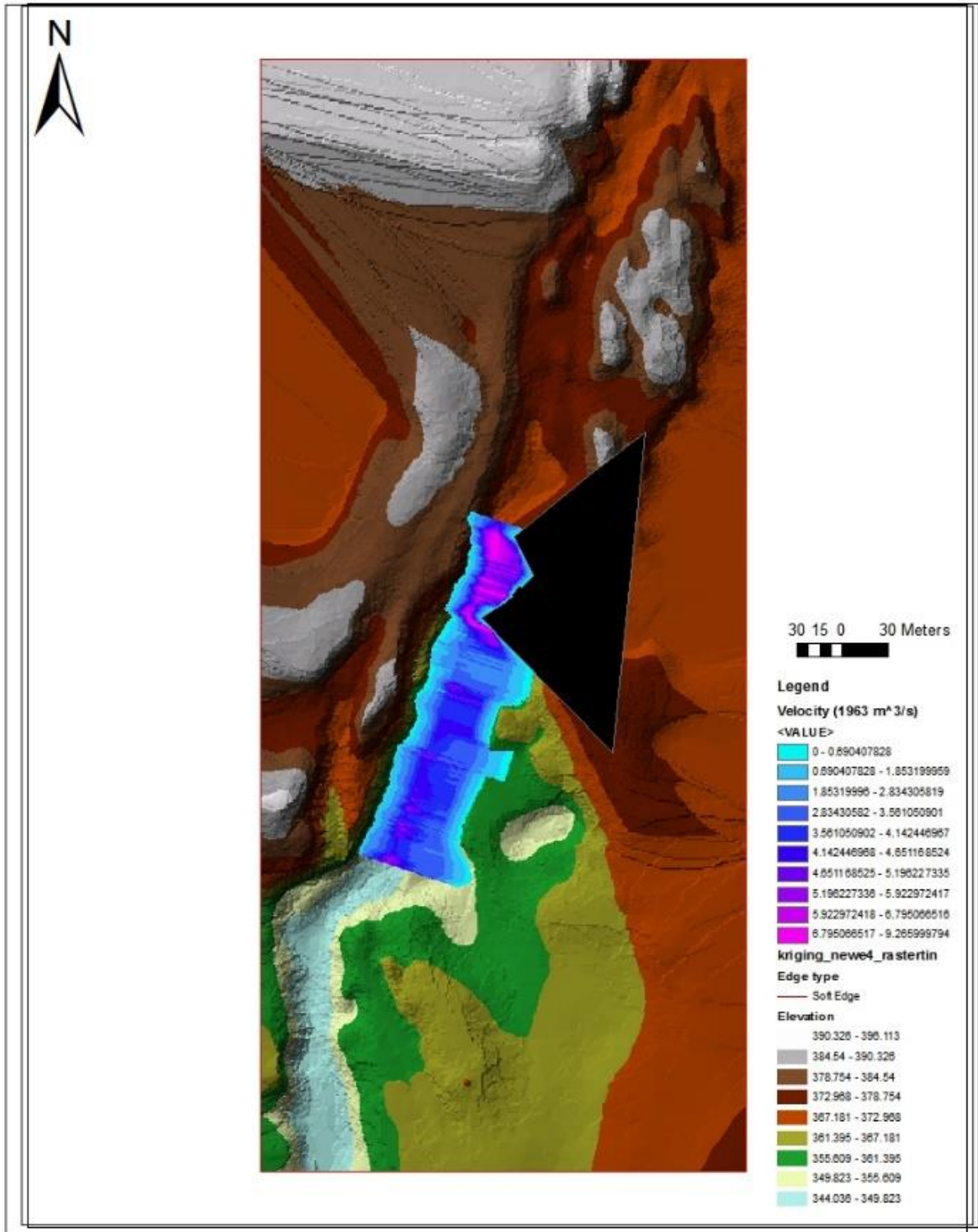


**Figure 51: Cheakamus Dam Emergency Spillway Velocity Map for 100% PMF and Lower Manning's Scenario**

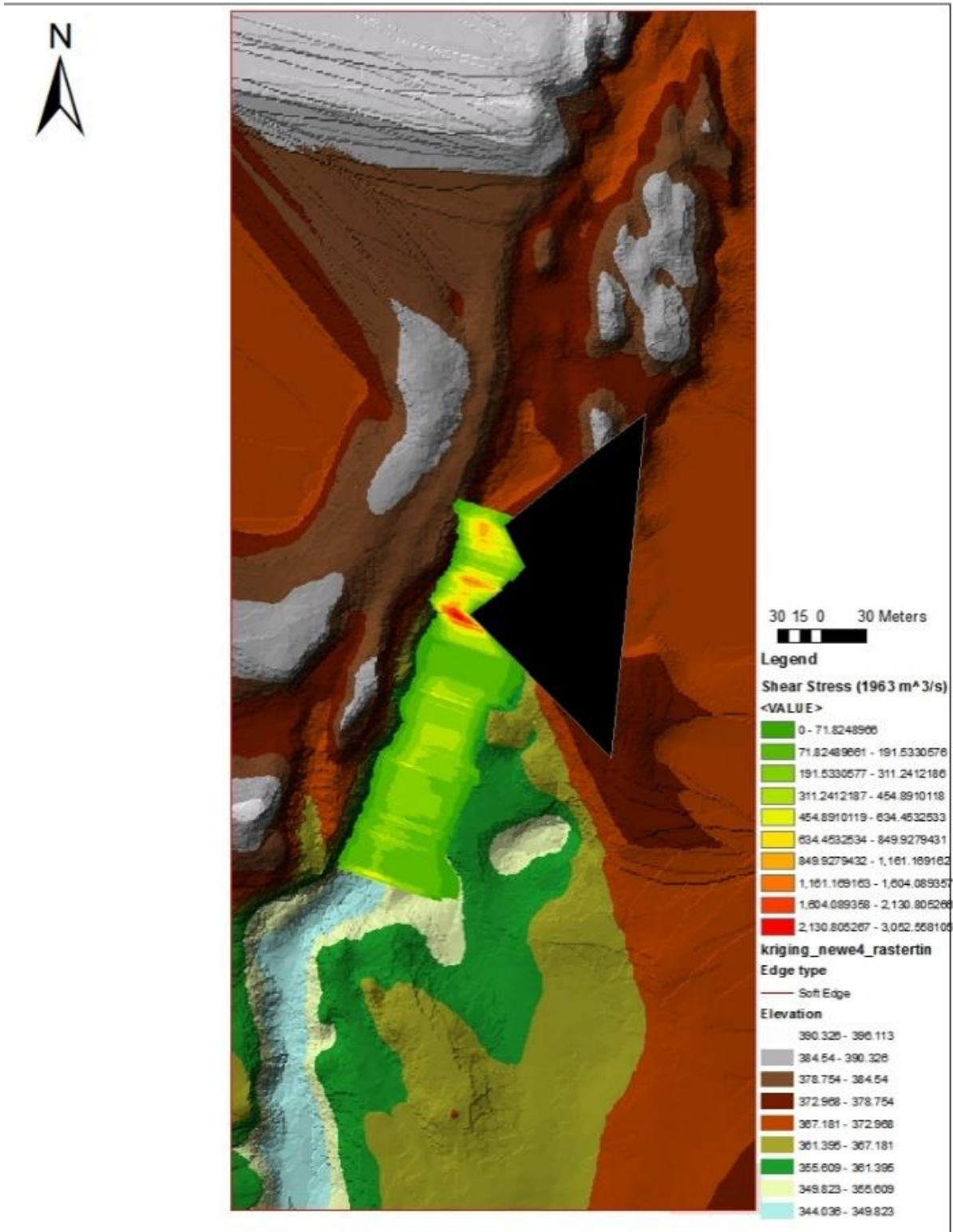


**Figure 52: Cheakamus Dam Emergency Spillway Shear Stress Map for 100% PMF and Normal Manning’s Scenario**



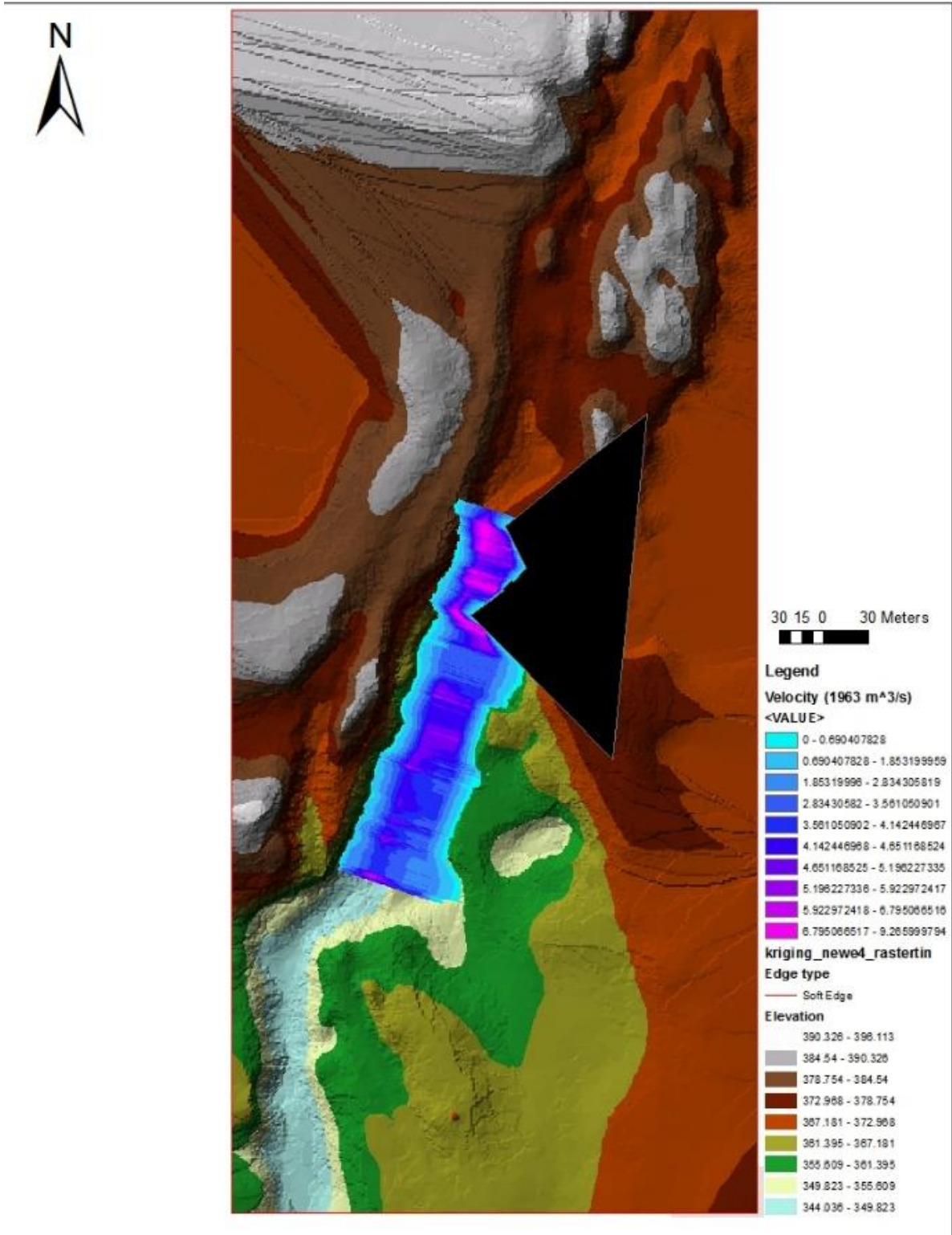


**Figure 53: Cheakamus Dam Emergency Spillway Velocity Map for 100% PMF and Normal Manning's Scenario**

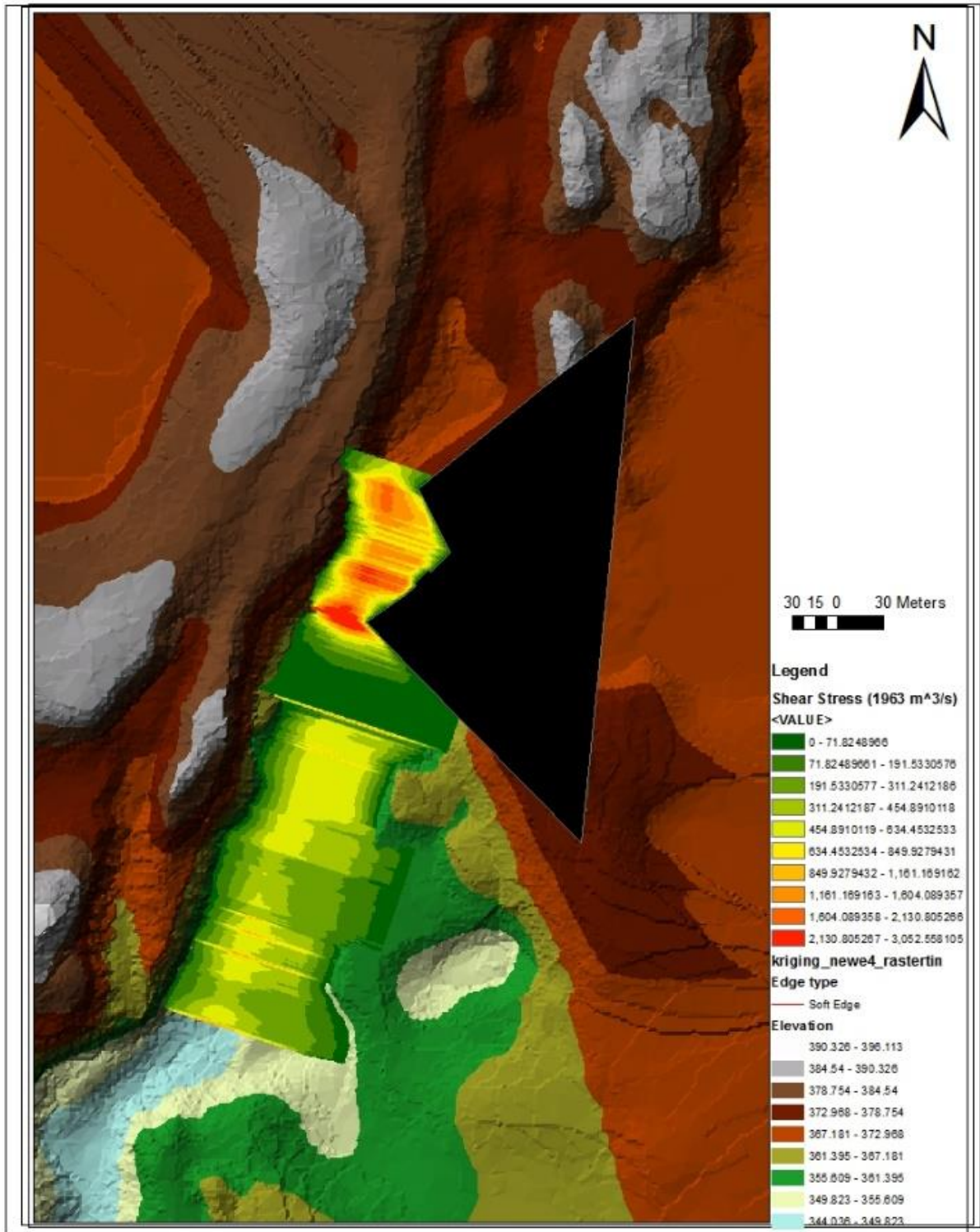


**Figure 54: Cheakamus Dam Emergency Spillway Shear Stress Map for 100% PMF and Upper Manning’s Scenario**

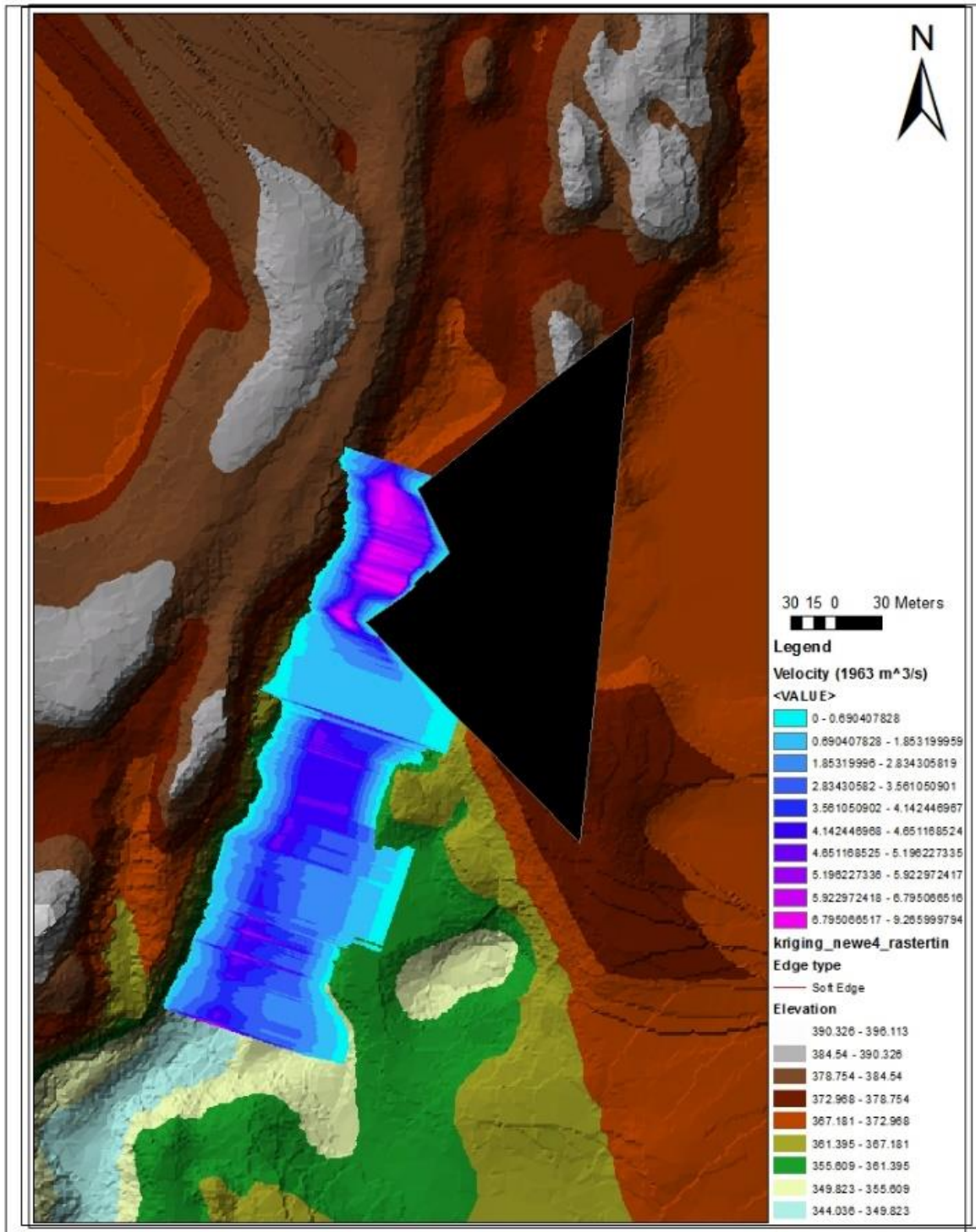


**Figure 55: Cheakamus Dam Emergency Spillway Velocity Map for 100% PMF and Upper Manning’s Scenario**

Several patterns can be observed from the presented maps. The values of shear stress increase with increase of Manning's value. Velocity is decreasing slightly as the Manning's values increase. It can also be noted that the general pattern does not change significantly with change of Manning's values. Most of the high values of shear stress and velocity are occurring in the steep section of the emergency spillway as expected. There is a portion along the concrete spillway where a high value of velocity and shear stress are occurring. This region could potentially have water seep underneath the concrete spillway, however this would need to be further investigated to determine whether or not there are any design features to prevent this from occurring.

As the emergency spillway is founded on the bedrock, the potential for erosion is limited and therefore the emergency spillway could not fail from erosion. There is however, a significant amount of damage that could occur.

### 3.4 Discussion

There are several strengths and weaknesses of the modelling approach. As a whole the model provides valuable insights and results that can be utilized by the dam safety systems simulation model (King et al 2017). However, when closely examined, the accuracy of the model is not at the acceptable level. HEC-RAS functions well as a simple tool to be used to evaluate possible erosion trends within an emergency spillway, however the program is not applicable to determining accurate sediment transport values within an emergency spillway like Cheakamus Dam.

The main weaknesses stem from both, the hydraulic and the sediment transport modelling. With the hydraulic modelling, the main limitation is 1-dimensional representation of the problem. Regardless of how much data is available, the accuracy will be limited based on the lack of 2-dimensional modelling. The second pitfall within the hydraulic model is the error associated with calculating surface water profiles within steep slopes. As discussed in the methodology, HEC-RAS makes a simplification in the

calculation of the pressure head that creates an error when the slope increases. And thirdly, the lack of data for the downstream boundary condition leads to imprecise water surface calculations. Typically, a downstream boundary condition of stage-flow is chosen so that feedback between water surface elevation and channel bed change can occur. Without the stage-flow data, the user must select normal depth as the downstream condition. This limits the accuracy of the model by keeping the downstream depth constant, instead of changing with the flow. These errors and shortcomings result in inaccurate values for velocities and surface water profile calculations.

As the hydraulic model is directly related to the sediment transport model, any errors or inaccuracies within the hydraulic calculations directly impact the accuracy of the sediment transport model. The sediment transport model has several flaws that also lead to potentially inaccurate results. The sediment transport equations within HEC-RAS are empirical formulas that were either developed for specific grain classes and in laboratory conditions (using flume experiments). The Meyer Peter Muller (MPM) equation is a very common excess shear relationship equation that is most applicable when dealing with larger grain sizes. However, this formula underestimates the transport capacity within steep slopes. The bed gradation at the Cheakamus Dam exceeds the maximum grain size of sediment that the Meyer-Peter Muller equation was developed for; resulting in inaccurate sediment transport values for the larger grain sizes. If HEC-RAS allowed for modifications to be made to the formula, as outlined by Smart (1984), the MPM method may have resulted in more accurate results.

Manning's roughness coefficient values had a significant impact on the results of the model simulations. Changing the Manning's coefficient values affected the stability of the model, due to the dynamic nature of the model. Increasing the Manning's value did decrease the velocity and increase the shear stress. As seen in the results, the downstream erosion was pushed further downstream as Manning's coefficient values increased.

Despite the shortcomings within the hydraulic and sediment transport model, there are strengths to be discussed. Many of the errors and shortcomings come from a lack of data. If downstream boundary conditions were known, instead of estimated, then the hydraulic

analyses would have a higher level of accuracy. Obtaining the downstream stage-flow relationship would greatly improve the model and would allow for the Manning's coefficient values to be calibrated. The model does well at showing overall erosion trends. Despite changing the Manning's values within the sensitivity analyses, the overall erosion and deposition trend remained the same. Although the values of erosion and deposition may be either under predicted or over predicted, the model still offers a relationship that satisfies the main objective of this research. The 1-dimensional model developed has fulfilled the objective by creating a computationally simple, easily repeatable model that can predict the erosion and deposition for any inflow event.

The main objective of this research is to create a model that describes the relationship between various inflow events and the damage that would occur to an emergency spillway. This was demonstrated with the case study of Cheakamus Dam. The limitations of 1-dimensional modeling and the lack of some hydraulic data may have resulted in under or over predicted erosion values, however a certain amount of uncertainty was anticipated from the beginning of the research. Despite the uncertainty of the model results, the model may still be utilized with the dam system safety simulation model proposed by King et al (2017). This 1-dimensional model developed for Cheakamus Dam provides a relationship between the eroded material and flow rates.

## Chapter 4

### 4 Conclusion

This section will provide a brief overview of the research and future work to come.

#### 4.1 Overview

The methodology presented in Chapter 2 was followed for the case study of the Cheakamus Dam. A 1-dimensional hydraulic and sediment transport model was built, and simulations were performed for various inflow events. The impact of various Manning's roughness coefficients were tested as well, and the impacts were discussed. The model shows the general trends and acts as an acceptable first iteration for modeling damage within the emergency spillway. With additional historical hydraulic data, the model accuracy could increase. To further increase the accuracy of the model, 2-dimensional modelling approach would need to be considered. The research objective set out in the introduction is achieved by the development of the relationship between various inflow events and the ensuing damage that could occur.

#### 4.2 Future Work

The model developed in this research provides an opportunity to be integrated into to the dam safety systems modeling of King et al (2017). The creation of damage-duration-flow graphs could be utilized by the dam safety simulation model to represent the current state of the emergency spillway. The damage, or percentage of material eroded, would be calculated for a broad range of inflow values that last for a range of time periods. Damage could then be interpolated between these values to arrive at a damage state given an inflow event. By linking the dam safety systems simulation model can provide that inflow data could feed directly from the dam safety system simulation model into the HEC-RAS sediment transport model on an hourly timestep. The sediment transport model would run for one hour at the provided flow rate and then generate a new set of cross sections with any erosion or deposition changes. The new cross sections would then be updated for the next time step. This could all be achieved with the use of a python

script, which would directly link the programs. The systems dynamics model would then show the damage that has occurred to the emergency spillway, represented as a percentage of eroded material versus available material to erode.



## Chapter 5

### 5 Bibliography

- Ackerman, C. (2009). HEC-GeoRAS: GIS Tools for Support of HEC-RAS using ArcGIS. 47-96. Davis: US Army Corps of Engineers. Retrieved August 14, 2017, from [http://www.hec.usace.army.mil/software/hec-georas/documentation/HEC-GeoRAS42\\_UsersManual.pdf](http://www.hec.usace.army.mil/software/hec-georas/documentation/HEC-GeoRAS42_UsersManual.pdf)
- Baecher, G., Ascila, R., & Hartford, D. (2013). Hydropower and dam safety. *STAMP/STPA Workshop*, (pp. 1-25). Cambridge, U.S.A.
- BC Hydro. (2005). *Cheakamus Project Water Use Plan*. Vancouver: BC Hydro.
- BC Hydro. (2008). *Engineering Report E591: Cheakamus Dam Deficiency Investigation*. Vancouver: BC Hydro.
- BC Hydro. (2013). *Cheakamus Project: Generation Operation Order*. Vancouver: BC Hydro.
- Brunner, G. (2016). HEC-RAS, River Analysis System Hydraulic Reference Manual. Davis, California, U.S.A.
- Brunner, G., & CEIWR-HEC. (2016). HEC-RAS, River Analysis System User's Manual Version 5. Davis, California, U.S.A.
- California Data Exchange Center. (2017). *Lake Oroville Spillway Incident: Timeline of Major Events February 4-25*. Retrieved January 15, 2018, from California Department of Water Resources: <https://www.water.ca.gov/LegacyFiles/oroville-spillway/pdf/2017/Lake%20Oroville%20events%20timeline.pdf>
- Cengel, Y., Turner, R., Cimbala, J., & Kanoglu, M. (2008). *Fundamentals of thermal-fluid sciences*. New York: McGraw-Hill.

- Chien, N. (1954). Meyer-Peter formula for bed-load transport and Einstein bed-load function. *M.R.D. Sediment Series No. 7*.
- Department of Natural Resources Indiana. (2007). *Indiana Dam Safety Inspection Manual*. Department of Natural Resources Indiana. Retrieved February 25, 2018, from <https://www.in.gov/dnr/water/3593.htm>
- Esri. (2016). *How Kriging works*. Retrieved 12 05, 2017, from ArcGIS for Desktop: <http://desktop.arcgis.com/en/arcmap/10.3/tools/3d-analyst-toolbox/how-kriging-works.htm>
- Fischenich, C. (2000). *Robert Manning (A Historical Perspective)*. Retrieved March 21, 2018, from <http://www.dtic.mil/dtic/tr/fulltext/u2/a378362.pdf>
- France, J., Alvi, I., Dickson, P., Falvey, H., Rigbey, S., & Trojanowski, J. (2018). *Independant Forensic Team Report Oroville Dam Spillway Incident*. Independant Forensic Team. Retrieved March 14, 2018, from <https://damsafety.org/sites/default/files/files/Independent%20Forensic%20Team%20Report%20Final%2001-05-18.pdf>
- Groenier, J. (2012, January). *Pocket Safety Guide for Dams and Impoundments*. Retrieved March 3, 2018, from United States Department of Agriculture: <https://www.fs.fed.us/eng/pubs/htmlpubs/htm12732805/longdesc/fig01ld.htm>
- Hager, W. (2005). Du Boys and sediment transport. *Journal of Hydraulic Research*, 43(3), 227-233.
- Hartford, D., & Baecher, G. (2004). *Risk and uncertainty in dam safety*. London, U.K.: Thomas Telford.
- Hunziker, R., & Jaeggi, M. (2002). Grain Sorting Processes. *Journal of Hydraulic Engineering*, 128(12), 1060-1068.
- Kasler, D. (2017, February 10). *Use of untested emergency spillway yet again a possibility at crippled Oroville Dam*. Retrieved March 3, 2018, from The

Sacramento Bee: <http://www.sacbee.com/news/state/california/water-and-drought/article132123804.html>

King, L., Simonovic, S., & Hartford, D. (2017). Using system dynamics simulation for assessment of hydropower system safety. *Water Resources Research*, 53(8).

Komey, A., Deng, Q., Baecher, G., Zielinski, P., & Atkinson, T. (2015). Systems reliability of flow control in dam safety. *12th International Conference on Application of Statistics and Probability in Civil Engineering*, (pp. 1-8). Vancouver, Canada.

Leliavsky, S. (1955). *An Introduction to Fluvial Hydraulics*. London: Constable.

Leveson, N. (2011). Engineering a safer world: Systems thinking applied to safety. *MIT Press*, 64-100.

Leveson, N., Daouk, M., Dulac, N., & Marais, K. (2003). Applying STAMP in accident analysis. 1-23.

MacArthur, R., Williams, D., & Thomas, W. (1990). *Status and New Capabilities of Computer Program HEC-6; 'Scour and Deposition in Rivers and Reservoirs'*. Retrieved 02 10, 2018, from <http://www.hec.usace.army.mil/publications/TechnicalPapers/TP-129.pdf>

Maeder, C. (2015, December 30). *The Road to HEC-RAS*. Retrieved from CivilGEO Engineering Software: <https://www.civilgeo.com/the-road-to-hec-ras/>

Manning, R. (1891). On the flow of water in open channels and pipes. *Transactions of the Institution of Civil Engineers*, pp. 161-207.

Meyer-Peter, E., & Muller, R. (1948). Formulas for bed-load transport. *International Association for Hydraulic Structures Research 2nd Meeting* (p. Appendix 2). Stockholm: International Association for Hydraulic Structures Research.

- Neelz, S., & Pender, G. (2009). *Desktop review of 2D hydraulic modelling packages*. Bristol: Environmental Agency. Retrieved January 8, 2018, from [http://evidence.environment-agency.gov.uk/FCERM/Libraries/FCERM\\_Project\\_Documents/SC080035\\_Desktop\\_review\\_of\\_2D\\_hydraulic\\_packages\\_Phase\\_1\\_Report.sflb.ashx](http://evidence.environment-agency.gov.uk/FCERM/Libraries/FCERM_Project_Documents/SC080035_Desktop_review_of_2D_hydraulic_packages_Phase_1_Report.sflb.ashx)
- Oroville Dam Spillway Incident Independent Forensic Team. (2017, September 5). Interim Status Memorandum. Retrieved October 20, 2017, from <https://damsafety.org/sites/default/files/files/IFT%20interim%20memo%20final%2009-05-17.pdf>
- Papanicolaou, A., Bdour, A., & Wicklein, E. (2004). One-dimensional hydrodynamic/sediment transport model applicable to steep mountain streams. *Journal of Hydraulic Research*, 42(4), 357-375.
- Regan, P. (2010). An Examination of Dam Failures vs. Age of Dams- How are dam failures distributed over the life of the dam? and does a long period of satisfactory performance mean there will be no significant incident over the remainder of its life? *Hydro Review*, 29(4), 62.
- Regan, P. (2010). Dams as systems - a holistic approach to dam safety. *30th Annual United States Society on Dams Conference*, (pp. 554-563). Sacramento.
- Smart, G. (1984). Sediment transport formula for steep channels. *Journal of Hydraulic Engineering*, 110(3), 267-276.
- State of California Department of Water Resources. (2005, January). Oroville Facilities FERC Project No. 2100. California, U.S.A. Retrieved March 01, 2018, from [https://water.ca.gov/LegacyFiles/orovillereicensing/docs/app\\_ferc\\_license\\_2005/Vol\\_I\\_Exhibit%20A.pdf](https://water.ca.gov/LegacyFiles/orovillereicensing/docs/app_ferc_license_2005/Vol_I_Exhibit%20A.pdf)
- Te Chow, V. (1959). *Open-channel Hydraulics (Vol. 1)*. New York: McGraw-Hill.
- Thomas, W. (1982). Mathematical modeling of sediment movement. In *Gravel Bed Rivers* (pp. 487-508). John Wiley & Sons Ltd.

- Toffaleti, F. (1968). *A Procedure for Computation of Total River Sand Discharge and Detailed Distribution, Bed to Surface*. Committee on Channel Stabilization, U.S. Army Corps of Engineers.
- U.S. Department of the Interior Bureau of Reclamation. (2014). *Appurtenant Structures for Dams (Spillways and Outlet Works) Design Standard*. U.S. Department of the Interior Bureau of Reclamation.
- Ventana Systems. (2017, December). *Vensim Version 7.2*. Retrieved from Vensim:  
<http://vensim.com/documentation/>
- Wolman, M., Miller, J., & Leopold, L. (1964). *Fluvial processes in geomorphology*. San Francisco: Courier Corporation.
- Wong, M., & Parker, G. (2006). Reanalysis and Correction of Bed-Load Relation of Meyer-Peter and Muller Using Thier Own Database. *Journal of Hydraulic Engineering*, 132(11), 1159-1168.

## Appendices

### Appendix 1: Meyer-Peter Muller Sample Calculation (Brunner, 2016)

#### Meyer-Peter Muller Sediment Transport Function

by Vanoni (1975), and Schlichting's Boundary Layer Theory, 1968

#### Input Parameters

Temperature, F	T = 55	Average Velocity, ft/s	V = 5.46
Kinematic viscosity, ft <sup>2</sup> /s	$\nu = 0.00001315$	Discharge, ft <sup>3</sup> /s	Q = 5000
Depth, ft	D = 22.9	Unit Weight water, lb/ft <sup>3</sup>	$\gamma_w = 62.385$
Slope	S = 0.0001	Overall d50, ft	$d_{90} = 0.00306$
Median Particle Diameter, ft $d_{50}$	$d_{50} = 0.00232$	Channel Width, ft	B = 40
Specific Gravity of Sediment,		s = 2.65	

#### Constants

Acceleration of gravity, ft/s<sup>2</sup>  $g = 32.2$

#### Solution

Shear velocity  $u_*$ ,

$$u_* = \sqrt{g \cdot D \cdot S} \qquad u_* = 0.272$$

Shear Reynold's number,  $R_s$ ,

$$R_s = \frac{u_* \cdot d_{90}}{\nu} \qquad R_s = 63.189$$

Schlichting's B coefficient, Bcoeff

$$BCoeff = \begin{cases} (5.5 + 2.5 \cdot \ln(R_s)) & \text{if } R_s \leq 5 \\ \left[ \begin{array}{l} 0.297918 + 24.8666 \cdot \log(R_s) - 22.9885 \cdot (\log(R_s))^2 \\ + 8.5199 \cdot (\log(R_s))^3 - 1.10752 \cdot (\log(R_s))^4 \end{array} \right] & \text{if } 5 < R_s \leq 70 \\ 8.5 & \text{otherwise} \end{cases}$$

Friction factor due to sand grains  $f'$ ,

$$f' = \left( \frac{2.82843}{BCoeff - 3.75 + 2.5 \cdot \ln\left(2 \cdot \frac{D}{d_{90}}\right)} \right)^2 \quad f' = 9.565 \times 10^{-3}$$

Nikaradse roughness ratio RKR,

$$RKR = \sqrt{\frac{f'}{8}} \cdot \frac{V}{\sqrt{g \cdot D \cdot S}} \quad RKR = 0.695$$

Sediment discharge lb/s,

$$g_s = \left[ \frac{(RKR)^{\frac{3}{2}} \cdot \gamma_w \cdot D \cdot S - 0.047 \cdot (\gamma_w \cdot s - \gamma_w) \cdot d_{si}}{0.25 \cdot \left(\frac{\gamma_w}{g}\right)^{\frac{1}{3}} \cdot \left(\frac{\gamma_w \cdot s - \gamma_w}{\gamma_w \cdot s}\right)^{\frac{2}{3}}} \right]^{\frac{3}{2}} \cdot B \quad g_s = 7.073$$

Sediment discharge ton/day,

$$G_s = g_s \cdot \frac{86400}{2000} \quad G_s = 306$$





### Appendix 3: Thomas Mixing Method Algorithm (Brunner, 2016)

Armoring Ratio: The Thomas and Copeland methods both use the equivalent particle diameter to compute an **Armor Ratio**. The Armor Ratio is a coefficient between 0 and 1, which reduces the sediment deficit HEC-RAS will erode from the sub-surface layer, if the cover layer includes enough coarser material.

The Thomas algorithm has five basic steps:

1. Compute Sediment Deficit by Grain Class: First HEC-RAS computes transport capacity for each grain class and compares it to supply. If capacity exceeds supply, it tries to erode the deficit from the bed.
2. Remove the Grain Class Mass from the Cover Layer: If the cover layer contains the enough of the grain class, HEC-RAS removes the entire deficit from the cover layer. If the cover layer does not have enough of the grain class to satisfy the deficit, HEC-RAS removes all of the grain class from the cover layer, and then tries to remove the balance from the sub-surface layer.
3. Sum the Equivalent Particle Diameters of all coarser grain classes in the cover layer: Before HEC-RAS removes any sediment from the sub-surface layer, it computes the equivalent particle diameter of every coarser grain class in the cover layer, and then sums them.

For example, in the simplified substrate in Figure 13-9, if HEC-RAS tried to remove the smallest grain class (green), it would sum the equivalent diameter of the two coarser grain classes. HEC-RAS uses the sum of the equivalent grain diameters for cover layer grain classes, coarser than the eroding grain class ( $\Sigma d_{eq}=0.9$  in Figure 13-9) to compute armor layer regulation (i.e. reduce the amount of deficit the model can erode from the sub-surface layer).

4. Compute an Armoring Ratio: The Thomas method computes an armor ratio from the cumulative coarser equivalent diameter according to the relationship in Figure 13-10. This relationship interpolates between a low bound, where the cover layer has no effect on erosion and an upper bound where the armor layer totally prevents erosion from the subsurface layer.

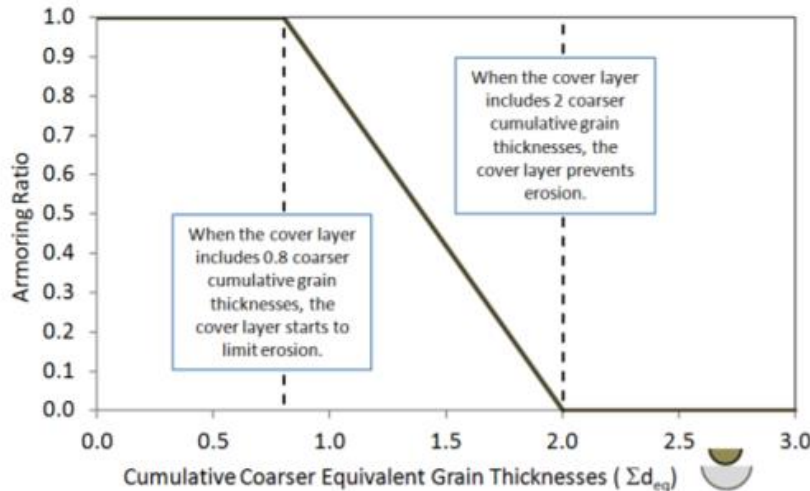


Figure 13-10: Armor ratio relationship used in the Thomas method.

**Low Bound:** If there is less than one total cumulative equivalent diameter of coarser material in the cover layer ( $\Sigma d_{eq} < 1$ ), then the cover

layer can't be continuous. For  $\Sigma d_{eq} < 0.8$ , 20% of the subsurface layer is exposed. At this thickness, the method assumes the cover layer has too many gaps to regulate the subsurface layer. The Thomas method does not reduce erosion for this case.

**High Bound:** On the other extreme, if the sum of the equivalent grain diameters of coarser grain classes is greater than 2 ( $\Sigma d_{eq} > 2$ ) the cover layer will not allow any erosion of that grain class from the sub surface layer. This end point comes from broad empirical evidence that flow cannot 'suction' fine sediment through more than two grain diameters of immobile armored layer.

The Thomas method interpolates linearly between these end points:

**No Armoring** (Armor Ratio = 1  $\rightarrow$  erosion = deficit) for  $\Sigma d_{eq} < 0.8$

and

**No Erosion** (Armor Ratio = 0  $\rightarrow$  erosion = 0) for  $\Sigma d_{eq} > 2$ .

5. **Erode the grain class from the sub-surface layer, reducing the deficit by the Armor Ratio:** HEC-RAS multiplies the sediment deficit for each grain class by the armor ratio such reducing erosion for each grain class (i) according to the expression:

$$\text{Erosion}_{(i)} = \text{Armor Ratio}_{(i)} * \text{Sediment Deficit}_{(i)}$$

For the example in Figure 13-9, where  $\Sigma d_{eq} = 0.9$ , the Thomas method returns an armor ratio of 0.91, and HEC-RAS would remove 91% of the deficit of the fines grain class from the subsurface layer.

### Cover Layer Reset: Destruction or Burial

The cover layer evolves during the simulation, coarsening or fining in response to capacity and upstream load. However, there are two situations which cause the cover layer to 'reset,' which introduce bed gradation non-linearity. Understanding these processes will help interpret bed gradation results.

Cover Layer Destruction: The cover layer can erode until it is too thin to regulate the bed. At that point, the Thomas method resets the layer, mixing it with the rest of the active layer, and cutting a new, thicker cover layer from the mixed active layer bed material.

At the beginning of *each* computation time step, HEC-RAS computes the **stratification weight** of the cover layer. The **stratification weight** is simply the combined **equivalent particle diameter** of *all* grain classes in the cover layer. If the stratification weight, the total cumulative equivalent particle diameter is less than 0.5, HEC-RAS destroys the cover layer. Thomas based the 0.5 threshold on Harrison's (1950) experiments, which demonstrated that equilibrium sediment transport dropped when 40% of the bed surface was covered in his flume experiments.

## Curriculum Vitae

**Name:** Ryan Mackenzie Weise

**Post-secondary Education and Degrees:** University of Western Ontario  
London, Ontario, Canada  
2012-2016 BEng Civil and Environmental Engineering

**Honours and Awards:** CEE Undergraduate Thesis  
2016  
1<sup>st</sup> Place for CEE Presentation of Undergraduate Thesis

**Related Work Experience** Teaching Assistant  
The University of Western Ontario  
2016-2017  
Courses: Project Management, Environmental Hydraulics, and Landfill Design